1. Report No. FHWA-SC-03-07	2. Government Accession No.	3. Recipient's Catalog No.
4. Title and Subtitle Guide for Estimating the Dynamic Properties of South Carolina Soils for Ground Response Analysis		5. Report Date November 13, 2003
		6. Performing Organization Code
7. Author(s) Ronald D. Andrus, Jianfeng Zhang, Brian S. Ellis, and C. Hsein Juang		8. Performing Organization Report No.
9. Performing Organization Name and Address Clemson University Civil Engineering Department Clemson, SC 29634-0911		10. Work Unit No. (TRAIS)
		11. Contract or Grant No. SC-DOT Research Project No. 623
12. Sponsoring Agency Name and Address South Carolina Department of Transportation P. O. Box 191 Columbia, SC 29202-0191		13. Type of Report and Period Covered Final Report March 14, 2001 to Nov. 13, 2003
		14. Sponsoring Agency Code

15. Supplementary Notes

16. Abstract

     South Carolina is the second most seismically active region in the eastern U.S. The 1886 Charleston earthquake caused about 60 deaths and an estimated $23 million (1886 dollars) in damage. An important step in the engineering design of new and the retrofit of existing structures in earthquake-prone regions is the prediction of strong ground motions. Required inputs for ground response analysis include the small-strain shear wave velocity, the variation of normalized shear modulus with shear strain, and the variation of material damping ratio with shear strain for each soil layer beneath the site in question. Collectively, these inputs are known as the dynamic soil properties. This report presents guidelines for estimating the dynamic properties of South Carolina soils for ground response analysis.

     Regression equations for estimating small-strain shear-wave velocity from CPT and SPT data are presented in this guide. The regression equations are based on findings in previous studies and 123 penetration-velocity data pairs from South Carolina. Variables in the CPT-velocity equations are: cone tip resistance, soil behavior type index, depth, and geology. In the SPT-velocity equations, variables are: corrected blow count, fines content, depth, and geology. Shear-wave velocity measurements in Pleistocene soils are 20 % to 30 % greater than velocity measurements in Holocene soils with the same penetration resistance. In Tertiary soils, shear-wave velocity measurements are 40 % to 130 % greater than velocity measurements in Holocene soils with the same penetration resistance, and appear to depend on the amount of carbonate in the soils.   (Continued)

17. Key Word Cone penetration test; earthquakes; ground motion; material damping; resonant column test; shear modulus; shear-wave velocity; site effects; South Carolina; standard penetration test; surface geology; torsional shear test	18. Distribution Statement		
19. Security Classif. (of this report) Unclassified	20. Security Classif. (of this page) Unclassified	21. No. of Pages 141	22. Price

Form DOT F 1700.7 (8-72)   Reproduction of completed page authorized

16. Abstract (Continued).

      Predictive equations for estimating normalized shear modulus and material damping ratio are also presented. They are based on a modified hyperbolic model and test results from Resonant Column and Torsional Shear tests on 122 samples. Input variables in the predictive equation for normalized shear modulus are: strain amplitude, confining stress, plasticity index (PI), and geology. In general, the recommended normalized shear modulus curve for Holocene soils with $PI = 0$ follows the Seed et al. upper range curve for sand, the Idriss curve for sand, and the Stokoe et al. curve for sand. On the other hand, the recommended normalized shear modulus curves for the older soils with $PI = 0$ generally follow the Seed et al. mean or lower range curves for sand and the Vucetic and Dobry curve for $PI = 0$ soil.

      The material damping ratio curves are expressed in terms of normalized shear modulus and minimum material damping ratio. Relationships between minimum damping and PI are developed based only on Torsional Shear test data. In general, the recommended damping curve for Holocene soils with $PI = 0$ follows the Seed et al. lower range curve for sand and the Idriss curve for sand and clay. The recommended damping curves for the older soils with $PI = 0$ generally follow the Seed et al. mean curve for sand and the Vucetic and Dobry curve for $PI = 0$ soils.

      Additional penetration-velocity data are needed from older soils, particularly the residual soils and saprolites in the Piedmont and natural sediments in the Middle and Upper Coastal Plain. Additional normalized shear modulus and material damping ratio data are needed from all deposit types in South Carolina, particularly the Lower Coastal Plain.

      The guidelines serve as a resource document for practitioners and researchers involved in predicting ground motions in the southeastern U.S.

Guide for Estimating the Dynamic Properties of South Carolina Soils for Ground Response Analysis

SCDOT

U.S. Department of Transportation

Federal Highway Administration

Final Report

November 13, 2003

By:

Ronald D. Andrus, Ph.D., Jianfeng Zhang, Brian S. Ellis,
and C. Hsein Juang, Ph.D., P.E.
Department of Civil Engineering
Lowry Hall, Box 340911
(864) 656-0488

**Department of Civil Engineering
College of Engineering and Science
Clemson University
Clemson, South Carolina USA**

ACKNOWLEDGMENTS

TABLE OF CONTENTS

x

LIST OF TABLES

LIST OF FIGURES

CHAPTER 1

INTRODUCTION

1.1 BACKGROUND

Earthquake hazards are a major concern for the state of South Carolina. The 1886 Charleston earthquake (moment magnitude, $M_w \approx 7.3$) was the strongest historic earthquake to occur in the eastern U. S., causing about 60 deaths and an estimated \$23 million (1886 dollars) in damage. Paleoliquefaction evidence suggests that at least five other large earthquakes have occurred in South Carolina during the last 2000 to 5000 years (Obermier *et al.*, 1985; Talwani and Cox, 1985; Amick and Gelinas, 1991). In a recent study by Talwani and Schaeffer (2001), they estimate the earthquakes prior to 1886 near Charleston occurred about 546 $\pm$ 17 and 1021 $\pm$ 30 years ago. This evidence has lead the U. S. Geological Survey (Frankel *et al.*, 2000; http://geohazards.cr.usgs.gov/eq/) to map significantly higher expected ground shaking levels than indicated on previous maps for South Carolina. Thus, future large earthquakes in the state are expected, and property damage during these future events will likely exceed several billion dollars (FEMA, 2000).

Required inputs for earthquake ground motion and site response analysis include stiffness and material damping information for each soil layer at the site in question. Soil stiffness is represented by either shear-wave velocity or shear modulus. Small-strain shear-wave velocity, V_S, is directly related to small-strain shear modulus, G_{max}, by:

$$G_{\max} = \rho V_S{}^2 \qquad\qquad (1.1)$$

where ρ is the mass density of soil (total unit weight of the soil divided by the acceleration of gravity). Illustrated in Figure 1.1 is the relationship between G_{max}, shear strain, γ, and shear stress, τ. At moderate to high strains, the secant modulus, G, is used to represent the average stiffness. It is common in engineering practice to normalize G by dividing by G_{max}. A plot showing the variation of G/G_{max} with shear strain is called a *normalized modulus reduction curve,* and is illustrated in Figure 1.2.
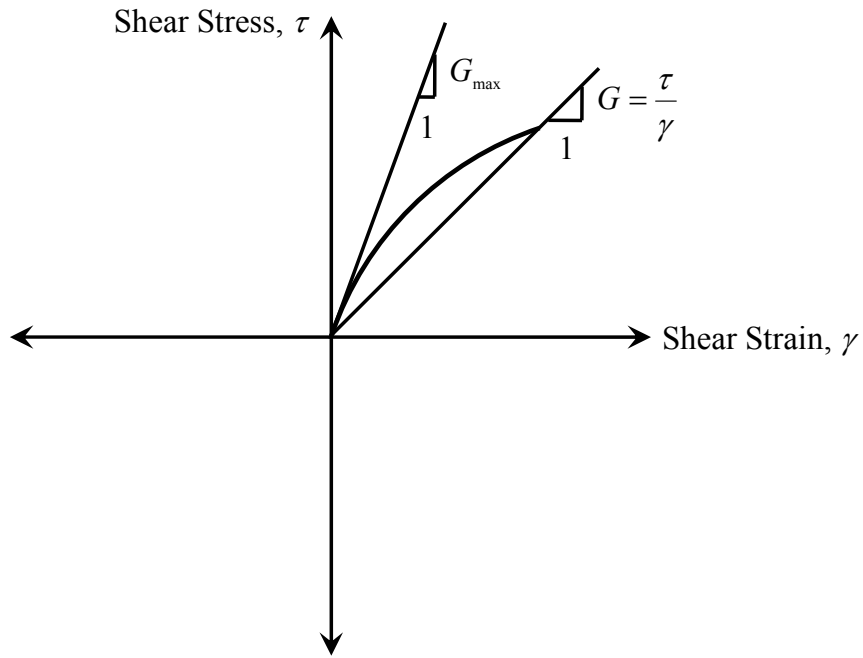
Figure 1.1 – Stress-strain curve showing G_{max} and G.
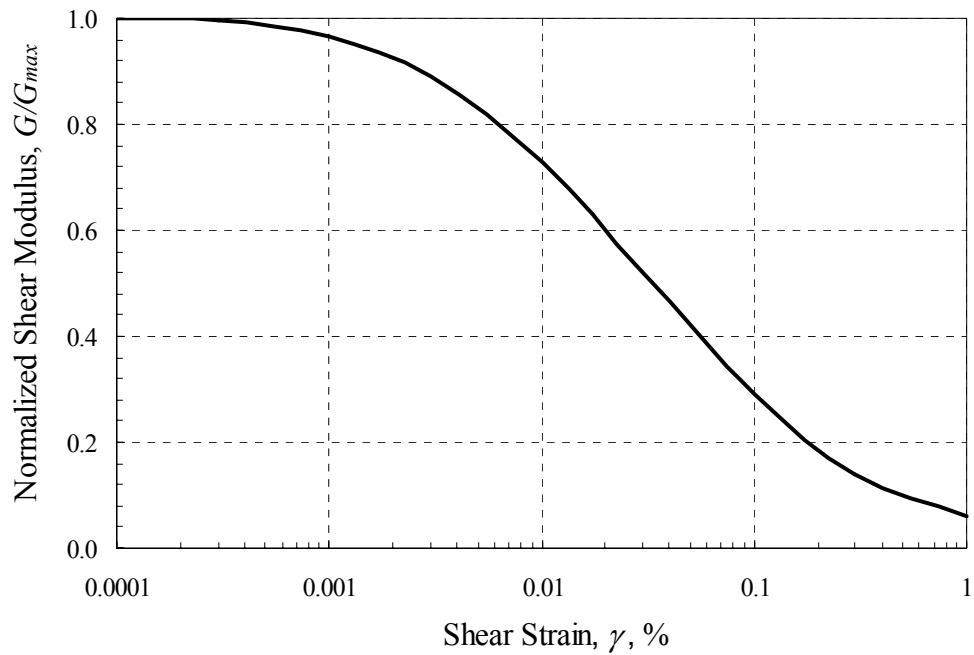
Figure 1.2 – Typical normalized shear modulus reduction curve.

Material damping ratio, D, represents the energy dissipated by the soil and is related to the stress-strain hysteresis loops generated during cyclic loading. Mechanisms that contribute to material damping are friction between soil particles, strain rate effect, and nonlinear soil behavior. Hysteretic damping can be defined by:

$$D = \frac{W_D}{4\pi W_S}$$ (1.2)

where W_D is the energy dissipated in one cycle of loading, and W_S is the maximum strain energy stored during the cycle. A hysteresis loop is shown in Figure 1.3. The area inside the loop is W_D. The area of the triangle is W_S. A typical curve representing the variation of material damping with shear strain for soil is illustrated in Figure 1.4.

Theoretically, there should be no dissipation of energy at the linear elastic behavior stage. However, even at very low strain levels, there is always some energy dissipation measured in the laboratory testing and the material damping ratio of soils never goes to zero. In the linear range, the damping ratio is a constant value and is referred to as the small-strain material damping, D_{min}. At higher strains, nonlinearity in the stress-strain relationship (see Figure 1.1) leads to an increase in material damping with increasing strain amplitude.

The field V_S, the shear modulus reduction curve, and the damping versus shear strain curve are collectively referred in this document as the dynamic soil properties that are required for earthquake ground motion and site response analysis.

1.2 PURPOSE

The current state of practice for determining the dynamic soil properties for ground response analysis involves 1) measuring or estimating the field V_S, and 2) measuring or estimating the modulus reduction and material damping versus strain curves. While good direct measurements are always preferred, it is often not economically feasible to make these measurements for all locations and soil layers. In addition, measurements for the modulus reduction and damping curves are particularly expensive to make, and are usually made for only critical projects.

This guide addresses the need for procedures for estimating the dynamic properties of soils in South Carolina that can be used to improve current earthquake ground motion and site response maps of the state, as well as provide inputs for site-specific response analysis. The procedures recommended in this guide are based on a review of earlier general procedures proposed for soils worldwide and a statistical analysis of existing data.
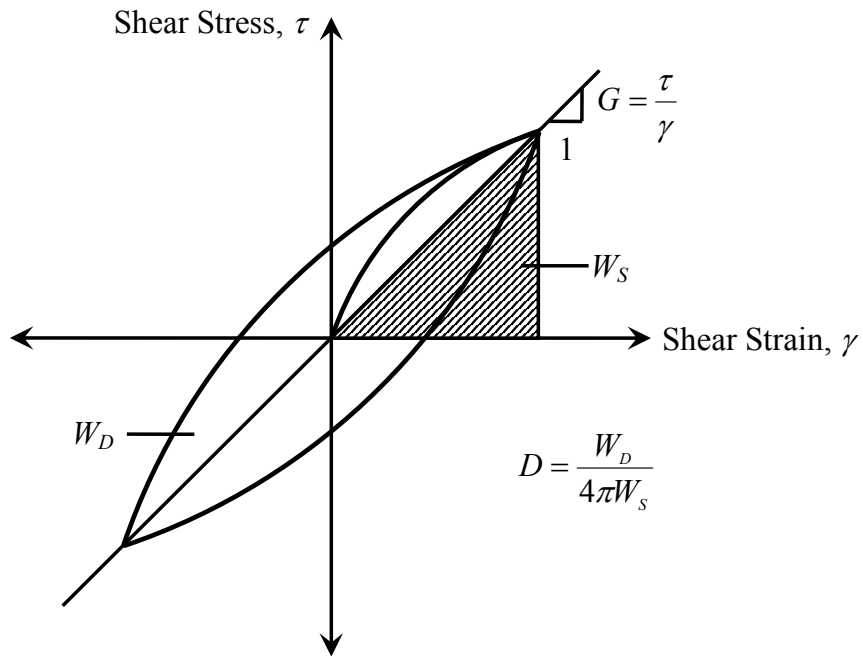
Figure 1.3 – Hysteresis loop for one cycle of loading.
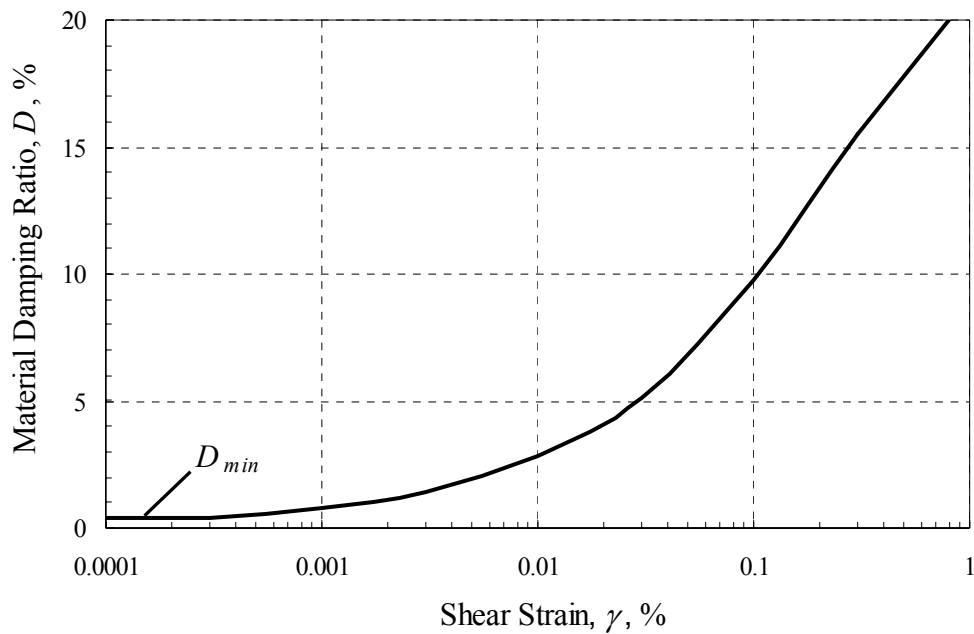
Figure 1.4 – Typical relationship between material damping ratio and shear strain.

4

1.3 REPORT OVERVIEW

Following this introduction, procedures for estimating V_S from penetration measurements are discussed in Chapter 2. Procedures for estimating the variation of G/G_{max} and material damping with shear strain are discussed in Chapter 3. In Chapter 4, an application of the recommended procedures using a case study from the new Cooper River Bridge in Charleston, South Carolina is presented. And, in Chapter 5, the recommended procedures are summarized and issues that remain to be resolved are identified.

Six appendixes are included to assist the reader, and to provide information used in the development of the guidelines. A list of references cited in the guidelines is presented in Appendix A. A list of Symbols and Notation is presented in Appendix B. The compiled field V_S and penetration data from South Carolina are summarized in Appendix C. Selected earlier penetration-V_S equations are summarized in Appendix D. Tables summarizing CPT-V_S and SPT-V_S regression equations derived for this study are presented in Appendix E. Finally, the compiled dynamic laboratory test data from South Carolina and surrounding states are summarized in Appendix F.

CHAPTER 2

ESTIMATING IN SITU SHEAR-WAVE VELOCITY FROM PENETRATION DATA

Empirical equations for estimating the small-strain shear-wave velocity, V_S, of South Carolina soils from the Cone Penetration Test (CPT) and Standard Penetration Test (SPT) are presented in this chapter. The equations are particularly useful for regional seismic ground response hazard mapping, where it is not economically feasible to measure V_S at all desired locations. They may be also useful for preliminary site-specific response analysis. However, V_S should be measured directly for final site-specific response analysis. The empirical equations are based on statistical analysis of existing field data from primarily South Carolina.

2.1 DATA FROM SOUTH CAROLINA

The existing SPT blow counts, CPT tip and sleeve resistances, and V_S measurements are compiled for this study from various published and unpublished sources. The general locations of V_S and penetration test sites are shown on the map in Figure 2.1 and summarized in Table 2.1. From the compiled data, 123 penetration and V_S data pairs from South Carolina soil deposits are obtained. A detailed listing of the 123 penetration-V_S data pairs is given in Appendix C.

The general criteria used for selecting the penetration-V_S data pairs are as follows: 1) Measurements are from below the groundwater table where reasonable estimates of effective stress can be made. 2) Measurements are from thick, uniform soil layers identified using CPT measurements. A distinct advantage of the CPT is that a nearly continuous profile of penetration resistance is obtained for detailed soil layer determination. By requiring V_S and penetration resistance data to be from only thick, uniform soil layers, scatter in the data due to soil variability is minimized. When no CPT measurements are available, exceptions to Criterion 2 are allowed if there are several V_S and SPT measurements within the layer that follow a consistent trend. 3) Penetration test locations are within 6 m of velocity test locations. 4) At least two V_S measurements, and the corresponding test intervals, are within the uniform layer. 5) Time history records used for V_S determination exhibit easy-to-pick shear-wave arrivals. Thus, values of V_S determined from difficult-to-pick wave arrivals are not used. When time history records are not available, exceptions to Criterion 5 are allowed if there are at least 3 V_S measurements within the selected layer above 20 m, or at least 5 V_S measurements below 20 m.
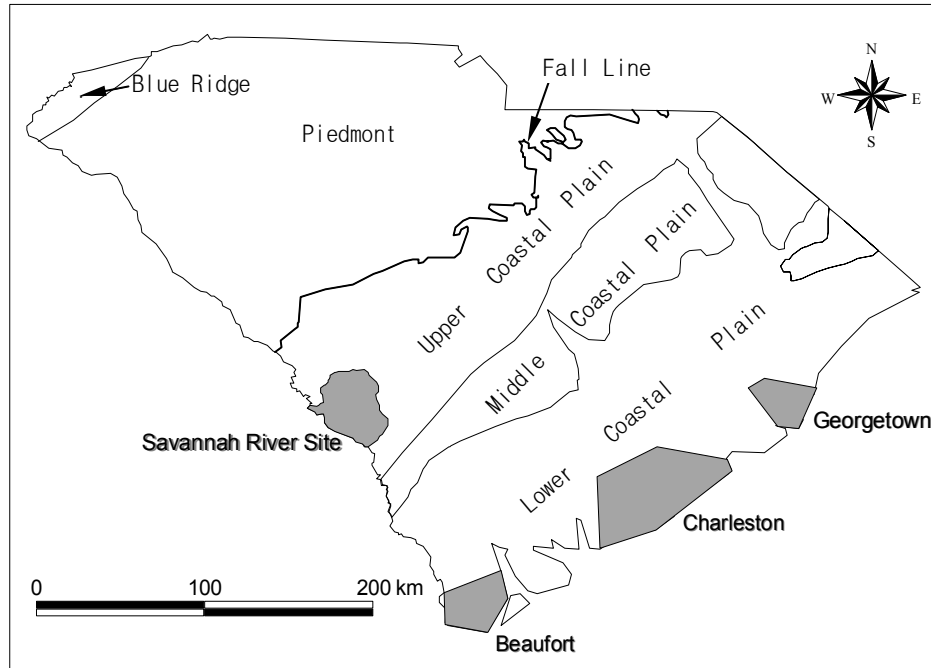
Figure 2.1 – Map of South Carolina showing general locations of V_S and penetration test sites for data compiled for this study

Table 2.1 – Sites and references of field data used to develop the penetration-velocity predictive equations.

Counties	Site	Reference
Charleston	Cooper River Bridge; Maybank Highway (SC Highway 700); Ashley Phosphate/I-26 Interchange	S&ME (1998-2000)
Charleston, Berkeley, Beaufort, and Jasper; Savannah, Ga.	SC Highway 170; various areas	WPC (1999-2002)
Charleston and Georgetown	Ten Mile Hill, Gapway, Sampit	Talwani *et al.* (2002); Hu *et al.* (2002)
Aiken and Barnwell	Savannah River Site	WSRC (2000)

2.1.1 General Characteristics of the Compiled Data

Distributions of the compiled data pairs with respect to average measurement depth, depth to water table, soil type, and inferred geologic age are presented in Figure 2.2. Of the 123 data pairs, about 98 % correspond to average measurement depths less than 28 m (Figure 2.2a). These depths correspond to calculated average values of σ'_v ranging from 36 kPa to 343 kPa, with only 6 average values from the Savannah River Site exceeding 300 kPa. The thickness of the selected layer vary from 2 m to 18 m, with 70 % less than 7 m. Nearly all the data pairs are from sites where the water table is between the ground surface and a depth of 14 m (Figure 2.2b). The Unified Soil Classification System (USCS) soil type is known for 26 % of the data pairs, and ranges from clean sand to organic clay (Figure 2.2c). Concerning the inferred geologic age of the deposits, 17 % are Holocene in age (< 10,000 years), 42 % are Pleistocene in age (10,000 to 1.8 million years), 36 % are Tertiary in age (1.8 to 65 million years), and 5 % are of unknown age (Figure 2.2d).

The geologic ages of the selected soil layers are inferred from information provided in reports, maps produced by the South Carolina Geological Survey and U.S. Geological Survey, and communications with the investigator(s). The majority of the Holocene data are from the Charleston area. The Pleistocene and Tertiary data are from the lower and upper coastal plain areas in South Carolina. For the Pleistocene data, the distinguishable formations are the Wando and Ten Mile Hill. For the Tertiary data, the distinguishable formations are the Ashley (locally known as the Cooper Marl) in Charleston, and the Tobacco Road and Dry Branch at the Savannah River site. The influence that geologic age and formation have on the SPT-V_S and CPT-V_S equations will be discussed later in this chapter.

2.1.2 Standard Penetration Test Blow Count

As specified in ASTM D-1586-84, the SPT involves driving a 51-mm (2.0-inch) outside diameter, split-barrel sampler 0.46 m (18 inches) into the ground using a 0.624-kN (140-lb) hammer dropped from a height of 0.76 m (30 inches). The number of blows to penetration the last 0.3 m (12 inches) is called the blow count or N-value. One distinct advantage of the SPT is that it provides a sample.

Because there are many variations of SPT equipment and procedures, it is recommended that the measured blow count (N_m) be corrected to reference test conditions by the following equation (Youd *et al.*, 2001):

$$N_{60} = N_m C_E C_B C_R C_S \tag{2.1}$$

(a) Average Measurement Depth

0m - <7m
7m - <14m
14m - <21m
21m - <28m
28m - 35m

j = 123

(b) Depth to Water Table

0m - <2m
2m - <4m
4m - <6m
6m - <14m
14m - 22m

j = 123

(c) Soil Type

CL, CH, OH
ML, MH
SM, SC
SP, SW, SP-SM, SP-SC
Unknown

j = 123

(d) Geologic Age

Holocene
Pleistocene
Tertiary
Unknown

j = 123
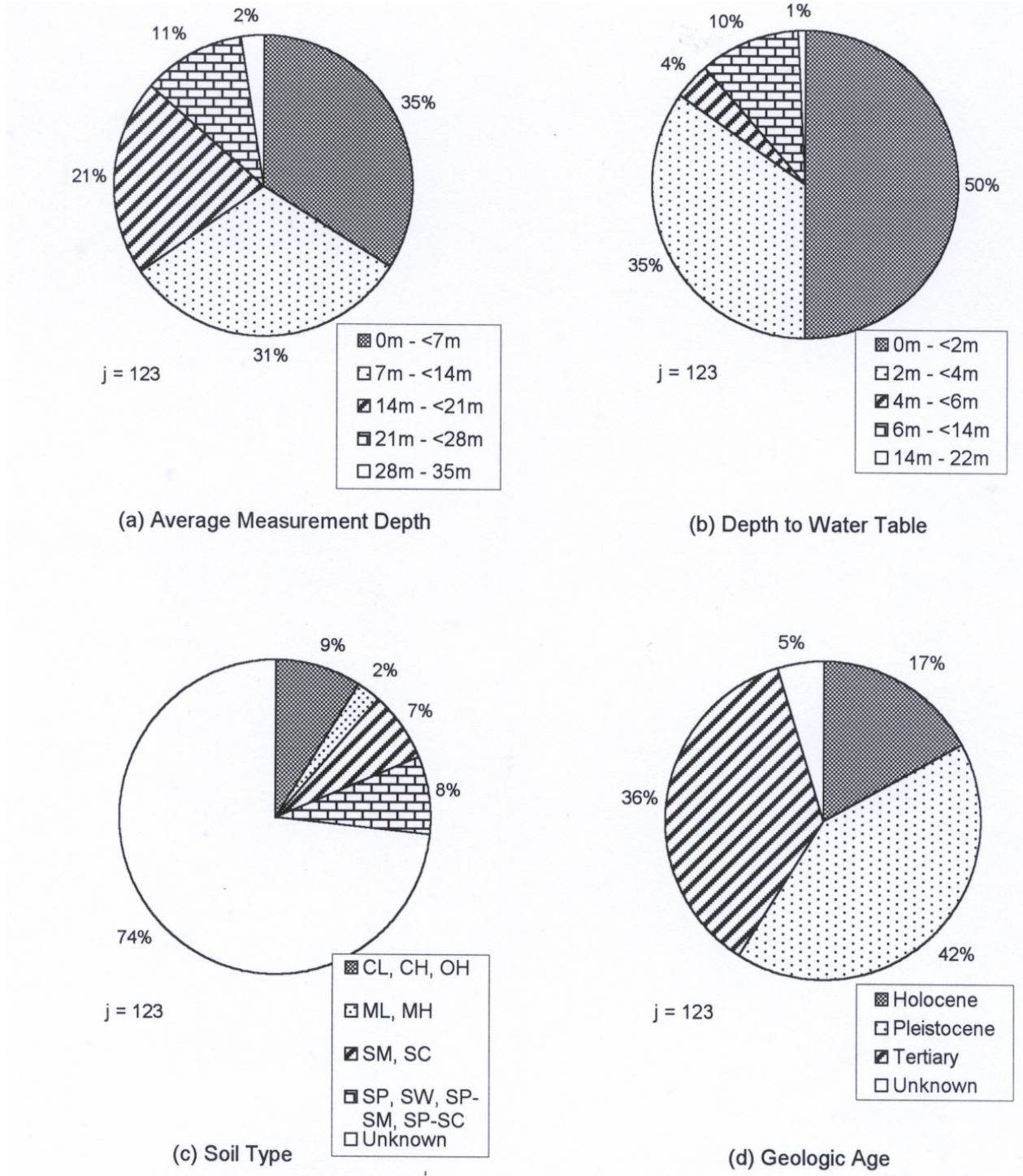
Figure 2.2 – Characteristics of the compiled penetration-V_S data from South Carolina.

where N_{60} is the equipment-corrected blow count, C_E is the correction for hammer energy ratio (*ER*), C_B is the correction factor for borehole diameter, C_R is the correction for rod length, and C_S is the correction for samplers with or without liners. Approximate values for C_E, C_B, C_R, and C_S are listed in Table 2.2. An *ER* of 60 % is commonly assumed as the average for U.S. testing practice and a reference value for the energy correction ($C_E = ER/60$). Youd *et al.* (2001) recommend that hammer energy measurements be made at each site where the SPT is used. Where energy measurements cannot be made, the values listed in Table 2.2 may be used to approximate C_E.

For this study, the corrections factors listed in Table 2.2 are generally used to correct the compiled N_m values. Energy measurements reported for several SPT drill rigs employed during the new Cooper River Bridge field investigations are used directly to correct those data. Where no energy measurements were reported, the average values listed in Table 2.2 are assumed based on the type of hammer used. Detailed borehole diameter, rod length, and sampling method information are typically not included in the project reports. Therefore, additional information was requested from the engineer in charge. Based on the additional information provided by the engineer, reasonable assumptions are made. Estimates of borehole diameters ranged from 100 mm to 150 mm. Rod lengths are assumed equal to the measurement depth plus 1 m. The value of C_S is assumed 1.0 for all measurements (i.e., all samplers are assumed to have a constant inside diameter of 34.9 mm).

Table 2.2 – Corrections to SPT (modified from Skempton, 1986) as listed by Robertson and Wride (1998).

Factor	Term	Equipment Variable	Correction
Energy ratio	C_E	Donut hammer	0.5-1.0
		Safety hammer	0.7-1.2
		Automatic-trip donut type hammer	0.8-1.3
Borehole diameter	C_B	65-115 mm	1.0
		150 mm	1.05
		200 mm	1.15
Rod length	C_R	<3 m	0.75
		3-4 m	0.8
		4-6 m	0.85
		6-10 m	0.95
		10-30 m	1.0
Sampling method	C_S	Standard sampler	1.0
		Sampler without liners	1.1-1.3

For some applications, SPT blow counts are further corrected to a reference overburden stress using the following equation:

$$(N_1)_{60} = N_{60}C_N \tag{2.2}$$

where the correction factor C_N is commonly calculated by the following equation (Liao and Whitman, 1986):

$$C_N = \left(\frac{P_a}{\sigma'_v}\right)^{0.5} \tag{2.3}$$

where σ'_v is the effective vertical or overburden stress, and P_a is a reference stress of 100 kPa (or 1 atm). Equation 2.3 is an approximation to the original correction curve proposed by Seed and Idriss (1982), and is limited to a maximum value of 1.7. Youd *et al.* (2001) endorse the use of Equation 2.3 for overburden pressures up to 300 kPa. For pressures greater than 300 kPa, they recommend that Equation 2.3 not be applied.

2.1.3 Cone Penetration Test Tip and Sleeve Resistances

As specified in ASTM D-3441-94, the CPT consists of measuring the load on the tip of a cone with an apex angle of 60° and the skin friction over a short length of rod above the tip during penetration through soil deposits. Tip and sleeve resistances are typically recorded every 1 cm, providing a nearly continuous profile of subsurface stratigraphy. In addition, other measurements such as pore pressure and V_S can be made at the same time (Lunne *et al.*, 1997).

Because samples are usually not collected during cone testing, CPT data are grouped in this study using a simplified version of the soil behavior type chart developed by Robertson (1990) shown in Figure 2.3. The value on the vertical axis represents a dimensionless cone tip resistance (Q) defined by (Robertson and Wride, 1998):

$$Q = \left(\frac{q_c - \sigma_v}{P_a}\right)\left(\frac{P_a}{\sigma'_v}\right)^n \tag{2.4}$$

12
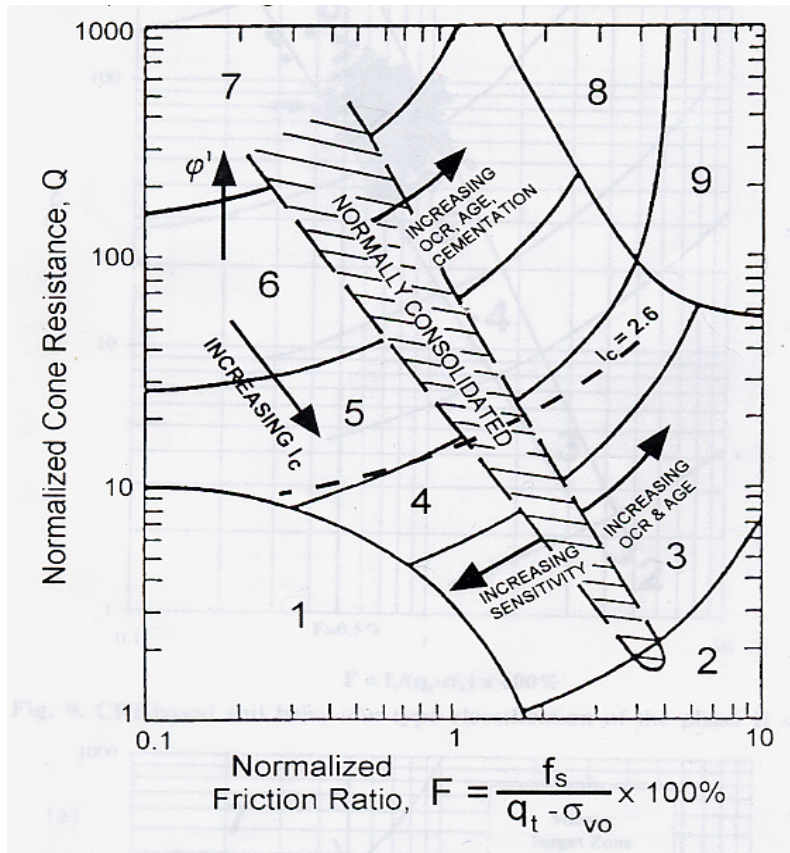
Figure 2.3 – Normalized CPT soil behavior type chart by Robertson (1990).

Table 2.3 – Boundaries of soil behavior type and zones (after Robertson, 1990).

Zone	Soil Behavior Type	Soil Behavior Type Index I_c
1	Sensitive, fine grained	-----
2	Organic soils--peats	$I_c > 3.60$
3	Clays--silty clay to clay	$2.95 < I_c < 3.60$
4	Silt mixtures--clayey silt to silty clay	$2.60 < I_c < 2.95$
5	Sand mixtures--silty sand to sandy silt	$2.05 < I_c < 2.60$
6	Sands--clean sand to silty sand	$1.31 < I_c < 2.05$
7	Gravelly sand to sand	$I_c < 1.31$
8	Very stiff sand to clayey sand*	-----
9	Very stiff, fine grained*	-----

*Heavily overconsolidated or cemented

where q_c is the measured cone tip resistance, σ_v is the total overburden stress in the same units as q_c and P_a, and n is an exponent ranging from 0.5 to 1.0. The value on the horizontal axis represents normalized friction ratio (F) defined by (Wroth, 1988):

$$F = \left(\frac{f_s}{q_c - \sigma_v} \right) 100\% \tag{2.5}$$

where f_s is the measured cone sleeve friction in the same units as q_c.

The boundaries separating soil behavior type zones 2 to 7 shown in Figure 2.3 can be approximated as concentric circles, with the radius of each circle, term the soil behavior type index (I_c) defined by:

$$I_c = \left[(3.47 - \log Q)^2 + (1.22 + \log F)^2 \right]^{0.5} \tag{2.6}$$

General soil behavior type descriptions and corresponding I_c values for each zone are given in Table 2.3. To select the suitable value of n for Equation 2.4, the iterative procedure by Robertson and Wride (1998) is followed. The first step is to calculate I_c assuming $n = 1.0$. If the I_c calculated with $n = 1.0$ is greater than 2.6, then 1.0 is selected for n. If the calculated I_c is less than 2.6, it is recalculated using $n = 0.5$. If the recalculated I_c is less than 2.6, then 0.5 is selected for n and the recalculated I_c is used to group the data. However, if the recalculated I_c is greater than 2.6, I_c is again recalculated using $n = 0.7$ for the final value to be used in grouping the data.

A simplified version of the soil behavior type chart by Robertson (1990) is shown in Figure 2.4. The vertical axis of this simplified chart is based on normalized cone tip resistance expressed by (Robertson and Wride, 1998):

$$q_{c1N} = \left(\frac{q_c}{P_a} \right) C_Q = \left(\frac{q_c}{P_a} \right) \left(\frac{P_a}{\sigma'_v} \right)^n \tag{2.7}$$

where q_{c1N} is the normalized cone tip resistance. Similar to the SPT, a maximum value of C_Q of 1.7 is applied at shallow depths. The parameter I_c defining the radius of the circles plotted in Figure 2.4 is calculated using Equation 2.6. Also plotted in Figure 2.4 are the compiled data grouped by soil type, as determined by USCS. The chart accurately predicts the soil type for the plotted data, with 6 exceptions.
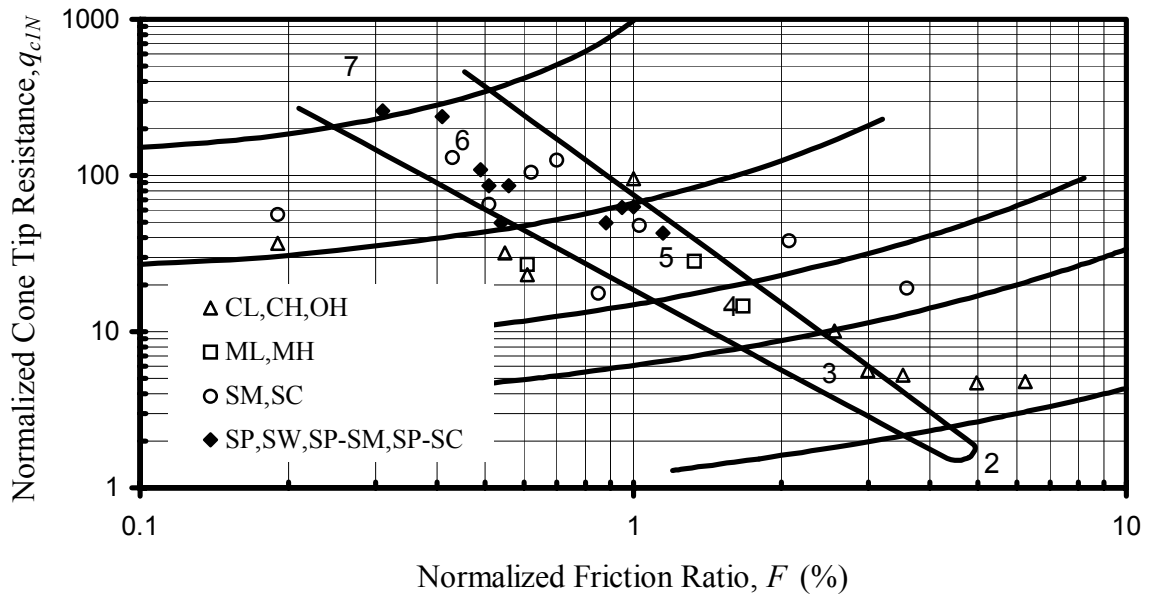
Figure 2.4 – Simplified CPT soil behavior type chart (modified from Robertson, 1990) with data compiled for this study grouped by USCS soil type.
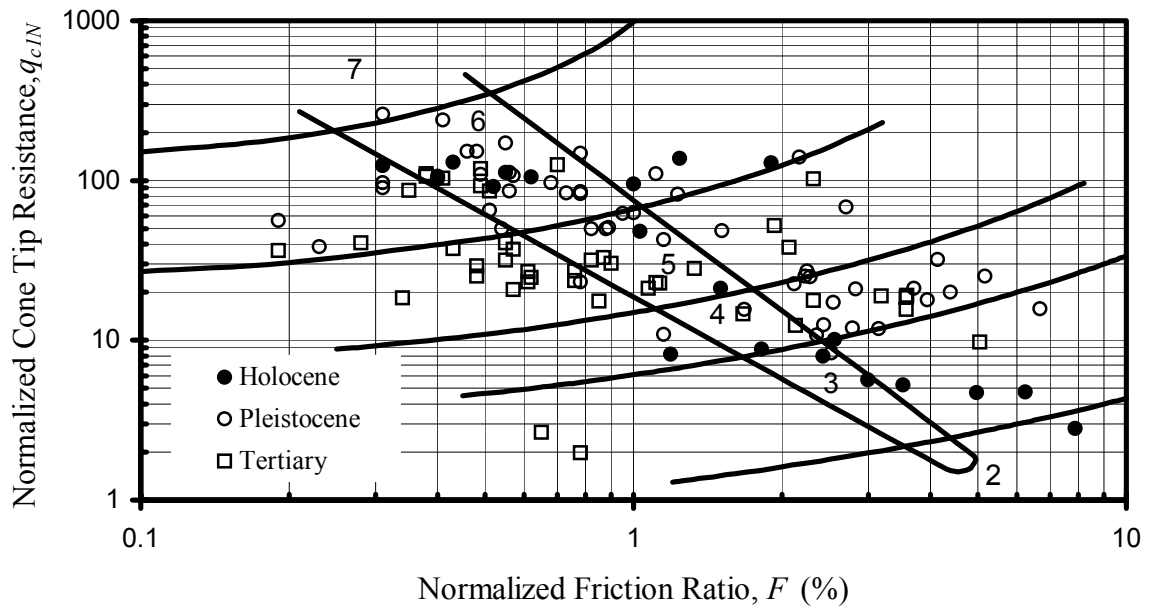
Figure 2.5 – Simplified CPT soil behavior type chart (modified from Robertson, 1990) with data compiled for this study grouped by geologic age.

Dividing the zones 2 to 7 in the soil behavior type charts shown in Figures 2.3 and 2.4 is a normally consolidated region that trends diagonally downward from left to right. According to Robertson (1990), data plotting above the normally consolidated region tend to indicate soils that are over-consolidated and older. Below the normally consolidated region, soils generally tend to exhibit higher sensitivity. Plotted in the chart shown in Figure 2.5 are the compiled data grouped by inferred geologic age. It can be seen that many of the data from Holocene deposits plot within the normally consolidated region. However, there are several Holocene data points above the normally consolidated region. Also contrary to expected behavior, the data from Pleistocene and Tertiary deposits plot in all areas of the chart.

2.1.4 Shear-Wave Velocity

The field V_S can be measured by several seismic test methods including seismic crosshole, seismic downhole, seismic cone penetrometer (SCPT), suspension logger, and Spectral-Analysis-of-Surface-Waves (SASW). General reviews of these methods are given in Woods (1994) and Ishihara (1996). All of the V_S measurements in the 123 penetration-V_S data pairs compiled for this study were determined by the SCPT method and calculated by the psuedo-interval method (Pantel, 1981; Campanella and Stewart, 1992).

Following the traditional procedures for correcting penetration resistance to a reference overburden stress, V_S is often corrected using the following equation (Sykora, 1987; Robertson *et al.*, 1992):

$$V_{S1} = V_S C_{vs} = V_S \left(\frac{P_a}{\sigma'_v} \right)^{0.25} \tag{2.8}$$

where V_{S1} is the stress-corrected shear-wave velocity, and σ'_v and P_a are in the same units. Similar to the equations for correcting penetration resistance, Equation 2.8 implicitly assumes a constant coefficient of earth pressure at rest, K'_0. Also implicitly assumed is that V_S is measured with both the directions of particle motion and wave propagation polarized along principal stress directions and that one of those directions is vertical (Stokoe *et al.*, 1985). Similar to the SPT and CPT, a maximum value of C_{vs} of 1.4 is applied at shallow depths (Andrus and Stokoe 2000).

2.2 CPT-VELOCITY EQUATIONS

The CPT-V_S equations are considered first because more CPT-V_S data pairs are available than SPT-V_S data pairs. All of the 123 penetration-V_S data pairs from South Carolina include CPT measurements. The compiled data with known geologic age are plotted in Figure 2.6. The plotted data are grouped by the providing organization and geologic age. The providing organizations include: S&ME, Inc. (S&ME), University of South Carolina (USC), WrightPadgettChristopher (WPC), and Westinghouse Savannah River Company (WSRC). It can be seen in the figure that V_S generally increases with age for a given cone tip resistance. Because the data from Holocene-age soils are limited, the recommended equations are based, in part, on the compiled data and, in part, on earlier CPT-V_S studies.

2.2.1 Earlier Equations for Holocene-Age Soils

The relationship between CPT resistances and V_S has been studied since about 1983, as reviewed in Piratheepan and Andrus (2002). A listing of selected earlier equations for Holocene-age sands, clays, and all soils is given in Appendix D. For comparison, several of these equations are plotted in Figures 2.7 and 2.8. Also plotted are data from South Carolina, along with data from California and Japan compiled by Piratheepan and Andrus (2002).

Figure 2.6 – Comparison of q_c versus V_s measurements from South Carolina grouped by providing organization and inferred geologic age.

17

Figure 2.7 - Comparison of earlier CPT-V_{S1} equations for Holocene sandy soils along with data from Holocene soils with $I_c < 2.05$.

Figure 2.8 - Comparison of earlier CPT-V_S equations for Holocene clayey soils along with data from Holocene soils with $I_c > 2.6$.

18

In Figure 2.7, earlier equations based on normalized cone tip resistance, as well as data for Holocene-age sands, are plotted. There is good agreement between the data from California and Japan compiled by Piratheepan and Andrus (2002) and equations proposed by Robertson *et al.* (1992), Hegazy and Mayne (1995), Andrus *et al.* (1999), and Piratheepan and Andrus (2002). On the other hand, the relationships by Rix and Stokoe (1991) and Fear and Robertson (1995) plot significantly above most of the data and other proposed relationships. The relationship by Baldi *et al.* (1986) plots between these two groups. Also, 6 of the 7 data points for South Carolina plot on high side of the data compiled by Piratheepan and Andrus (2002). It is likely that aging processes increased the velocities associated with the South Carolina data, because they are from natural soil deposits where the geologic age could be early Holocene.

In Figure 2.8, earlier equations based on uncorrect cone tip resistances, as well as data for Holocene-age clays, are plotted. The equation by Hegazy and Mayne (1995) indicates that f_s is somewhat of a significant parameter. However, based on the regression analysis by Piratheepan and Andrus (2002) and this study, I_c appears to be a more significant parameter than f_s. Thus, the equation by Piratheepan and Andrus (2002) based on q_c, f_s, and I_c is plotted. As noted in Figure 2.8, when I_c is introduced into the regression equation the exponent on f_s becomes very small (-0.004), indicating that most of the variability can be explained by q_c and I_c. The relationship by Hegazy and Mayne (1995) for clays appears to be most appropriate for soils with I_c of about 3.3, which corresponds to silty clay to clay soil behavior according to Robertson's (1990) chart. The plotted data from South Carolina and California are in good agreement with the plotted equations.

Based on this review, the significant variables affecting CPT-V_S relationships are: cone tip resistance, confining stress (or depth), soil type (or I_c), and geologic age. Considering these variables and combining the data from South Carolina with data from California, Canada and Japan, several new regressions are derived (Ellis, 2003). These new regression equations are listed in Appendix E.

2.2.2 Recommended Equations for South Carolina Soils

Listed in Table 2.4 are the recommended CPT-V_S equations for use in ground response studies in South Carolina. These equations are based on regression analysis of Holocene data from South Carolina, California, Canada, and Japan. They are recommended because they include all the significant variables identified in the previous section. Also, they provide some of the highest values of coefficient of multiple determination and lowest values of residual standard deviation of the equations listed in Appendix E. Equations that predict uncorrected V_S are preferred because it is V_S, and not V_{S1}, that is needed for ground response analysis.

Table 2.4 – Recommended CPT-V_S equations for use in ground response studies in South Carolina.

Soil Behavior Type, I_c	Equation for Predicting V_S [a], m/s	Equation
All values	$V_S = 4.63 q_c^{0.342} I_c^{0.688} Z^{0.092} ASF$	2.9 [b]
< 2.05	$V_S = 8.27 q_c^{0.285} I_c^{0.406} Z^{0.122} ASF$	2.10 [c]
> 2.60	$V_S = 0.208 q_c^{0.654} I_c^{1.910} Z^{-0.108} ASF$	2.11 [c]

[a] q_c in kPa, and Z is depth in meters.
[b] Equation 2.9 is the simplest equation recommended for estimating V_S for all soil types.
[c] Somewhat better predictions of V_S may be obtained using Equations 2.10 and 2.11 for soils with $I_c < 2.05$ and $I_c > 2.60$, respectively. For $2.05 < I_c < 2.60$, use Equation 2.9.

Table 2.5 – Age scaling factors and statistical characteristics for the recommended CPT-V_S equations

Location and Geologic Age of Deposit	Soil Behavior Type, I_c	Age Scaling Factor, ASF	R^2	Residual Standard Deviation, s, m/s	No. of Samples, j	Range of V_S, m/s
South Carolina Coastal Plain – Holocene	All values	1.00	0.731[a]	25	81	60-260
	< 2.05	1.00	0.684[a]	17	33	110-260
	> 2.60	1.00	0.899[a]	15	31	60-230
South Carolina Coastal Plain – Pleistocene	All values	1.23	----[b]	37	52	130-300
	< 2.05	1.34	----[b]	46	22	160-300
	> 2.60	1.16	----[b]	40	17	130-250
South Carolina Coastal Plain –Tertiary-age Ashley Formation (or "Cooper Marl")	All values	2.29	----[a]	64	30	230-540
South Carolina Coastal Plain – Tertiary-age Tobacco Road Formation	All values	1.65	----[b]	48	4	310-350
	> 2.60	1.42	----[b]	31	3	330-350
South Carolina Coastal Plain – Tertiary-age Dry Branch Formation	All values	1.38	----[b]	32	10	310-360
	< 2.05	1.33	----[b]	20	8	310-360

[a] Data from California, Canada and Japan.
[b] R^2 not calculated.

Age scaling factors and statistical characteristics for the recommended equations are given in Table 2.5. The age scaling factor (ASF) is an adjustment to the "reference" model (equations for Holocene soils) for use in the older aged soils. It is defined as the measured V_S divided by the predicted V_S using the equation for Holocene-age soils. The residual standard deviation (s) is defined as the square root of [$\sum$(measured V_S – predicted $V_S)^2$]/(j-2), where j is the number of samples. It reflects how much the data fluctuate from the developed equation. Example calculations of ASF and s are given in Table E.11 of Appendix E. The coefficient of multiple determination (R^2) is the ratio of the deviation due to regression to the total variation in the dependent variable, which is velocity. The closer R^2 is to 1, the more the regression equation is said to explain the total variation. Predictions of V_S outside the ranges indicated in Table 2.5 should be used with greater care.

A plot of measured and predicted V_S for the Holocene data using Equation 2.9 with ASF = 1.0 is shown in Figure 2.9. It can be seen in the figure that the V_S measurements compiled for this study and V_S measurements compiled by Piratheepan and Andrus (2002) are equally well predicted by Equation 2.9. The value of s associated with the plotted data and Equation 2.9 is 25 m/s. Considering that soil variability also contributes to scatter in the data, this s value is not unreasonable for ground response analysis. Even good V_S measurements generally have errors of 5 %. Somewhat better predictions of V_S can be achieved using Equations 2.10 and 2.11 for soils with $I_c < 2.05$ and $I_c > 2.6$, respectively.

Presented in Figure 2.10 is a direct comparison the Holocene CPT-V_S data pairs and Equation 2.9, using the average depth of the measurements of 7 m. Despite the fact that two of the variables are fixed in the plotted curves (i.e., $Z = 7$ m and $q_c =$ values between 1.4 and 3.9), the plotted data compare will with the curves.

Shown in Figure 2.11 is a plot of measured and predicted V_S for the Pleistocene data using Equation 2.9 with $ASF = 1.23$. The ASF value of 1.23 suggests that V_S is, on average, 23 % higher in Pleistocene soils of the South Carolina Coastal Plain than in Holocene soils with similar cone resistances. A comparison of the Pleistocene CPT-V_S data pairs and Equation 2.9 using the average depth for the measurements of 7 m is presented in Figure 2.12. The value of s associated with the plotted data and Equation 2.9 is 37 m/s. An s value of 37 m/s is about 1.5 times as large as the value determined for the Holocene data, indicating greater fluctuation about the equation. When Equations 2.10 and 2.11 are considered, the values of ASF and s are similar to values associated with Equation 2.9.
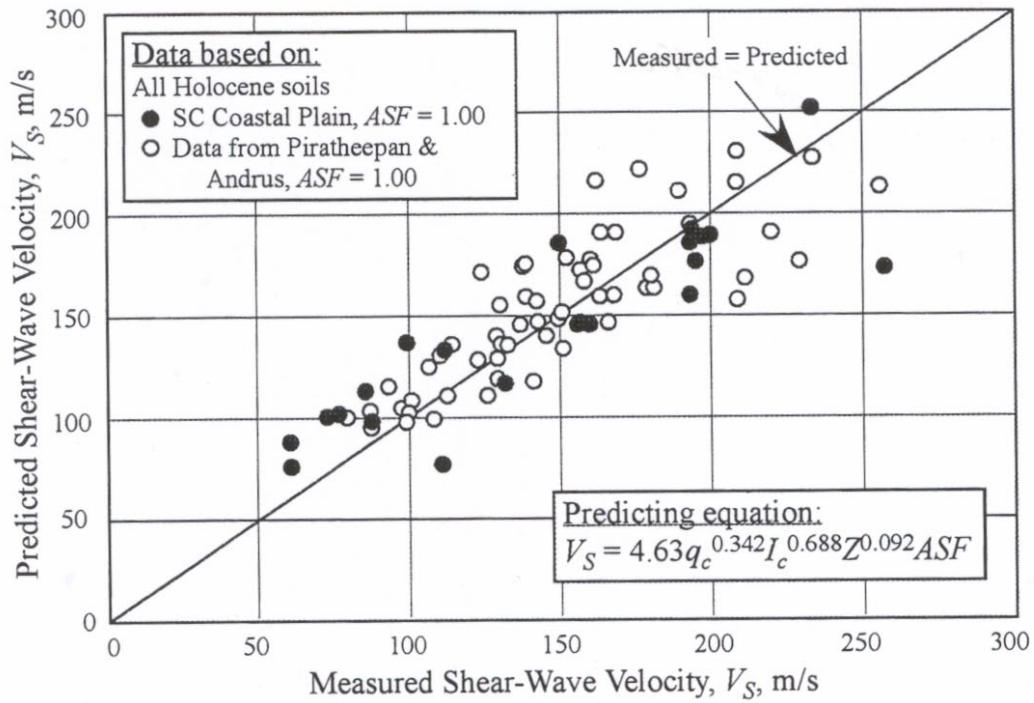
Figure 2.9 – Comparison of measured and predicted V_S as a function of q_c, I_c, and depth for Holocene data primarily from South Carolina and California.
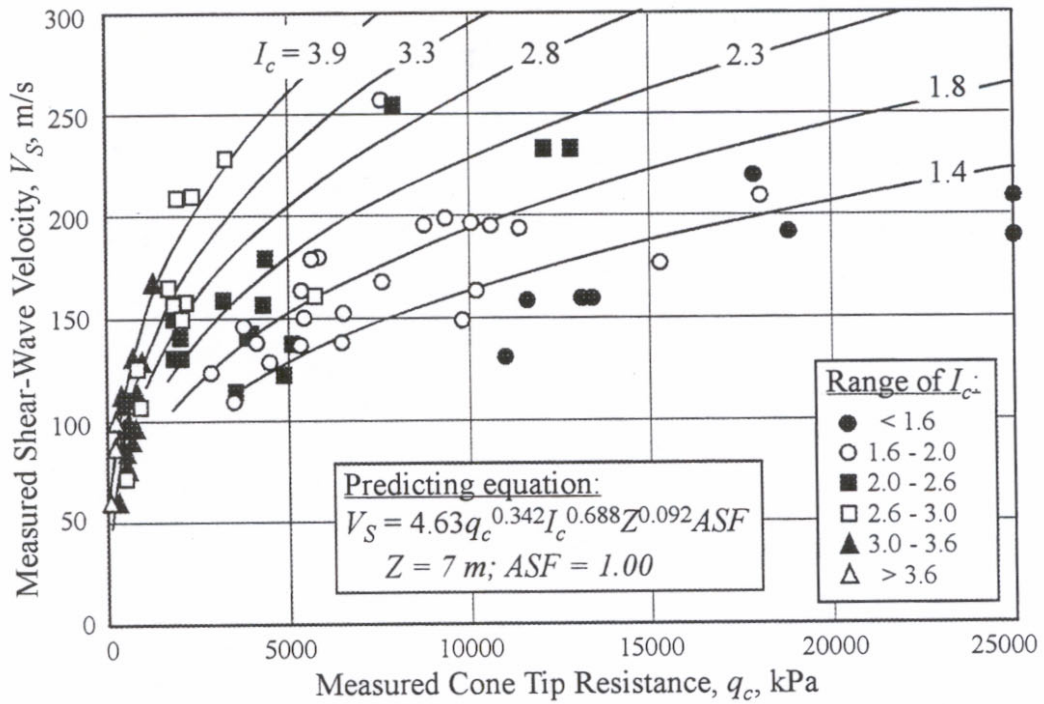
Figure 2.10 – Comparison of the recommended CPT-V_S relationship for Holocene soils and data primarily from South Carolina and California.
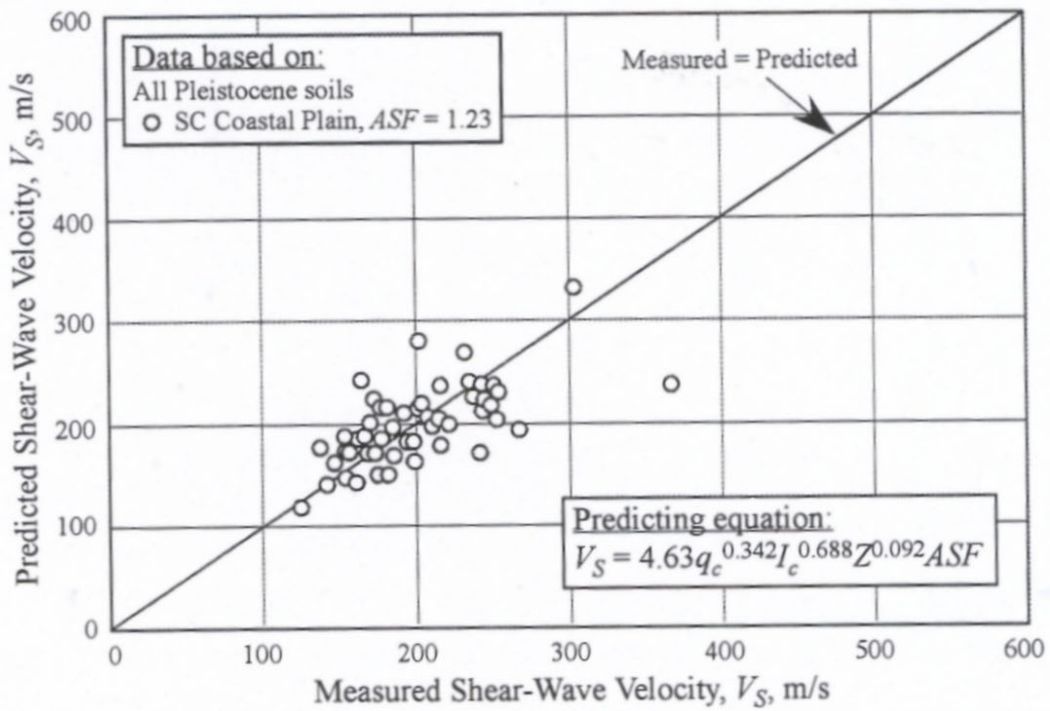
Figure 2.11 – Comparison of measured and predicted V_S as a function of q_c, I_c, and depth for Pleistocene data from South Carolina.
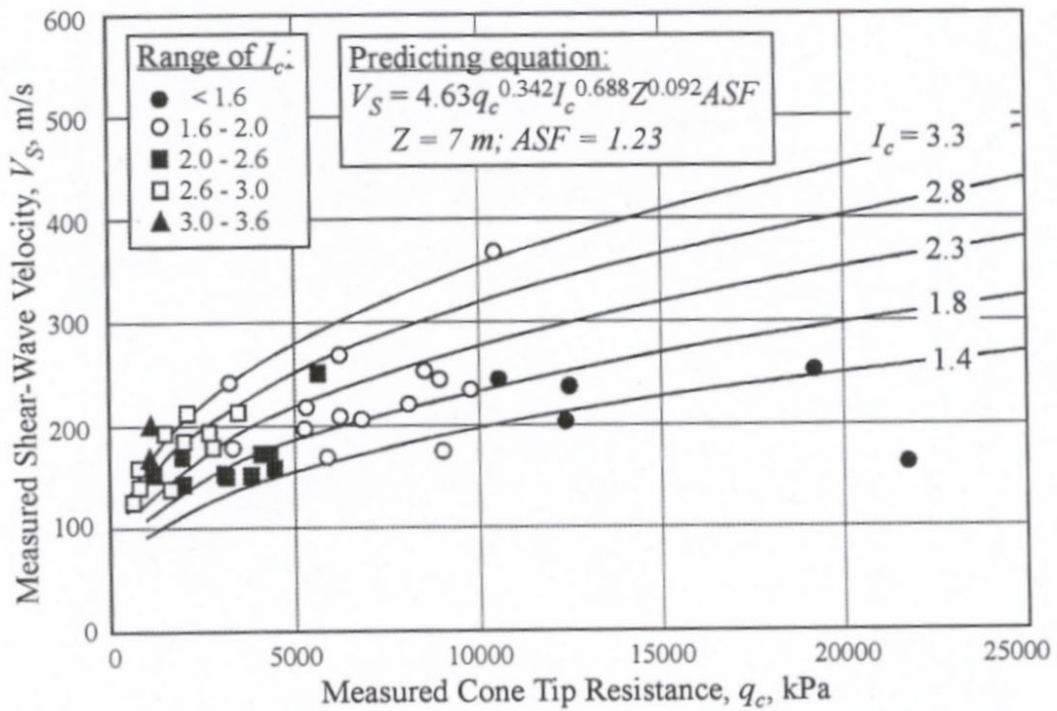
Figure 2.12 – Comparison of the recommended CPT-V_S relationship for Pleistocene soils and data from South Carolina.

A plot of measured and predicted V_S for the Tertiary data using Equation 2.9 is shown in Figure 2.13. The calculated *ASF* values for the Ashley, Tobacco Road, and Dry Branch Formations are on the order of 2.29, 1.65 and 1.38, respectively. These values are significantly higher than *ASF* values calculated for the Pleistocene soils. They suggest that, on average, V_S is 38 % to 129 % higher in Tertiary soils than in Holocene soils with similar cone resistances. Equation 2.9 is plotted in Figure 2.14 using average values of depth, ASF and I_c for the Ashley and Dry Branch Formations. Also plotted in Figure 2.14 are the Tertiary data grouped by geologic age and I_c. The fluctuation of the plotted data about Equation 2.9 is characterized with *s* values of 64, 48 and 32 for the Ashley, Tobacco Road and Dry Branch Formations, respectively.

It is interesting to note that all three Tertiary formations are similar in age. The Ashley Formation dates at about 30 million years before present (Weems and Lemon, 1993; Raymond A. Christopher, personal communication, November 2002), and is a deep marine deposit with an overconsolidation ratio (*OCR*) of about 3 to 7 and a calcium carbonate content of 60 to 70 %. The Tobacco Road and Dry Branch Formations date at about 25 to 29.5 million years and 34 to 36 million years, respectively (Raymond A. Christopher, personal communication, November 2002). According to the description given in WSRC (2000), the Tobacco Road Formation is a shallow marine deposit with OCR of 1 to 3 and contains some calcium carbonate. The Dry Branch Formation is a near shore and bay deposit. It is characterized as having an *OCR* of 1 to 3 and consisting of primarily quartz sand. The higher *OCR* associated with the Ashley Formation only partially explains the higher *ASF*, because the Tobacco Road and Dry Branch Formations have similar *OCR* values but different *ASF* values. On the other hand, the concentration of carbonate might explain the difference in calculated values of *ASF*. The Ashley Formation, having the highest amount, has the largest *ASF* value; and the Dry Branch Formation, having the lowest amount, has the smallest *ASF* value. Calcium carbonate is relatively easy to dissolve and re-crystallize. Its presence often suggests at least some weak cementing of soil particles. Based on these observations, it is likely that *ASF* is also dependent on the concentration of natural cementing agents, such as calcium carbonate, in addition to age.

2.3 SPT-VELOCITY EQUATIONS

Twenty-six SPT-V_S data pairs from South Carolina are available for this study. The reason for this small number is because SPTs are usually not performed close to CPTs. Of the 26 data pairs, 1 is for Holocene sands, 6 are for Holocene clays, 9 are for Pleistocene soils, and 10 are for Tertiary soils. The compiled data are plotted in Figure 2.15. The data are grouped by the providing organization and inferred geologic age. Similar to the CPT-V_S data, it can be seen that V_S generally increases with age for a given SPT blow count. Given the limited amount of data, the recommend equations are based primarily on earlier SPT-V_S studies.
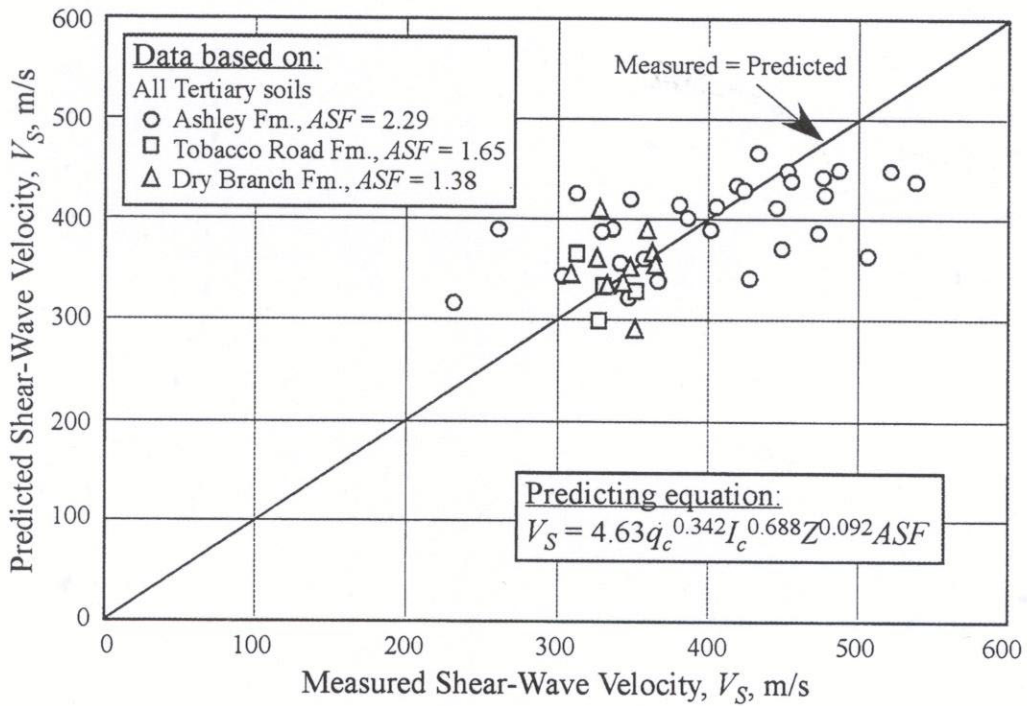
Figure 2.13 – Comparison of measured and predicted V_S as a function of q_c, I_c, and depth for Tertiary data from South Carolina.
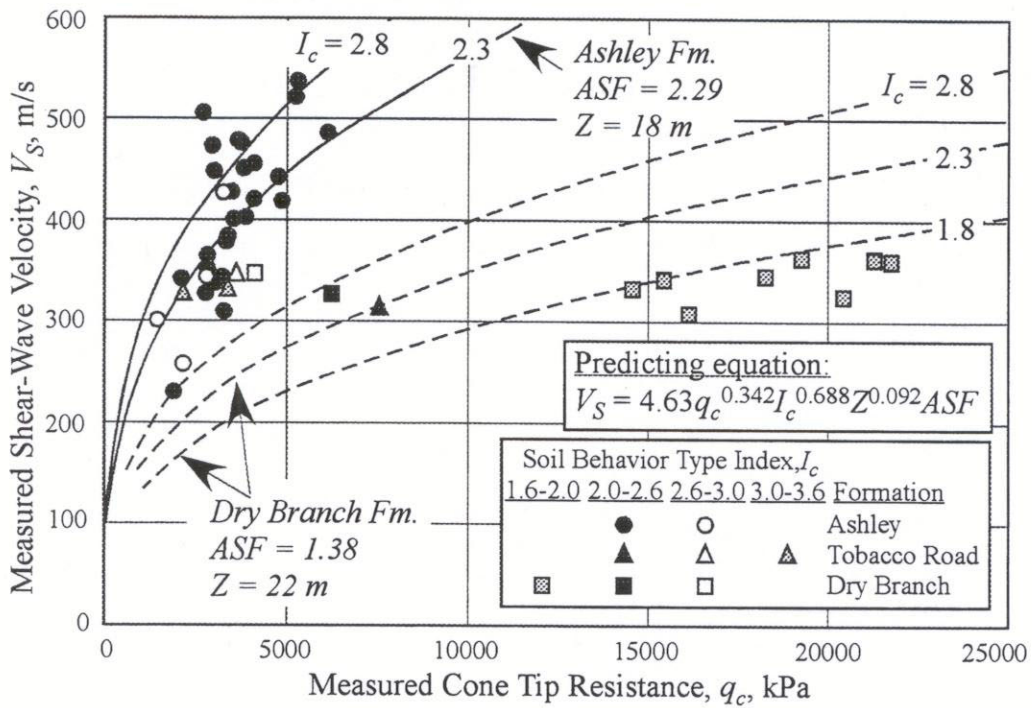
Figure 2.14 – Comparison of the recommended CPT-V_S relationship for Tertiary soils and data from South Carolina.

25

2.3.1 Earlier Equations for Holocene-Age Soils

Several investigators have studied SPT-V_S relationships, since about 1966. Most of the relationships are for sandy soils. Relationships for clays are not common, likely because the blow count in soft clay is close to zero. General reviews of the earlier relationships are given in Sykora (1987) and Piratheepan and Andrus (2002). A listing of selected equations for Holocene sands that consider both corrected blow count and confining stress (or depth) is given in Appendix D. For comparison, several of the equations are plotted in Figures 2.16 and 2.17. Also plotted are data from South Carolina, California, Canada, and Japan.

In Figure 2.16, earlier equations for Holocene sands based on energy-corrected SPT blow count and depth are plotted, using a depth value of 10 m. As can be seen in the figure, there is fairly good agreement between equations despite the fact that the equation by Ohta and Goto (1978) is based on field data from Japan and the equation by Piratheepan and Andrus (2002) is based on field data from primarily California. The effect of grain size is unclear, however. The Ohta and Goto (1978) curves suggest that V_S increases with increasing grain size for a given blow count, although the fine sand and medium sand curves are not consistent with this trend. On the other hand, the Piratheepan and Andrus (2002) curves suggest that V_S increases with increasing fines content for a given blow count.
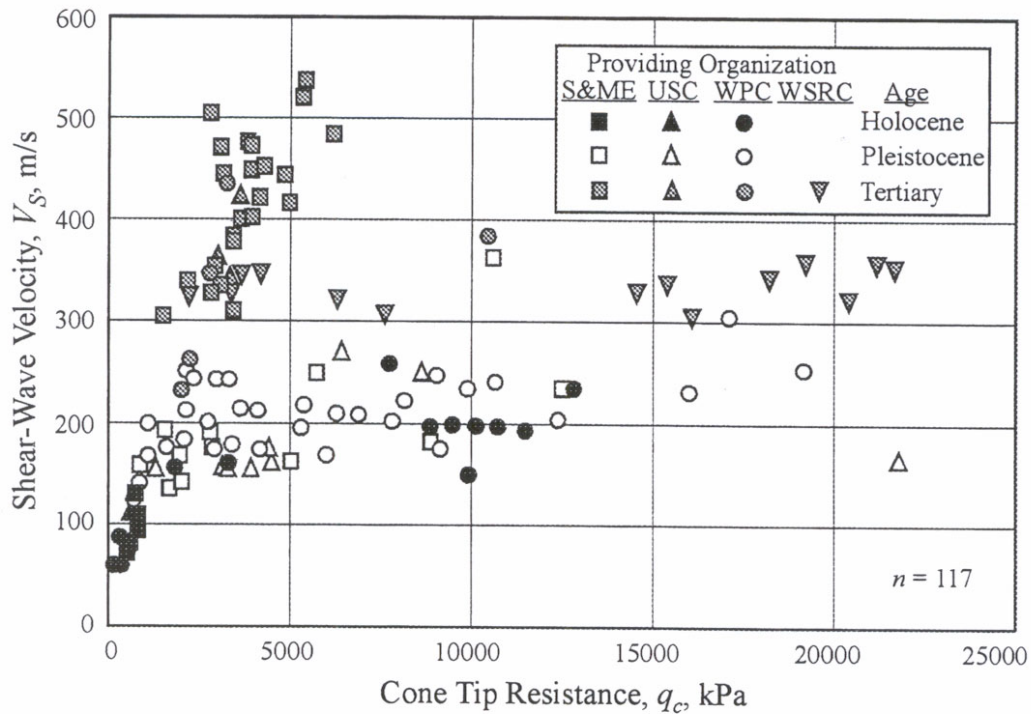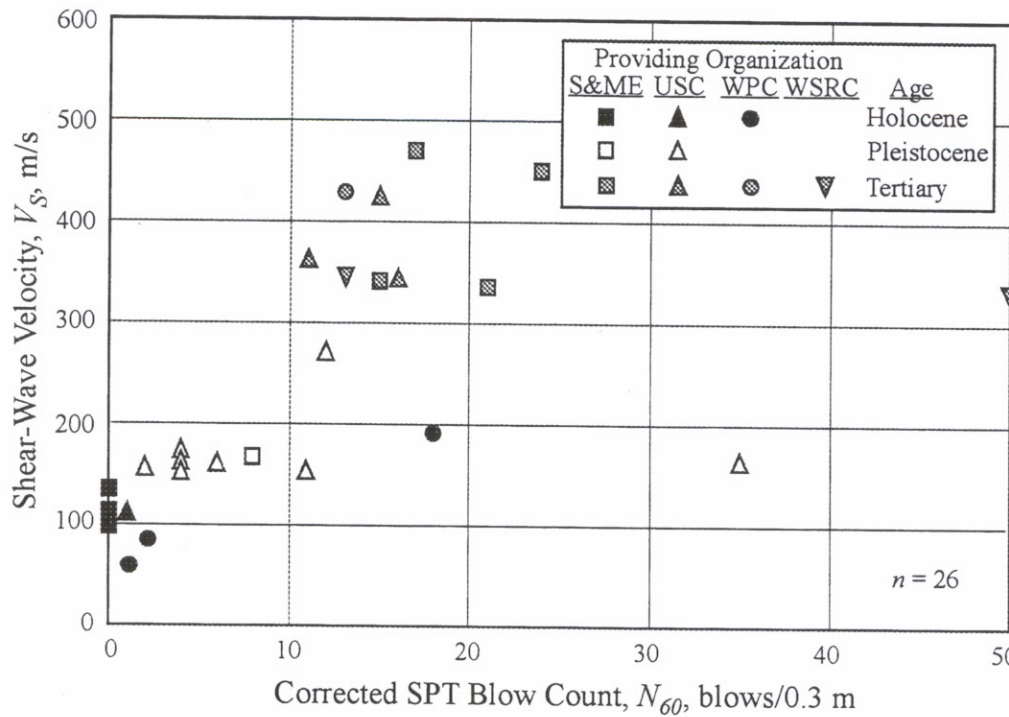

Figure 2.15 – Comparison of N_{60} versus V_s measurements from South Carolina grouped by providing organization and inferred geologic age.
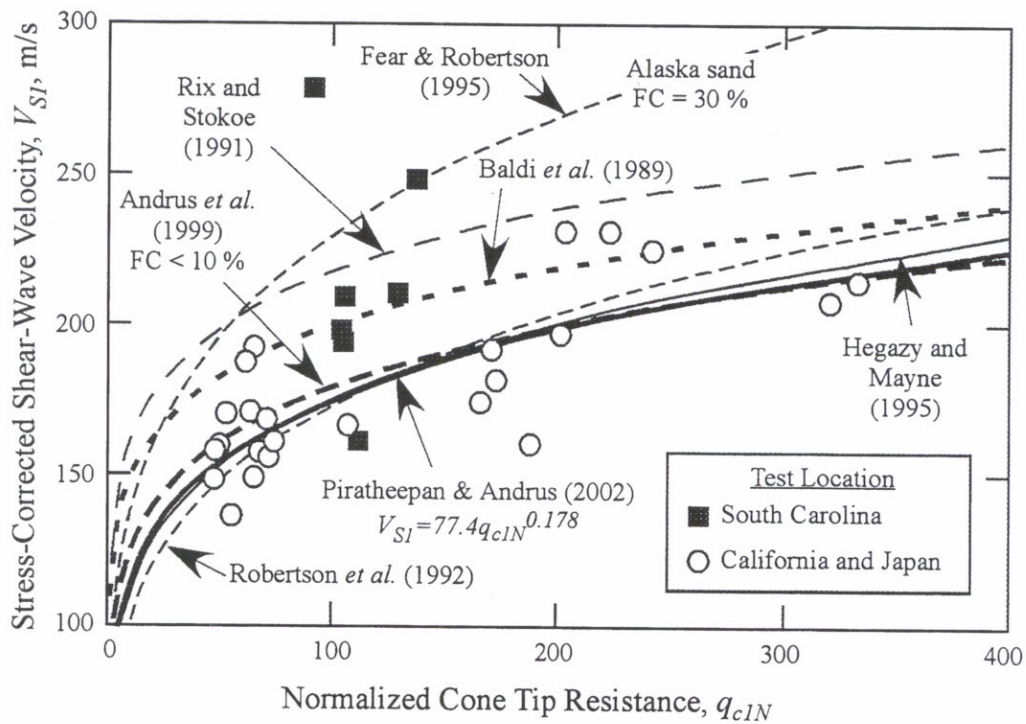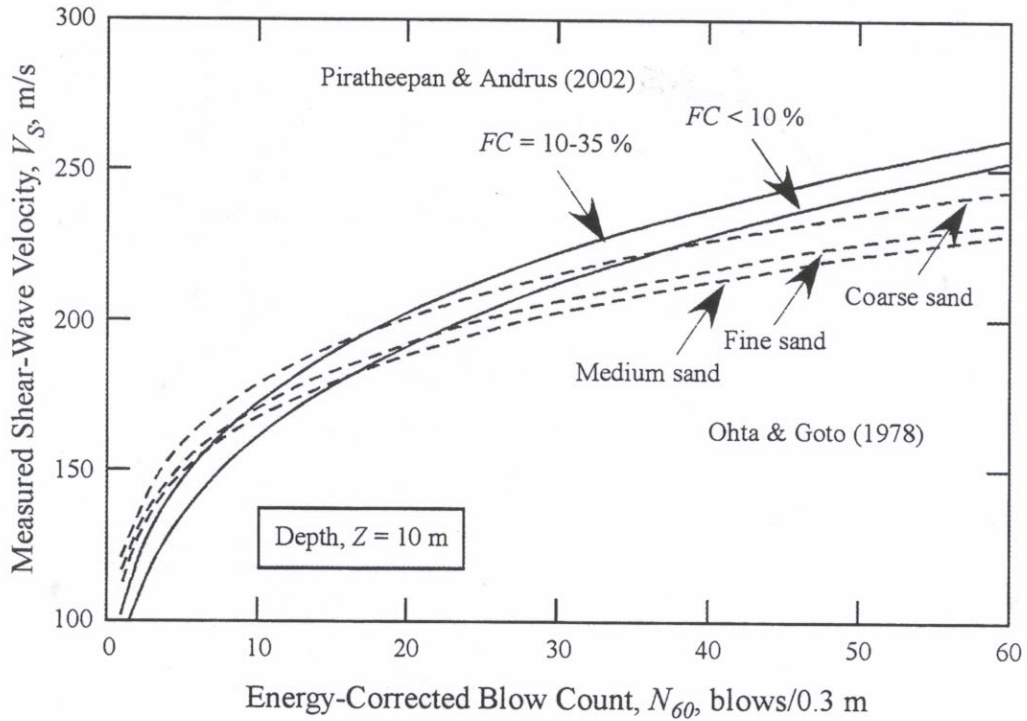
Figure 2.16 – Comparison of earlier SPT-V_S equations for Holocene sandy soils.

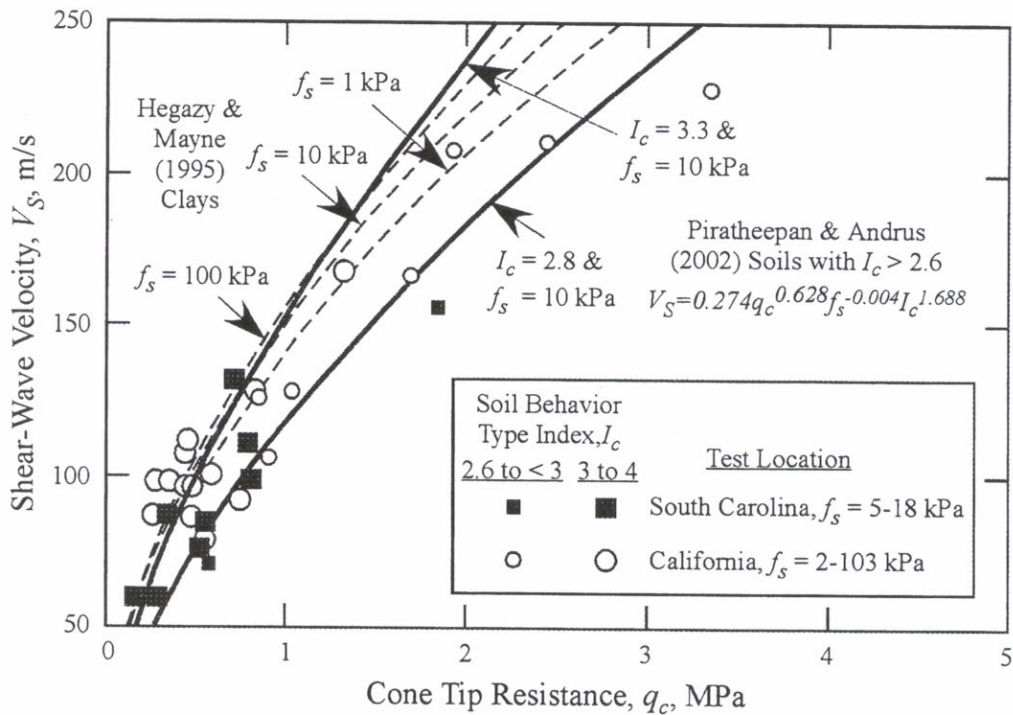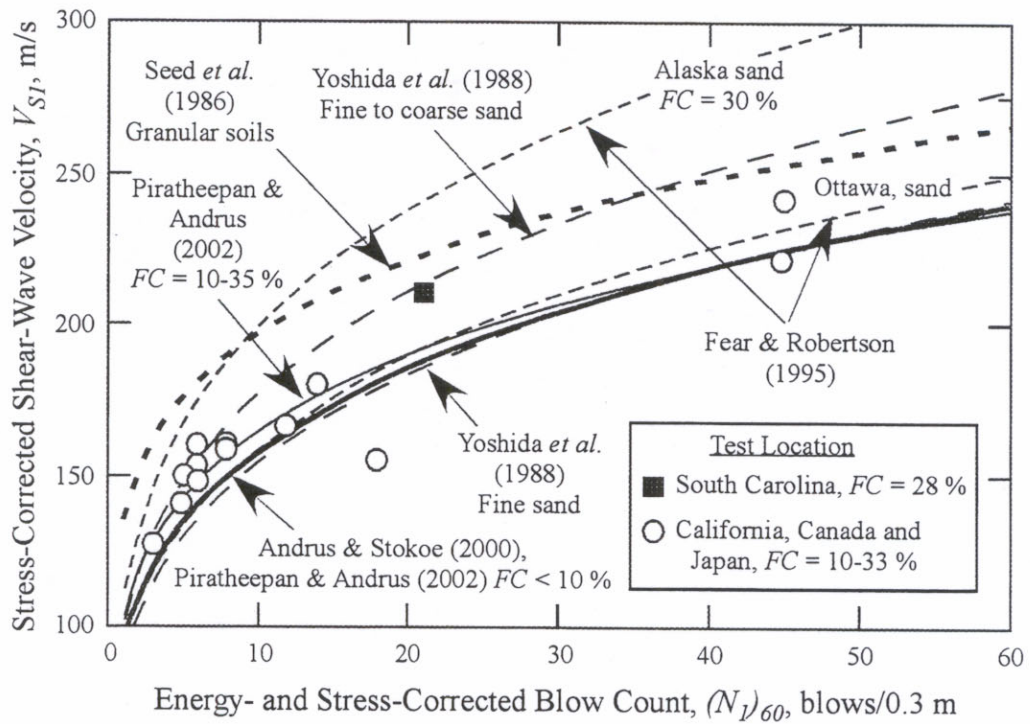Figure 2.17 – Comparison of earlier SPT-V_{S1} equations for Holocene sandy soils along with data from soils with $FC = 10\%$ to 33%.

In Figure 2.17, earlier equations for Holocene sands based on energy- and stress-corrected SPT blow count are compared graphically. Also plotted in the figure are data from South Carolina, California, Canada, and Japan soils with fines content of 10 % to 33 %. The relationships by Piratheepan and Andrus (2002), Andrus and Stokoe (2000), Fear and Robertson (1995) for Ottawa sand, and Yoshida *et al.* (1988) for fine sand compare well. On the other hand, the relationships by Seed *et al.* (1986) for granular soils, Yoshida *et al.* (1988) for fine to coarse sand, and Fear and Robertson (1995) for Alaska sand suggest higher values of V_{S1} than the other relationships for the same blow count. The plotted data from California, Canada and Japan were used by Piratheepan and Andrus (2002) to derive their relationship for soils with fines content of 10 % to 35 %. The one data point from South Carolina (with $FC = 28$ %) plots on the high side of the other data.

It is interesting to note that the relationships by Piratheepan and Andrus (2002) plotted in Figures 2.16 and 2.17 are based on the same data set. Seed *et al.* (1986) derived their relationship by assuming the Ohta and Goto (1978) equation for sandy gravel, which would plot above the curve for coarse sand shown in Figure 2.16. This observation suggests that the assumption made by Seed *et al.* (1986) resulted in a relationship that predicts V_S (or G_{max}) on the high side for many Holocene soils. The relationships by Yoshida *et al.* (1988) are based on calibration chamber tests. Fear and Robertson (1995) described Alaska sand as tailings composed of large amount of carbonate shell material and suggested that the shell material significantly increased its compressibility, which resulted in lower penetration resistances. An alternative hypothesis is that the high concentration of carbonate resulted in a weakly cemented soil skeleton having significantly higher V_S measurements. Predicting V_S on the high side may not be the best approach for ground response analysis. Earthquake records and analytical studies indicate that soft, low V_S, soil deposits subjected to low accelerations, less than about 0.4 g, can amplify the bedrock motion (Idriss, 1990). Thus, the relationships by Ohta and Goto (1978), Yoshida *et al.* (1988) for fine sand, Fear and Robertson (1995) for Ottawa sand, Andrus and Stokoe (2000), and Piratheepan and Andrus (2002) are suggested as better general equations for predicting V_S in uncemented, Holocene-age sands.

Using the equations proposed by Piratheepan and Andrus (2002) and the available data, age scaling factors are derived for various soils in the South Carolina Coastal Plain (Ellis, 2003). These age scaling factors along with the associated statistics are listed in Appendix E.

2.3.2 Recommended Equations for South Carolina Sands

Listed in Table 2.6 are the recommended SPT-V_S equations for use in ground response analyses. The recommended equations are those derived by Piratheepan and Andrus (2002) using data from Holocene soils in California, Canada, and Japan. These equations are recommended because they 1) include all the significant parameters identified in the previous section (i.e., blow count, depth, fines content, and geologic age), 2) provide some of the highest values of R^2 and lowest values of s for the compiled data (see Appendix E), 3) predict V_S (and not V_{S1}), the required parameter for ground response analysis, and 4) provide a reasonable fit for the two data pairs from South Carolina. In addition, the results of the regression analysis given in Appendix E show that equations based on uncorrected and stress-corrected have similar values of R^2 and s associated with them.

Age scaling factors and statistical characteristics for the recommended SPT-V_S equations are given in Table 2.7. Similar to the CPT-V_S equations, the ASF is equal to 1.0 for Holocene soils. The computed ASF for the 8 Pleistocene SPT-V_S data pairs and Equation 2.12 is 1.23, which is practically the same as the computed ASF for the Pleistocene CPT-V_S data pairs (see Table 2.5). The age scaling factors listed for Tertiary soils are tentative and should be used cautiously, because they are based on few SPT-V_S data pairs. It is possible that the age scaling factors listed in Table 2.5 for Tertiary soils may be more representative. Nevertheless, the limited data provide a greater ASF for the Ashley Formation than for the Dry Branch Formation. These findings generally agree with the CPT-V_S age scaling factors and suggest that aging processes may affect both SPT blow count and CPT tip resistance similarly.

Presented in Figure 2.18 is a comparison of measured and predicted V_S for the SPT-V_S data pairs from South Carolina. The two Holocene data points fall within 25 m/s of the "measured=predicted" line. This generally agrees with the s value of 16 m/s associated with Equation 12 and Holocene soils with fines content less than 40 % (see Table 2.7). The value of s associated with the plotted Pleistocene data plotted in Figure 2.18 is 50 m/s. These values of s are similar to s values calculated for the Holocene and Pleistocene CPT-V_S data (see Table 2.5). Somewhat lower s values are expected if Equations 2.13 and 2.14 are used for soils with fines content < 10 % and 10-35 %, respectively. Predictions of V_S outside the ranges indicated in Table 2.7 should be used with greater care.

Presented in Figure 2.19 is a direct comparison the SPT-V_S data pairs and Equation 2.12, using the average depth of the measurements of 5 m, 15 m, or 18 m. It can be seen that the few data plot fairly well about the predicting curves.

Table 2.6 – SPT-V_S equations by Piratheepan and Andrus (2002) recommended for use in ground response studies in South Carolina.

Fines Content, FC, %	Equation for Predicting V_S [a], m/s	Equation
< 40	$V_S = 72.9(N_{60})^{0.224} Z^{0.130} ASF$	2.12[b]
< 10	$V_S = 66.7(N_{60})^{0.248} Z^{0.138} ASF$	2.13[c]
10 to 35	$V_S = 72.3(N_{60})^{0.228} Z^{0.152} ASF$	2.14[c]

[a]N_{60} in blows/0.3 meter, and Z is depth in meters.
[b]Equation 2.12 is the simplest equation recommended for estimating V_S for soils with FC < 40 %.
[c] Somewhat better predictions may be obtained using Equations 2.13 and 2.14 for soils with FC < 10 % and FC = 10 % to 30 %, respectively.

Table 2.7 – Age scaling factors and statistical characteristics for the recommended SPT-V_S equations

Location and Geologic Age of Deposit	Fines Content, FC, %	Age Scaling Factor, ASF	R^2	Residual Standard Deviation, s, m/s	No. of Samples, j	Range of V_S, m/s
South Carolina Coastal Plain – Holocene	< 40	1.00	0.788 [a]	16 [a]	81[a]	110-260 [a]
	< 10	1.00	0.823 [a]	15 [a]	25 [a]	110-260 [a]
	10 to 35	1.00	0.951 [a]	8 [a]	10 [a]	120-240 [a]
South Carolina Coastal Plain – Pleistocene	< 40	1.23	---- [b]	50	8	150-270
	< 10	1.28	---- [b]	58	7	150-270
	10 to 35	1.08 [c]	---- [b]	---- [d]	1	160
South Carolina Coastal Plain – Tertiary-age Ashley Formation (or "Cooper Marl")	< 40	1.82 [c]	---- [b]	---- [d]	1	340
	10 to 35	1.71 [c]	---- [b]	---- [d]	1	340
South Carolina Coastal Plain – Tertiary-age Dry Branch Formation	< 40	1.59 [c]	---- [b]	---- [d]	2	330-350
	10 to 35	1.48 [c]	---- [b]	---- [d]	2	330-350

[a]Data from California, Canada and Japan.
[b]R^2 not calculated.
[c]Tentative ASF based on few measurements. ASF based on CPT data may be more representative.
[d]At least 3 data pairs or samples needed to calculate s.
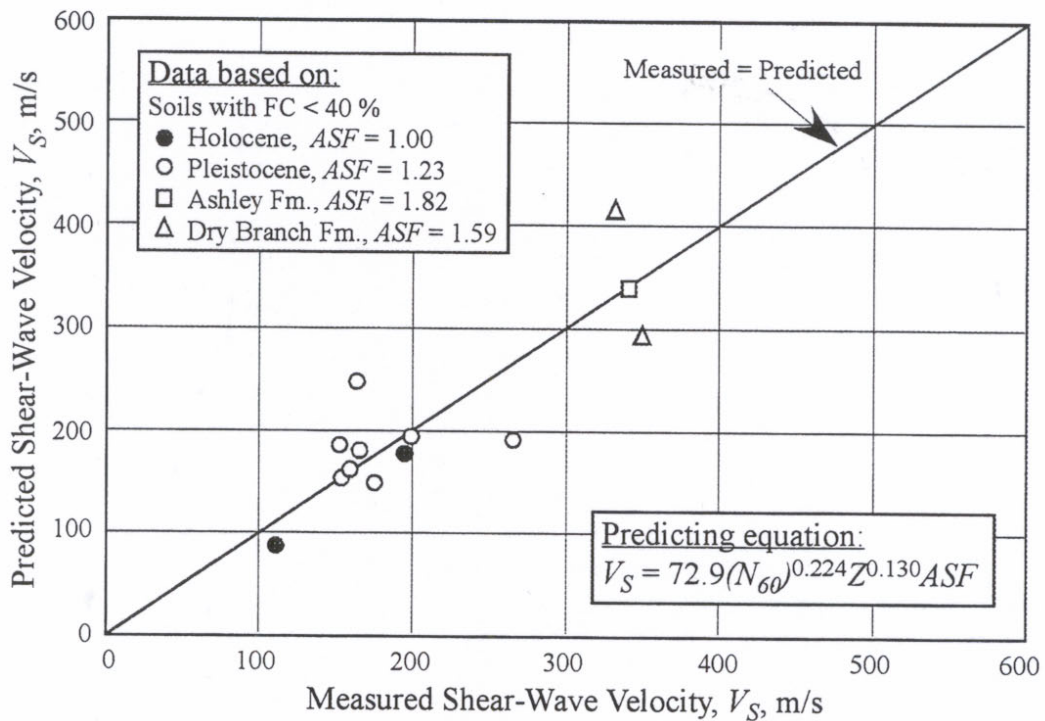
Figure 2.18 – Comparison of measured and predicted V_S as a function of N_{60} for data from South Carolina soils with fines content less than 40 %.
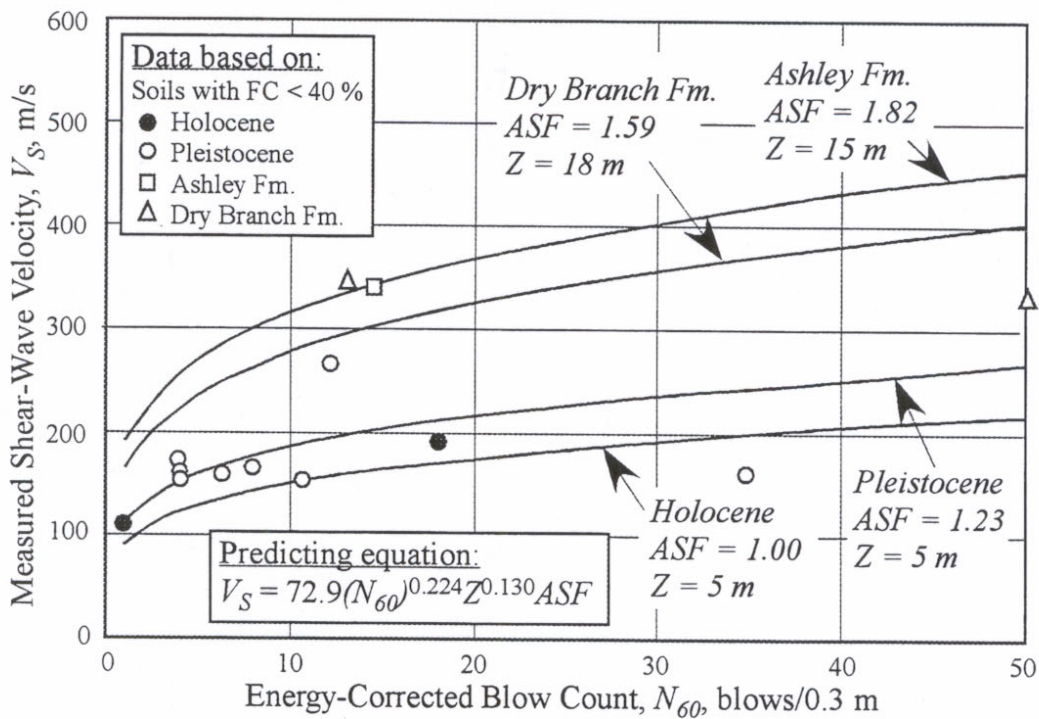
Figure 2.19 – Comparison of the recommended SPT-V_S relationships with the compiled data.

31

2.4 SUMMARY

Guidelines and procedures for estimating V_S of South Carolina Coastal Plain soils from CPT and SPT data were presented in this chapter. The recommended procedure for estimating V_S from CPT data can be summarized in the following five steps:

1. Identify the major geologic units beneath the site in question. This involves determining the approximate age (e.g., Holocene, Pleistocene, Tertiary) and/or formation of each major geologic unit.

2. Calculate the soil behavior type index for each measurement depth in the CPT profile following the iterative procedure described in Section 2.1.3.

3. If necessary, convert the CPT tip resistances and depths to kPa and meters, respectively.

4. Calculate V_S for each measurement depth using Equation 2.9 and the appropriate age scaling factors listed in Table 2.5. Note that Equation 2.9 was the simplest regression equation recommended for all soil types. Somewhat better estimates of V_S may be obtained using Equation 2.10 for $I_c < 2.05$, Equation 2.9 for $2.05 \leq I_c \leq 2.60$, and Equation 2.11 for $I_c > 2.6$.

5. Plot the profile of calculated V_S values. At locations where V_S measurements have been made in close proximity to CPT measurements, compare the measured and predicted values of V_S to verify the accuracy of the CPT-V_S equations and age scaling factors.

The recommended procedure for estimating V_S from SPT data can be summarized in the following five steps:

1. Identify the major geologic units beneath the site in question. This involves determining the approximate age and/or formation of each major geologic unit.

2. Determine the fines content for each measurement depth.

3. Correct the measured blow count, N_m, to the equipment-correct blow count, N_{60}, for each measurement depth following the procedures summarized in Section 2.1.2.

4. Calculate V_S for each measurement depth using Equation 2.12 and the appropriate age scaling factors listed in Table 2.7. Note that Equation 2.12 was the simplest regression equation recommended for soils with fines content < 40 %. Somewhat better estimates of V_S may be obtained using Equation 2.13 for soils with fines content < 10 %, and Equation 2.14 for soils with fines content between 10 and 35. Also, note that age scaling factors listed in Table 2.7 are tentative for the older formations because they are based on limited data.

5. Plot the profile of calculated V_S values. At locations where V_S measurements have been made in close proximity to SPT measurements, compare the measured and predicted values of V_S to verify the accuracy of the SPT-V_S equations and age scaling factors.

Based on both CPT and SPT data, age scaling factors are 1.00 for Holocene soils and 1.2 to 1.3 for Pleistocene soils. For Tertiary soils, computed age scaling factors range from 1.4 to 2.3, and appear to depend on the amount of carbonate in the soil. Residual standard deviations for the recommended equations are about 15 m/s to 25 m/s for the Holocene soils, 40 m/s to 50 m/s for the Pleistocene soils, and 20 m/s to 60 m/s for the Tertiary soils.

Greater care should be exercised with using the recommended equations outside the ranges of V_S listed in Tables 2.5 and 2.7. More data are needed to further validate the recommended equations for South Carolina soils, particularly the SPT-V_S equations. Additional data are needed before equations can be recommended for soils of the Piedmont physiographic province.

CHAPTER 3

**ESTIMATING NORMALIZED SHEAR MODULUS AND
MATERIAL DAMPING RATIO FROM SITE CHARACTERISTICS**

Equations for estimating normalized shear modulus and material damping ratio from site characteristics are presented in this chapter. The equations are particularly useful for regional seismic ground response hazard mapping and preliminary site-specific response analysis in South Carolina. They may also be useful for final site-specific response analysis of non-critical structures. For final site-specific analysis involving critical structures, however, direct measurements should be made. The recommended equations are based on a review of earlier relationships and a statistical analysis of available laboratory test data.

3.1 FACTORS AFFECTING NORMALIZED SHEAR MODULUS AND MATERIAL DAMPING RATIO

Many studies have been conducted to characterize the factors that affect normalized shear modulus and material damping ratio of soils (*e.g.*, Seed and Idriss, 1970; Hardin and Drnevich, 1972a; Lee and Finn, 1978; Zen *et al.*, 1978; Iwasaki *et al.*, 1978; Kokusho *et al.*, 1982; Ni, 1987; Sun *et al.*, 1988; Vucetic and Dobry, 1991; Ishibashi and Zhang, 1993; Stokoe *et al.*, 1995; Rollins *et al.*, 1998, Vucetic *et al.* 1998, Stokoe *et al.*, 1999; Darendeli, 2001). A summary of the relative importance of various factors is given in Table 3.1. The most important factors that affect normalized shear modulus, G/G_{max}, are: strain amplitude, confining pressure, and soil type and plasticity. Other factors that affect G/G_{max}, but are of less importance, include: number of loading cycles, frequency of loading, over-consolidation ratio, void ratio, degree of saturation, and grain characteristics. In general, G/G_{max} curves degrade more slowly with shear strain as confining pressure and plasticity index (*PI*) increase. Iwasaki *et al.* (1978) and Kokusho *et al.* (1982) found that lower plasticity soils are more affected by effective confining pressure than higher plasticity soils. Other studies like Ishibashi and Zhang (1993) and Stokoe *et al.* (1999) showed that G/G_{max} decreases generally less with increasing shear strain as confining pressure increases.

Concerning material damping ratio, *D,* the most important influencing factors are: strain amplitude, confining pressure, soil type and plasticity, number of loading cycles, and frequency of loading. With increase of confining pressure, *D* tends to decrease for all strain amplitudes. The effect of soil plasticity on *D* is complex, however. EPRI (1993), Stokoe *et al.* (1994) and Vucetic *et al.* (1998) found that values of small-strain damping, D_{min}, increase with

increasing *PI*, while values of *D* at high strains decrease with increasing *PI*. Earlier studies like Seed *et al.* (1986) and Vucetic and Dobry (1991) did not show this complex effect of *PI* on damping. As explained by Stokoe *et al.* (1999), one problem with laboratory *D* measurements lies in the identification of equipment-related energy loss. This effect must be quantified and deducted from the measured values to obtain the correct *D*. In addition, it has been suggested that *D* should be measured at frequencies and number of loading cycles similar to those of the anticipated cyclic loadings, to account for the effects of these factors. Considerations for the most important factors affecting G/G_{max} and *D* are made in the development of the predictive equations.

Table 3.1 – Relative importance of various factors on G/G_{max} and *D* of soils (after Darendeli, 2001).

Parameter	Importance on G/G_{max}	Importance on *D*
Strain Amplitude	Very Important	Very Important
Confining Pressure	Very Important	Very Important
Soil Type and Plasticity	Very Important	Very Important
Number of Loading Cycles	Less Important	Very Important
Frequency of Loading	Less Important	Important
Over-Consolidation Ratio	Less Important	Less Important
Void Ratio	Less Important	Less Important
Degree of Saturation	Less Important	Less Important
Grain Characteristics, Size, Shape, Gradation, Mineralogy	Less Important	Less Important

3.2 LABORATORY DATA FROM SOUTH CAROLINA AND SURROUNDING STATES

The available laboratory G/G_{max} and *D* data from South Carolina and surrounding states are compiled from various published and unpublished sources, as summarized in Table 3.2. They include Resonant Column (RC) and Torsional Shear (TS) test data for 78 samples taken from three general areas in South Carolina: Charleston, Savannah River Site (SRS), and Richard B. Russell Dam (RBRD). In addition, RC and TS data for 44 samples taken from North Carolina and Alabama are included in the database. Locations of the Charleston, SRS and RBRD areas are plotted on the map of South Carolina shown in Figure 3.1. Because of the extensive earthquake hazard study conducted at SRS, laboratory results for 64 RC and 15 TS tests are available from that area. Lesser amounts of test data are available from the other areas. Although Cyclic Triaxial test data are also available, they are not considered in this report because of equipment-related concerns raised during an earlier evaluation of the SRS data set (Stokoe *et al.*, 1995; Lee, 1996). Test results for samples from Charleston are available

Table 3.2 – Sites and references of laboratory data used to develop the G/G_{max} and D predictive equations.

Location	Physiographic Province	No. of Tests	Reference
Charleston, SC-Mark Clark Expressway; Daniel Island Terminal	Lower Coastal Plain	6 RC 3 TS	S&ME (1993, 1998)
Savannah River Site, SC	Upper Coastal Plain	64 RC 15 TS	Stokoe *et al*. (1995); Lee (1996); Hwang (1997)
Richard B. Russell Dam, SC	Piedmont	8 RC	USACE (1973, 1979)
Seven sites (A to G) sampled by the North Carolina Department of Transportation	Piedmont	5 RC 27 TS	Borden *et al*. (1994, 1996)
Spring Villa NGES, Opelika, Alabama	Piedmont	12 RC	Hoyos and Macari (1999)
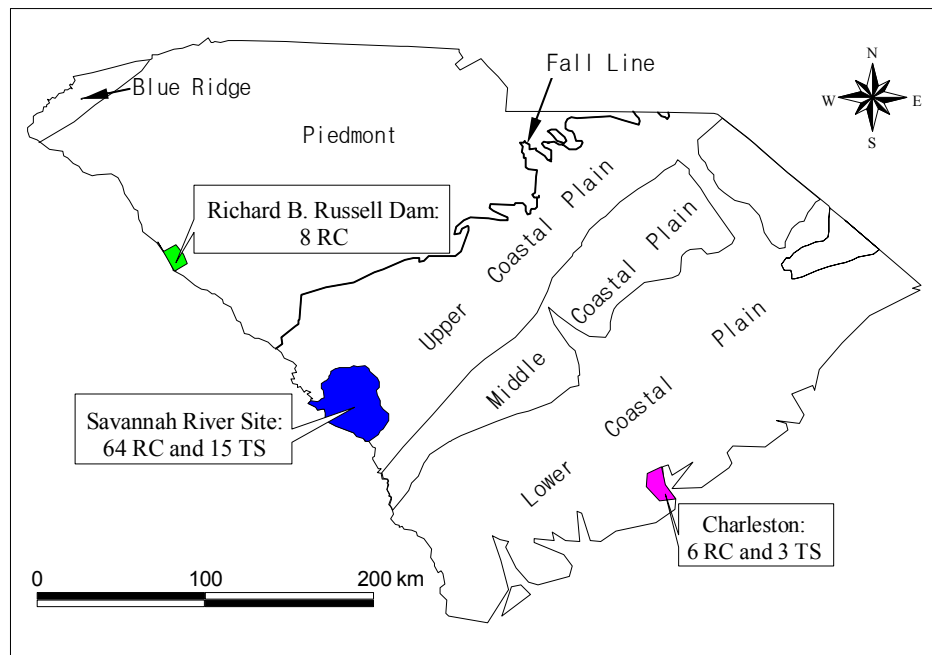
Figure 3.1 – Map of South Carolina showing general sample locations for compiled dynamic laboratory test data.

in tabular format. For samples from North Carolina, all shear modulus data and damping data for 5 RC and 3 TS tests are available in tabular format. Damping data for an additional 24 TS tests on samples from North Carolina are available in graphical form, but are difficult to read. Therefore, these data are not considered in this report. Test results for samples from other locations are read from plots of shear modulus and damping versus shear strain. Results for six deep samples from SRS are not used in this study because they do not follow the general trend displayed by other samples (Stokoe *et al.*, 1995). A detailed listing of the laboratory data is given in Appendix F. General characteristics of the data are described below.

The Charleston and SRS areas lie in the Lower Coastal Plain and Upper Coastal Plain, respectively (see Figure 3.1). The other three areas lie in the Piedmont physiographic province. The Coastal Plain physiographic province generally consists of soft Quaternary soils to relatively stiff Tertiary soils, with depth to hard rock increasing from near zero at the western boundary of the Upper Coastal Plain, called the Fall Line, to about 1 km at the coast (S&ME, 2000; Wheeler and Cramer, 2000). Above the Fall Line lie the Piedmont and Blue Ridge physiographic provinces (see Figure 3.1), which consist largely of shallow zones of residual soils and saprolites overlying hard rock.

Distributions of the 122 test samples with respect to the organization performing the test, sample depth, plasticity index, and geologic unit are presented in Figure 3.2. As shown in Figure 3.2(a), the RC and TS tests were performed by eight different laboratories. Of the 122 test samples: 3 were tested by Fugro-McClelland, Inc. (Fugro), 22 by GEI Consultants, Inc. (GEI), 14 by Law Engineering and Environmental Services, Inc. (Law), 13 by Purdue University (Purdue), 8 by the U.S. Department of the Army, South Atlantic Division Laboratory (SADEN-FL), 18 by The University of Texas at Austin (UTA), 32 by the North Carolina State University at Raleigh (NCSU), and 12 by the Georgia Institute of Technology (GT).

The test samples were collected from depths ranging from 0.6 m to 326 m. As shown in Figure 3.2(b), 50 % of the samples are from depths less than 10 m. About 72 % are from depths less than 30 m. Most samples were tested at mean confining pressures similar to the estimated in-situ mean effective confining pressures. Some were tested at several different confining pressure levels to reflect the confining pressure range that soils at the site were expected to experience.

Values of *PI* are known for 101 of the 122 test samples, ranging from 0 to 132. As illustrated in Figure 3.2(c), non-plastic (*PI* = 0) samples make up at least 35 % of the compiled samples. At least 73 % of the samples have *PI* values less than 30. Only about 10 % of the samples have *PI* values greater than 30, with just one sample having *PI* greater than 100.

38
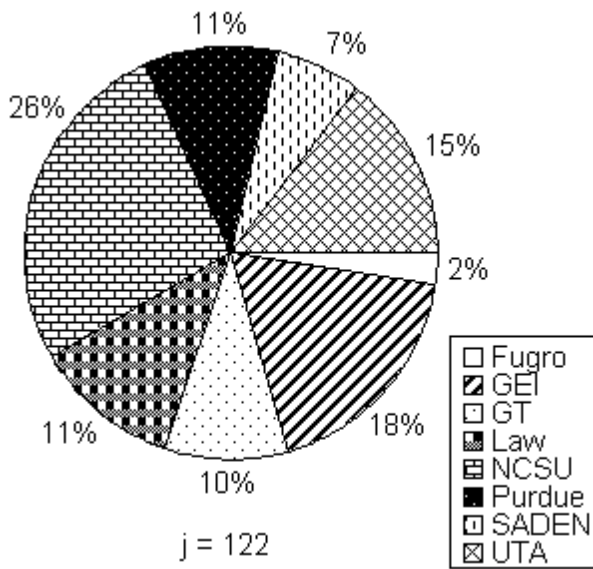
(a) Test Performing Organization   (b) Sample Depth
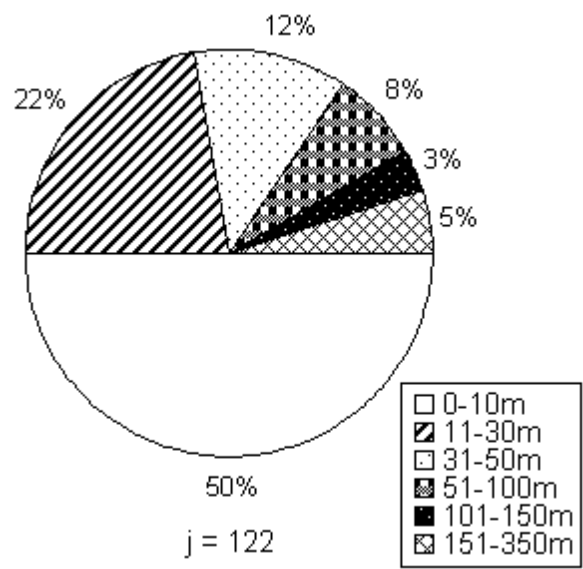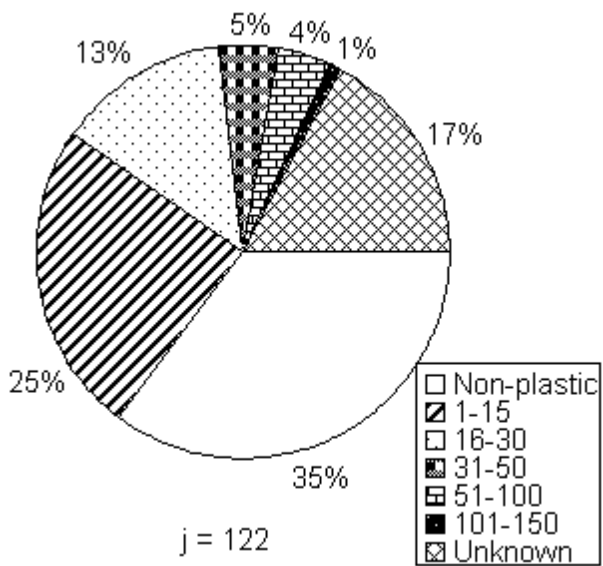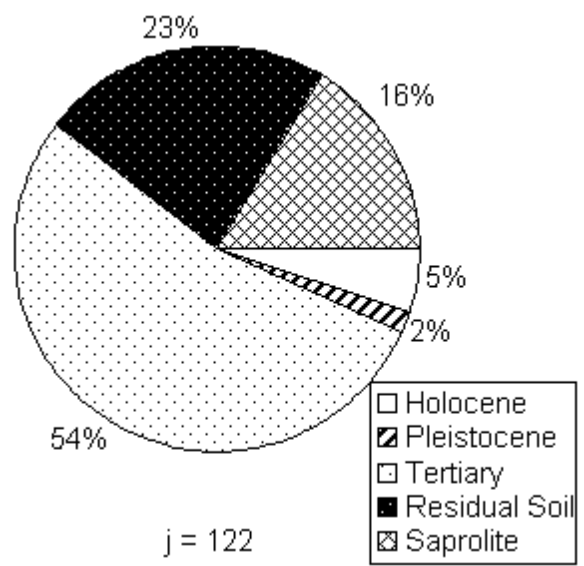
(c) Plasticity Index   (d) Geologic Unit

Figure 3.2 - Characteristics of the compiled dynamic laboratory data.

Geologic unit distribution for the test samples is shown in Figure 3.2(d). Of the 122 test samples, 6 are Holocene in age, 2 are Pleistocene in age, and 66 are Tertiary in age or even older. The other 48 samples are from residual soils and saprolites. Residual soils are clay-rich earths that are the remains of completely weathered rock. Saprolites are highly decomposed rock without the clay accumulation. Generally, no parent rock structure can be found in residual soils, while saprolites retain the relict structure of the original rock but have soil texture. Among the 6 Holocene-age samples, 2 are from Charleston and 4 are from embankment soil at the RBRD site. Two of the Tertiary-age samples are from the Ashley Formation beneath Charleston. The 64 samples from SRS are from various formations of Tertiary age or older. Most test samples were described as "undisturbed," except for three samples from SRS that were described as somewhat disturbed (see Appendix F).

3.3 NORMALIZED SHEAR MODULUS

3.3.1 Earlier General Curves

A comparison of selected earlier general normalized shear modulus curves is presented in Figure 3.3. As can be seen, the Vucetic and Dobry (1991) curve for $PI = 0$ soil is similar to the Seed *et al*. (1986) mean curve for sand. This similarity suggests that the Vucetic and Dobry (1991) curves may be applicable to both fine- and coarse-grained soils. The curve proposed by Idriss (1990) for sand is practically identical to the Seed *et al*. (1986) upper range curve for sand. The Idriss (1990) curve for clay lies close to the Vucetic and Dobry (1991) curve for $PI = 50$ soil. The curve by Stokoe *et al*. (1999) for $PI = 0$ soil and depths (Z) = 7.5 - 100 m lies between the Seed *et al*. (1986) mean and upper range curves for sand, and their curve for $PI = 2$-26 soils and $Z = 7.5$ - 100 m lies above the Seed *et al*. (1986) upper range curve for sand.

Hardin and Drnevich (1972a and 1972b) made one of the early attempts to develop mathematical equations to predict the G/G_{max} curve using a hyperbolic model. The hyperbolic model assumes that the stress-strain curve of soil under cyclic loading can be represented by a hyperbola asymptotic to the maximum shear stress, τ_{max}, and is expressed as:

$$G/G_{max} = \frac{1}{1 + \dfrac{\gamma}{\gamma_r}} \tag{3.1}$$

where γ is the shear strain, and γ_r is the reference strain (= G_{max}/τ_{max}). One limitation of Equation 3.1 is its poor fit to some laboratory measurements because it involves only one fitting parameter, γ_r.
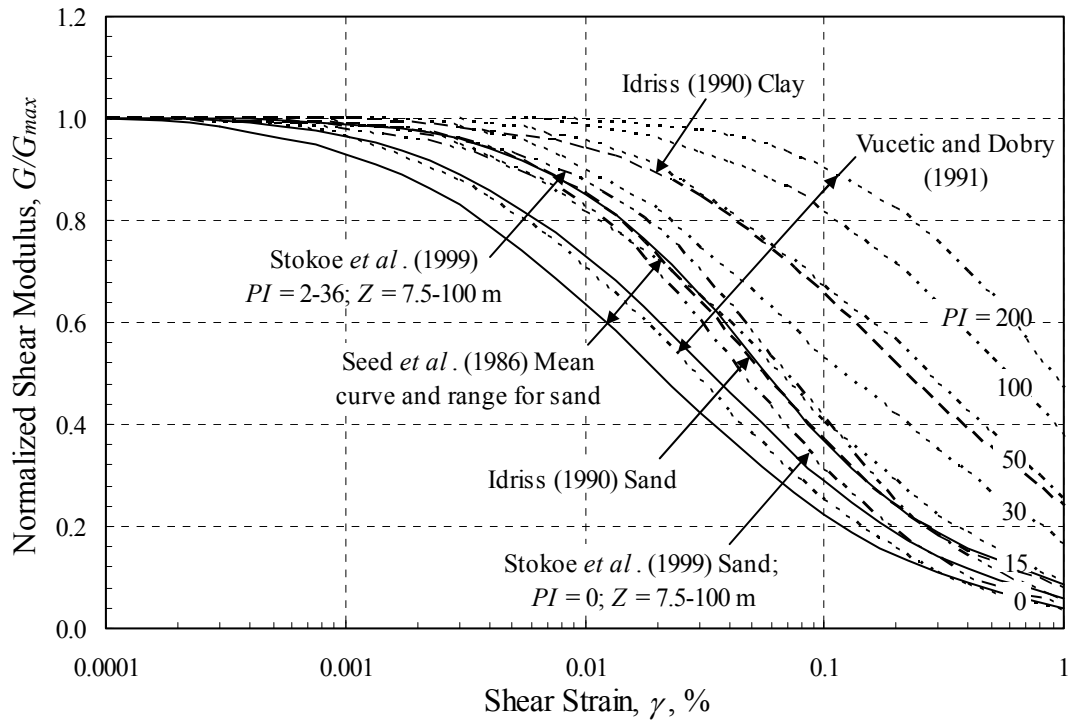
Figure 3.3 – Comparison of selected earlier general normalized shear modulus curves.
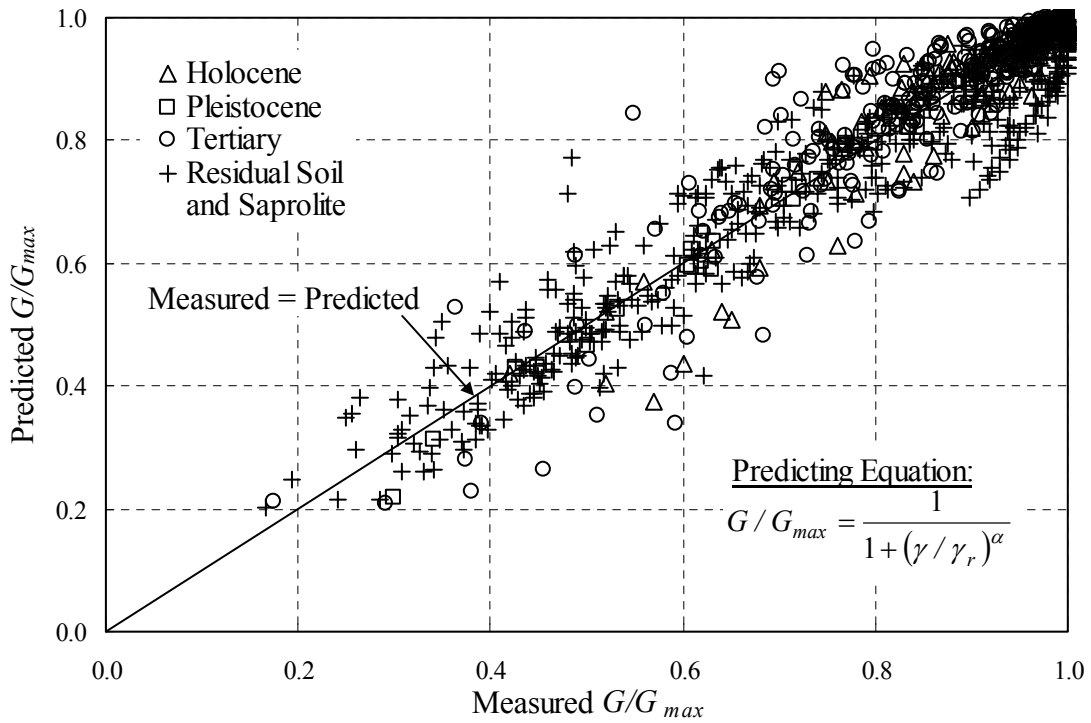
Figure 3.4 - Comparison of measured and predicted G/G_{max} for the compiled data.

41

Improved fits to laboratory test data can be obtained using a modified hyperbolic model expressed as (Stokoe *et al.*, 1999):

$$G/G_{\max} = \cfrac{1}{1 + \left(\cfrac{\gamma}{\gamma_r}\right)^{\alpha}} \qquad (3.2)$$

where α is an exponent called the curvature coefficient. Darendelli (2001) proposed an average α value of 0.919 for all soils. Equation 3.2 is adopted in this study to model the variation of G/G_{max} with shear strain for South Carolina soils.

3.3.2 Recommended Values of γ_r and α for South Carolina Soils

Values of γ_r and α that provide the best fits to Equation 3.2 are determined for each RC or TS test series. It is found that values of γ_r can vary greatly from one geologic unit to another, and generally increase with increasing plasticity and effective confining pressure. Assuming α is independent of confining pressure, calculated values of α are 1.00 for soils in SRS, but vary considerably for soils in Charleston and in the Piedmont. Listed in Table 3.3 are reference strains at a mean effective confining pressure of 100 kPa, γ_{r1}, and corresponding α for various geologic units and *PI* values. As noted in the table, some of these values have been extrapolated from the range of available laboratory data and should be used with greater care. For values of *PI* other than those listed, interpolation between listed values is acceptable.

For converting values of γ_{r1} listed in Table 3.3 to mean effective confining pressures other than 100 kPa, the following relationship is suggested (Stokoe *et al.*, 1995):

$$\gamma_r = \gamma_{r1}\left(\sigma'_m / P_a\right)^k \qquad (3.3)$$

where σ'_m is the mean effective confining pressure at the depth in question in kPa, P_a is a reference pressure of 100 kPa, and k is an exponent that varies with geologic formation and *PI*. Suggested values for k are also listed in Table 3.3. The mean effective pressure is calculated by:

$$\sigma'_m = \sigma'_v\left(\frac{1 + 2K'_0}{3}\right) \qquad (3.4)$$

where σ'_v is the vertical effective pressure, and K'_0 is the coefficient of effective earth pressures at rest. The coefficient K'_0 is defined as the horizontal effective pressure, σ'_h, divided by σ'_v. Procedures for estimating K'_0 can be found in most soil mechanics textbooks. Based on evaluations of laboratory data and analytical studies, Stokoe *et al.* (1995) suggested that actual σ'_m should be within ±50 % range of the estimated values. This suggestion is also supported by the fact that σ'_m (or depth) has been largely ignored in the earlier general G/G_{max} curves.

Table 3.3 – Recommended values of γ_{r1}, α, k and D_{min1} for South Carolina soils.

Geologic Unit (Formation)	No. of Samples	Location	Variable	Soil Plasticity Index, PI						COV for Ln (γ_{r1})	R^2
				0	15	30	50	100	150		
Holocene	6	Charleston and Richard B. Russell Dam	γ_{r1}, %	0.073	0.114	0.156	0.211	0.350	0.488[a]	--	G/G$_{max}$: 0.878 Damping: 0.919
			α	0.95	0.96	0.97	0.98	1.01	1.04[a]	--	
			k	0.385	0.202	0.106	0.045	0.005	0.001[a]	--	
			D_{min1}, %	1.09	1.29	1.50	1.78	2.48	3.18[a]	--	
Pleistocene (Wando)	2	Charleston	γ_{r1}, %	0.018	0.032	0.047	0.067	0.117	0.166	--	G/G$_{max}$: 0.993 Damping: 0.807
			α	1.00	1.02	1.04	1.06	1.13	1.19	--	
			k	0.454	0.402	0.355	0.301	0.199	0.132	--	
			D_{min1}, %	0.59	0.66	0.73	0.83	1.08	1.32	--	
Tertiary (Ashley or "Cooper Marl")	2	Charleston	γ_{r1}, %	--[c]	--	0.030[a]	0.049	0.096[a]	--	--	G/G$_{max}$: 0.971 Damping: 0.915
			α	--	--	1.10[a]	1.15	1.28[a]	--	--	
			k	--	--	0.497[a]	0.455	0.362[a]	--	--	
			D_{min1}, %	--	--	1.14[a,b]	1.52[b]	2.49[a,b]	--	--	
Tertiary (stiff Upland soils)	2	Savannah River Site	γ_{r1}, %	--	--	0.023	0.041[a]	--	--	--	G/G$_{max}$: 0.987 Damping: 0.960
			α	--	--	1.00	1.00[a]	--	--	--	
			k	--	--	0.102	0.045[a]	--	--	--	
			D_{min1}, %	--	--	0.98	1.42[a]	--	--	--	
Tertiary (All soils at SRS except stiff Upland soils)	50	Savannah River Site	γ_{r1}, %	0.038	0.058	0.079	0.106	0.174[a]	--	12.0 %	G/G$_{max}$: 0.855 Damping: 0.785
			α	1.00	1.00	1.00	1.00	1.00[a]	--	--	
			k	0.277	0.240	0.208	0.172	0.106[a]	--	--	
			D_{min1}, %	0.68	0.94	1.19	1.53	2.37[a]	--	--	

[a] Tentative values; extrapolated from the range of available laboratory test data.
[b] Approximate; no Torsional Shear damping measurements available.
[c] Little or no data available.

Table 3.3 – Recommended values of γ_{r1}, α, k and D_{min1} for South Carolina soils (Cont'd).

| Geologic Unit (Formation) | No. of Samples | Location | Variable | Soil Plasticity Index, PI | | | | | | COV for Ln (γ_{r1}) | R^2 |
				0	15	30	50	100	150		
Tertiary (Tobacco Road, Snapp)	19	Savannah River Site	γ_{r1}, %	0.029	0.056	0.082	0.117	0.205[a]	--[c]	11.7 %	G/G$_{max}$: 0.838
			α	1.00	1.00	1.00	1.00	1.00[a]	--	--	
			k	0.220	0.185	0.156	0.124	0.070[a]	--	--	Damping: 0.799
			D_{min1}, %	0.68	0.94	1.19	1.53	2.37[a]	--	--	
Tertiary (soft Upland soils, Dry Branch, Santee, Warley Hill, Congaree)	30	Savannah River Site	γ_{r1}, %	0.047	0.059	0.071	0.086	0.125[a]	--	11.6 %	G/G$_{max}$: 0.887
			α	1.00	1.00	1.00	1.00	1.00[a]	--	--	
			k	0.313	0.299	0.285	0.268	0.229[a]	--	--	Damping: 0.813
			D_{min1}, %	0.68	0.94	1.19	1.53	2.37[a]	--	--	
Residual Soil and Saprolite	48	Piedmont	γ_{r1}, %	0.040	0.066	0.093	0.129[a]	--	--	14.8 %	G/G$_{max}$: 0.924
			α	0.72	0.80	0.89	1.01[a]	--	--	--	
			k	0.202	0.141	0.099	0.061[a]	--	--	--	Damping: 0.852
			D_{min1}, %	0.56[b]	0.85[b]	1.14[b]	1.52[a,b]	--	--	--	

[a] Tentative values; extrapolated from the range of available laboratory test data.
[b] Approximate; no Torsional Shear damping measurements available.
[c] Little or no data available.

Values of G/G_{max} predicted using Equations 3.2, 3.3, and 3.4 for the compiled data are compared with measured G/G_{max} values in Figure 3.4. As noted in Table 3.3, calculated values of R^2 range from 0.855 to 0.987. One point to keep in mind when interpreting the R^2 values is that most of the data are concentrated between G/G_{max} values from 0.8 to 1.0, where error is inherently small because of normalization. Thus, the R^2 values probably do not reflect the goodness-of-fit of the model at lower values of G/G_{max}. Perhaps more weight should be assigned to the G/G_{max} values smaller than 0.8. Nevertheless, the plotted data in Figure 3.4 are fairly evenly distributed about the "Measured = Predicted" line.

For geologic units where enough data exist, statistical variability of the compiled data is also provided in Table 3.3 in terms of coefficient of variation (COV) for reference strain. COV is defined as the standard deviation divided by the mean value, and is a measure of relative dispersion. Values of γ_{r1} for a certain geologic unit are found to be log-normally distributed and the COV values presented in the table are for Ln (γ_{r1}).

3.3.3 Comparison of Recommended and Earlier General Curves

In Figures 3.5 through 3.9, the recommended G/G_{max} curves are grouped by geologic unit and compared with the Vucetic and Dobry (1991) curves. Only the recommended curves for σ'_m of 100 kPa are shown for simplicity. Also shown in these figures are the compiled laboratory test data, which are converted to equivalent values with $\sigma'_m = 100$ kPa here through the correction of γ_r using Equations 3.3.

In Figure 3.5, the recommended curves for Holocene-age soils in Charleston and at RBRD are shown. As can be seen, the recommended curves for $PI = 0$ to 100 soils span a range narrower than the corresponding Vucetic and Dobry (1991) curves. The recommended curve for $PI = 0$ soils lies near the Vucetic and Dobry (1991) curve for $PI = 15$, where is also the position of the Seed *et al.* (1986) upper range curve for sand, the Idriss (1990) curve for sand, and the Stokoe *et al.* (1999) curve for sand (see Figure 3.3). The recommended curve for Holocene soils with $PI = 100$ lies between the Vucetic and Dobry (1991) curves for $PI = 50$ and 100.

Recommended curves for Pleistocene-age soils with $PI = 0$ to 150 are shown in Figure 3.6. They cover a range similar to the Vucetic and Dobry (1991) curves, but lie at lower positions compared to their counterparts, especially at medium to high strains. The difference between the recommended curves and the corresponding Vucetic and Dobry (1991) curves become increasingly greater with increasing PI. The recommended curve for $PI = 0$ soils would plot close to the Seed *et al.* (1986) lower range curve for sand (see Figure 3.3).
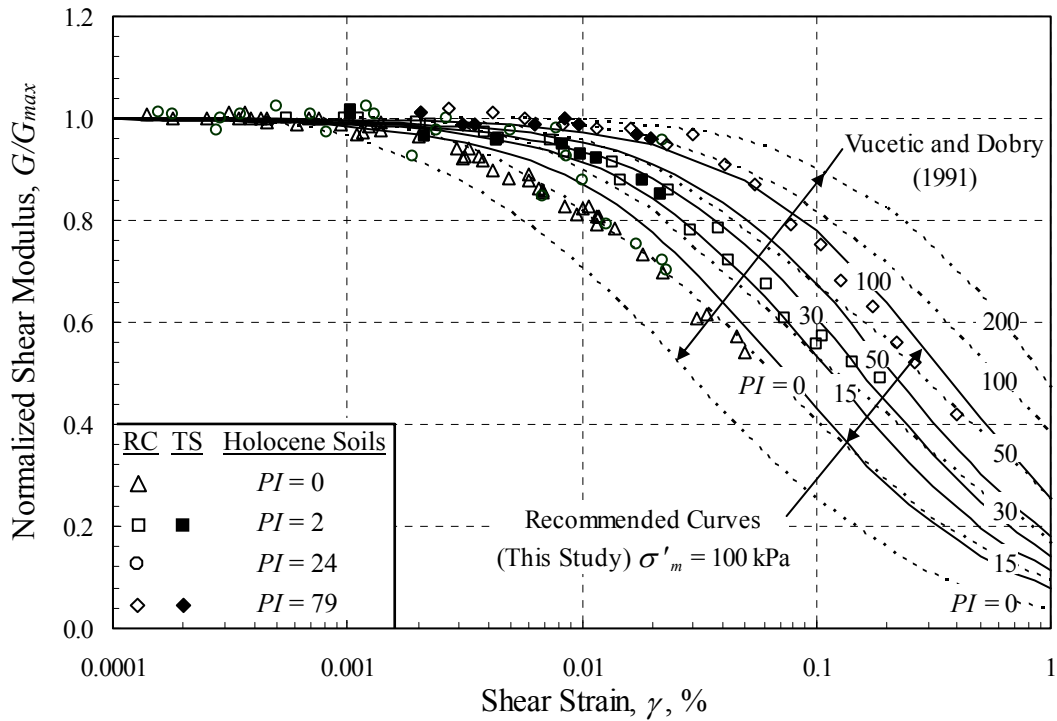
Figure 3.5 - Comparison of compiled data and recommended G/G_{max} - log γ curves for Holocene-age soils with curves proposed by Vucetic and Dobry (1991).
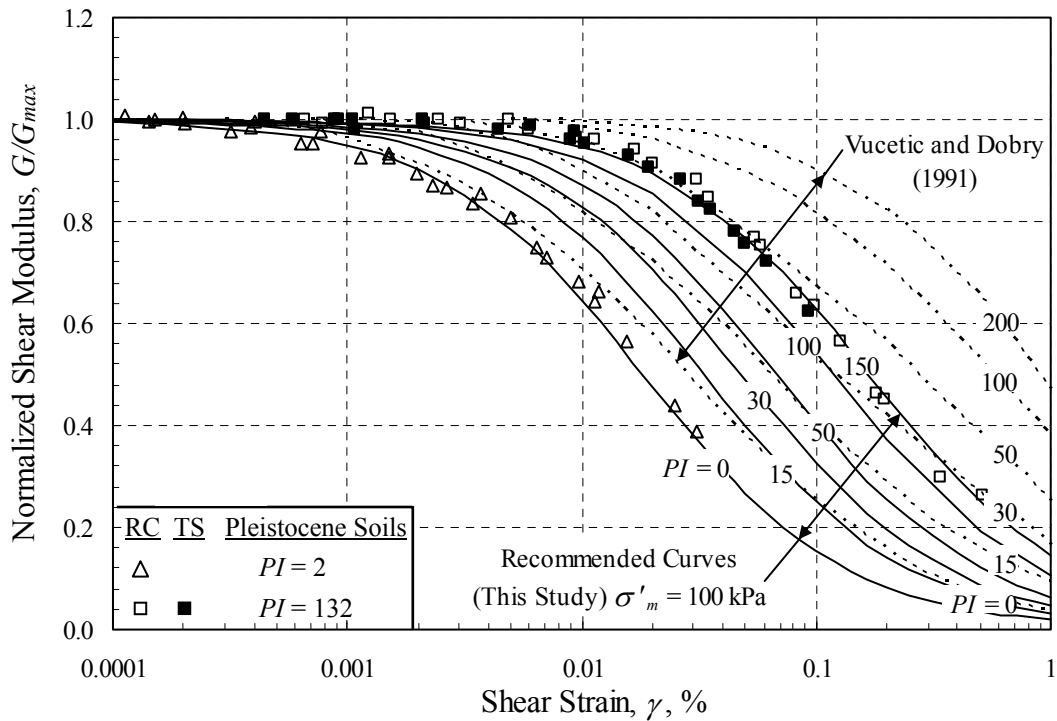
Figure 3.6 - Comparison of compiled data and recommended G/G_{max} - log γ curves for Pleistocene-age soils with curves proposed by Vucetic and Dobry (1991).

46
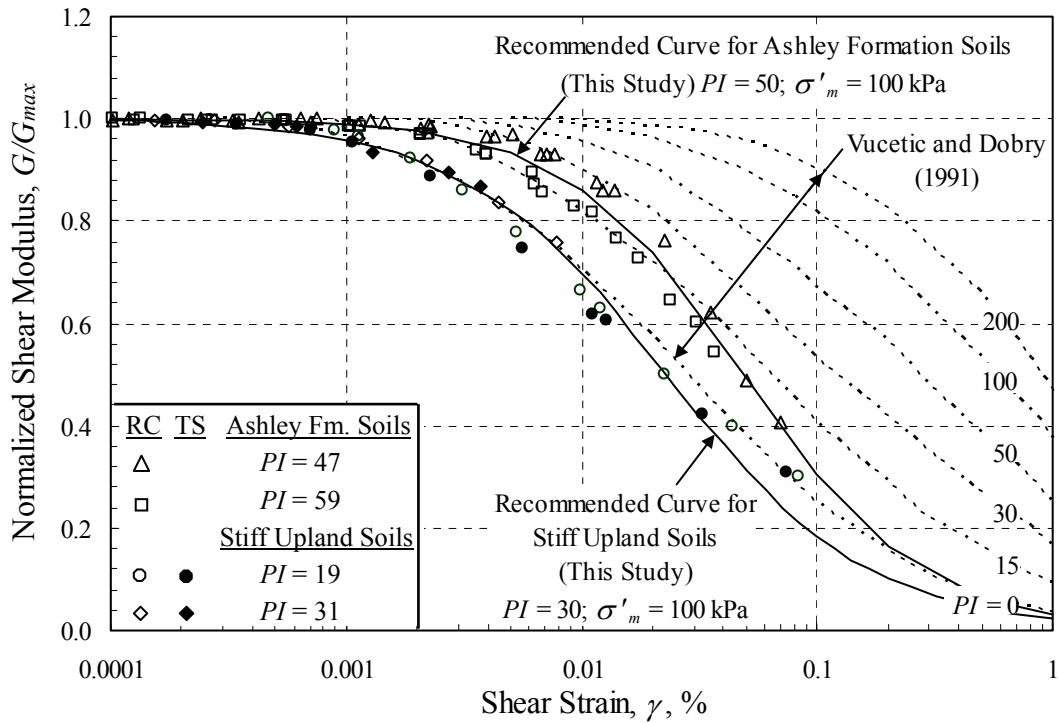
Figure 3.7 - Comparison of compiled data and recommended G/G_{max} - log γ curves for the Tertiary-age Ashley Formation and stiff Upland soils with curves proposed by Vucetic and Dobry (1991).
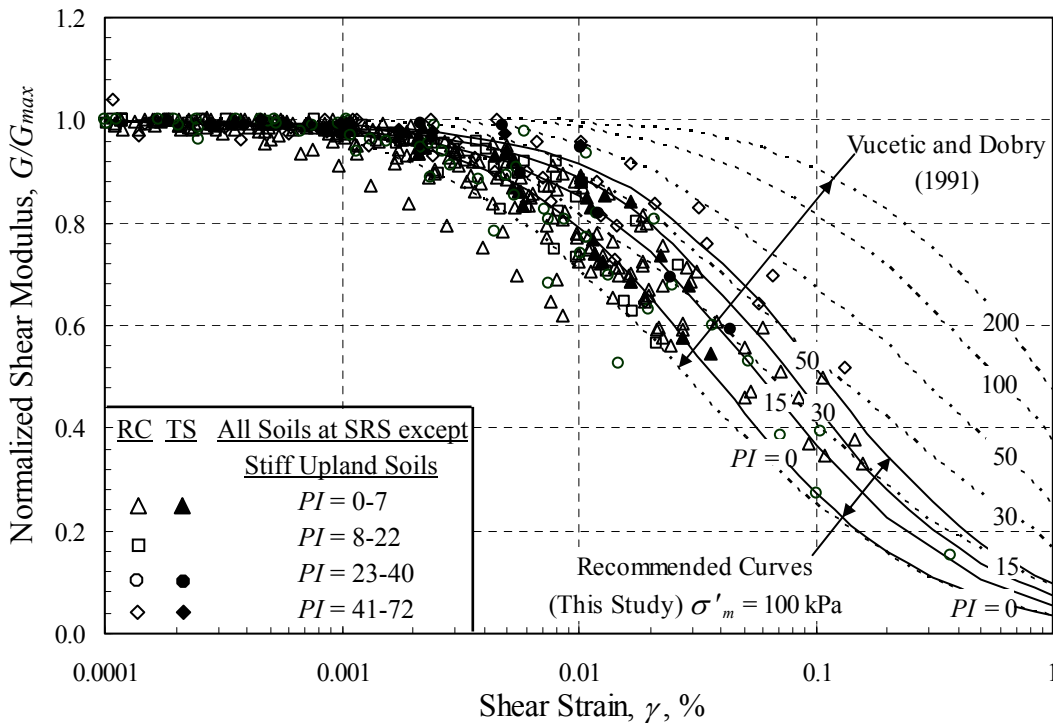
Figure 3.8 - Comparison of compiled data and recommended G/G_{max} - log γ curves for all Tertiary-age soils at SRS except stiff Upland soils with curves proposed by Vucetic and Dobry (1991).
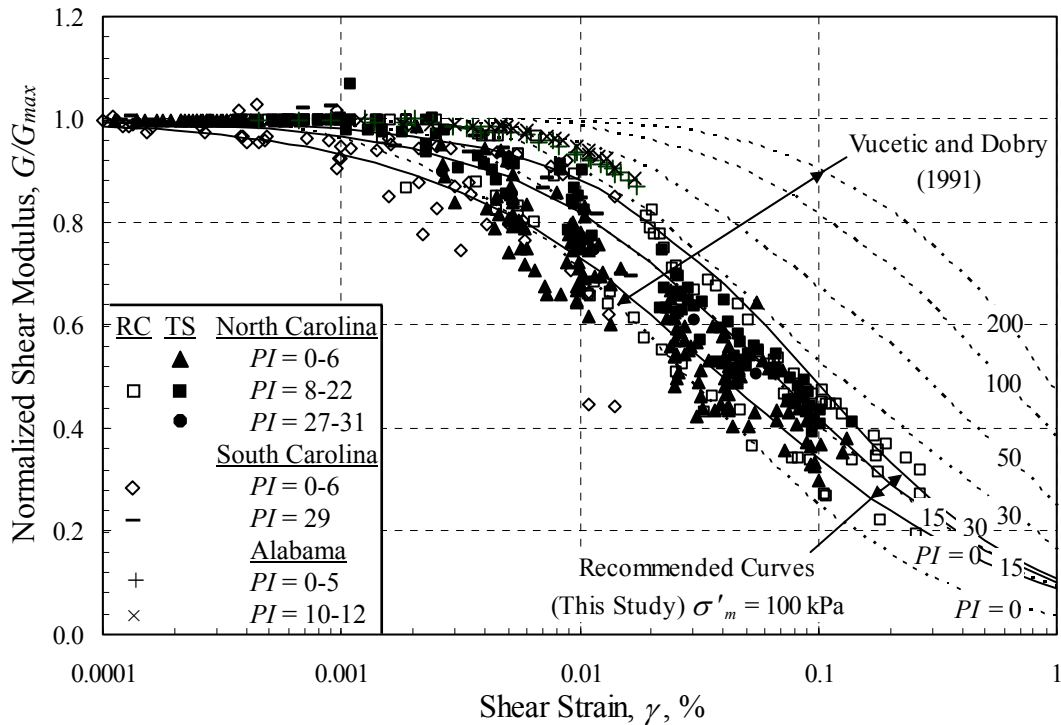
Figure 3.9 - Comparison of compiled data and recommended G/G_{max} - log γ curves for Piedmont residual soils and saprolites with curves proposed by Vucetic and Dobry (1991).

Shown in Figure 3.7 are the recommended curves for the Ashley Formation soils with $PI = 50$ and the stiff Upland soils with $PI = 30$. The recommended curve for the Ashley Formation appears between the Vucetic and Dobry (1991) curves for $PI = 15$ and 30 at small to medium strains and approaches the Vucetic and Dobry (1991) curve for $PI = 0$ at high strains. Unexpectedly, the recommended curve for the stiff Upland soils with $PI = 30$ generally follows the Vucetic and Dobry (1991) curve for $PI = 0$.

Presented in Figure 3.8 are the recommended curves for Tertiary-age soils at SRS with $PI = 0$ to 50, except the stiff Upland soils. The recommended $PI = 0$ curve follows the Vucetic and Dobry (1991) curve for $PI = 15$ soils at small strains, but is close to the Vucetic and Dobry (1991) curve for $PI = 0$ soils at high strains. The recommended $PI = 50$ curve is close to the Vucetic and Dobry (1991) curve for $PI = 30$ soils and falls below it at strains greater than 0.1 %. Somewhat improved predictions can be obtained if the specific formation at SRS is known, as noted in Table 3.3.

The recommended curves for Piedmont residual soils and saprolites are presented in Figure 3.9. They are based on samples from South Carolina, North Carolina, and Alabama. The recommended curve for $PI = 0$ is much flatter than the corresponding Vucetic and Dobry

48

(1991) curve. It plots lower than the Vucetic and Dobry (1991) curve for $PI = 0$ at small strains and rises above it with increasing strain amplitudes. The recommended curve for $PI = 15$ is similar to the Vucetic and Dobry (1991) curve for $PI = 15$. The recommended curve for $PI = 30$ generally follows the corresponding Vucetic and Dobry (1991) curve, except for high strains.

3.4 MATERIAL DAMPING RATIO

3.4.1 Earlier General Curves

A comparison of selected earlier general material damping ratio curves is presented in Figure 3.10. As can be seen in the figure, the Seed *et al*. (1986) mean curve for sand plots above the Vucetic and Dobry (1991) curve for $PI = 0$ soil. The Idriss (1990) curve for sand and clay is almost identical to the Seed *et al*. (1986) lower range curve for sand. Both the Seed *et al*. (1986) lower range curve and the Idriss (1990) curve follow the Vucetic and Dobry (1991) curve for $PI = 200$ soil at strains around 0.001 %, but increase rapidly with increasing strain and merge with the Vucetic and Dobry (1991) curve for $PI = 15$ soil at strains greater than 0.3 %. The Vucetic and Dobry (1991) curves only show the trend for damping at medium to high strains, and no clear trend is established between PI and D_{min}. Later research found that D_{min} increases with increasing PI and damping curves for soils of different PI values cross over each other at a certain strain range (EPRI, 1993; Stokoe *et al*., 1994; Vucetic *et al*., 1998).

One approach to modeling D is relating it to G/G_{max}. The advantage of such a relationship is it makes use of the better-understood G/G_{max} results to calculate D, which is usually more difficult to obtain. Relationships between D and G/G_{max} have been studied by several researchers. Hardin and Drnevich (1972b) assumed that D is proportional to $1-G/G_{max}$. Others, such as Ishibashi and Zhang (1993) and Borden *et al*. (1996), associated D with G/G_{max} using a polynomial expression. None of these models, however, reflect the complex relationship between PI and D. Pyke (1993) developed a computer program to calculate D based on γ_r fitted from the hyperbolic model and D_{min} measured in laboratory. Darendeli (2001) modeled the hysteretic damping assuming Masing behavior and an adjusting function, then adding a D_{min} term to obtain the total damping. The general damping equation adopted for this study is expressed as:

$$D = f(G/G_{max}) + D_{min} \qquad (3.5)$$

where $f(G/G_{max})$ is a function of the normalized shear modulus.
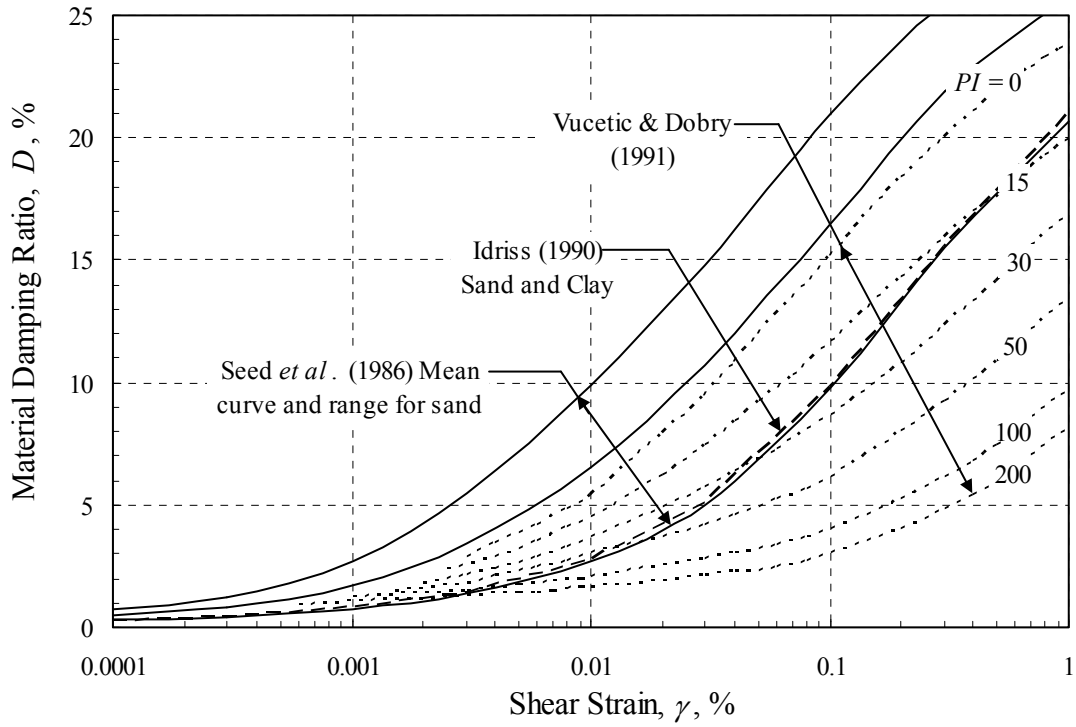
Figure 3.10 – Comparison of selected earlier general material damping ratio curves.
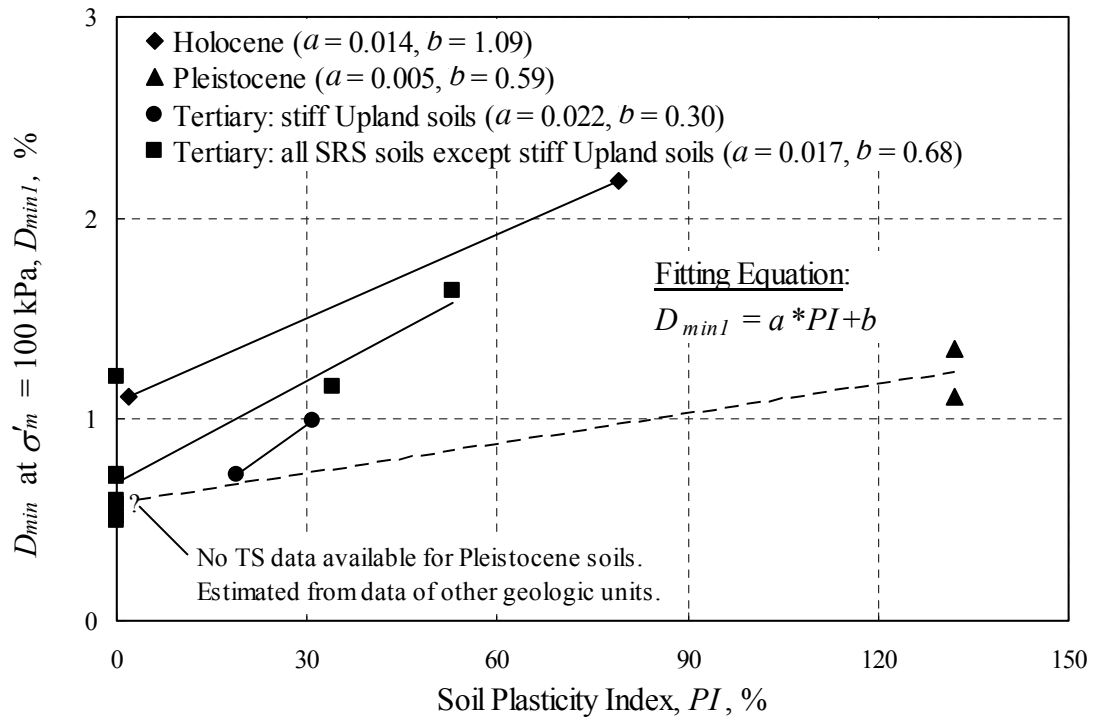
Figure 3.11 – Relationship between D_{min1} and PI based on TS test results by UTA.

50

3.4.2 Recommended Values of D_{min} and $f(G/G_{max})$ for South Carolina Soils

As shown in Figure 3.11, approximately linear relationships are observed between PI and the small-strain damping at σ'_m of 100 kPa, D_{min1}, for various geologic units. These linear relationships can be defined as (simplified from Darendeli, 2001):

$$D_{\text{min}1} = a(PI) + b \tag{3.6}$$

where a and b are fitting parameters. Values of a and b determined for four geologic units are given in Figure 3.11. Only TS data from Charleston and SRS are used in developing Equation 3.6 because they are measured at frequencies and number of loading cycles similar to typical earthquake loadings. The RC data are usually obtained at much higher frequency and number of loading cycles. No TS tests were conducted on samples from RBRD and Alabama. Although Borden *et al.* (1996) conducted TS test on samples from North Carolina, most of their TS damping data are in graphical form and are difficult to read off the published plots. Only data for 3 of their 27 TS test samples are available in tabular form. Recommended values of D_{min1} calculated from Equation 3.6 are presented in Table 3.3 for various geologic units at selected PI values.

Similar to Equation 3.3, the following equation is used to obtain D_{min} at σ'_m values other than 100 kPa (modified from Stokoe *et al.* 1995):

$$D_{min} = D_{min1}\left(\sigma'_m / P_a\right)^{-k/2} \tag{3.7}$$

where k is the same exponent used in Equation 3.3.

In Figure 3.12, the compiled data for D minus D_{min} and G/G_{max} by UTA are plotted. Also shown in the figure is the best-fit equation for the plotted data, which is defined by:

$$D - D_{min} = f(G/G_{max}) = 12.2(G/G_{max})^2 - 34.2(G/G_{max}) + 22.0 \tag{3.8}$$

When the value of G/G_{max} is 1 at small strains, $f(G/G_{max}) = 0$ and $D = D_{min}$. Equation 3.8 is based on data from Charleston and SRS.

Equations 3.5, 3.6, 3.7 and 3.8 along with the factors listed in Table 3.3 represent the recommended damping relationships for South Carolina soils. Material damping values predicted for the compiled data using these equations are compared with the measured values in Figure 3.13. Values of R^2 range from 0.785 to 0.960. Because most of the damping data are concentrated between 0 % and 5 %, the R^2 values probably do not reflect the goodness-of-fit of the model at higher values of D. Perhaps more weight should be assigned to damping of higher values. No statistical variability analyses are performed on the damping because there are not enough TS test data.
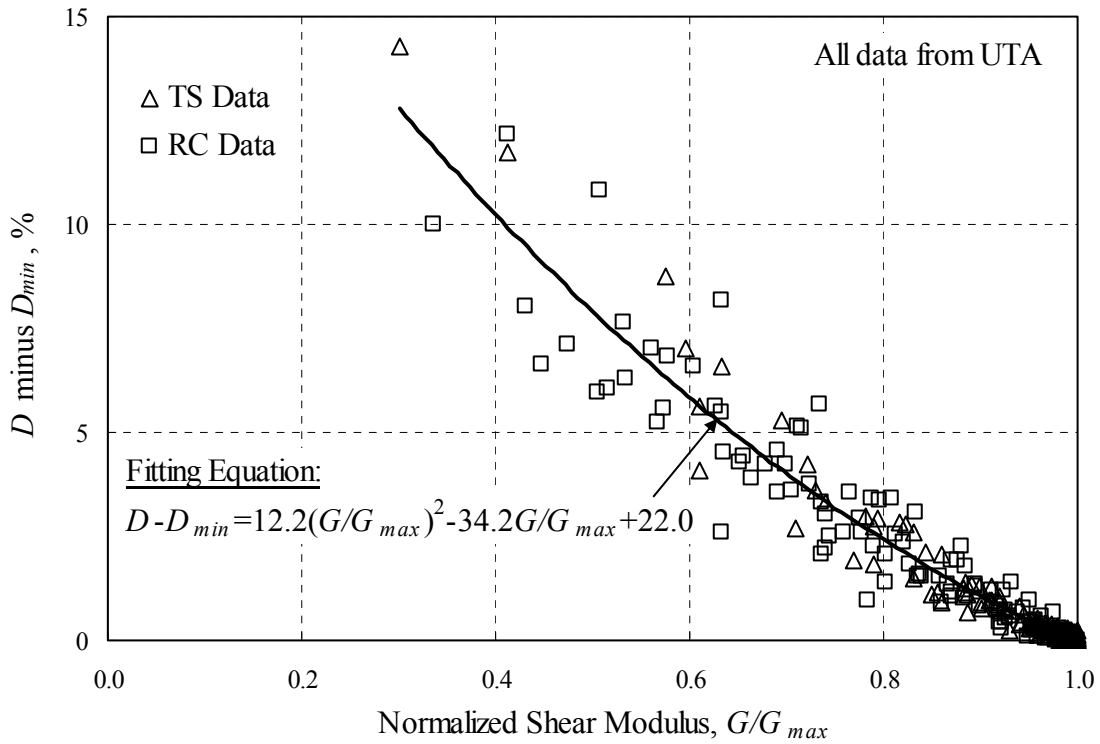
Figure 3.12 – Relationship between G/G_{max} and D minus D_{min}.
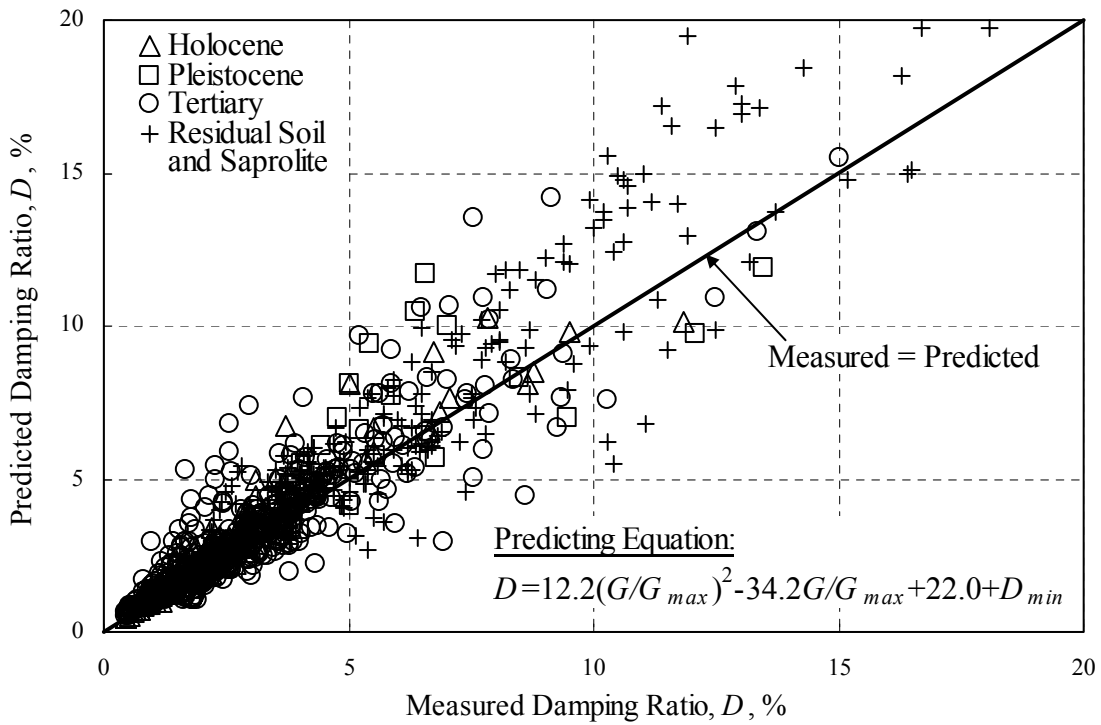
Figure 3.13 - Comparison of measured and predicted D for the compiled data.

3.4.3 Comparison of Recommended and Earlier General Curves

Comparisons of the recommended D curves by geologic unit with the Vucetic and Dobry (1991) curves are shown in Figures 3.14 through 3.18. For simplicity, only the recommended curves corresponding to σ'_m of 100 kPa are shown. At small strains, D values of the recommended curves are estimated from the TS data only, which are much smaller than the RC data shown in the figures. The small-stain D values of TS test are much smaller than those of RC test because the cyclic loading frequencies applied in the TS test are much lower than those of the RC test. Also shown in these figures are the compiled data converted to a σ'_m of 100 kPa. The damping data are converted using Equation 3.5, the G/G_{max} values at $\sigma'_m = 100$ kPa, and Equation 3.7.

In Figure 3.14, the recommended damping curves for Holocene-age soils from Charleston and RBRD are shown. Similar to the G/G_{max} curves, the recommended damping curves for $PI = 0$ to 100 soils cover a range narrower than the corresponding Vucetic and Dobry (1991) damping curves. The recommended curve for $PI = 0$ soils lies much lower than the Vucetic and Dobry (1991) curve for $PI = 0$, and generally follows the Seed *et al*. (1986) lower range curve for sand and the Idriss (1990) curve for sand and clay (see Figure 3.10). The recommended curve for $PI = 100$ soils lies above the Vucetic and Dobry (1991) curve for $PI = 100$ soils, with the most significant difference at high strains.

Recommended damping curves for Pleistocene-age soils with $PI = 0$ to 150 are shown in Figure 3.15. They are similar to the corresponding curves proposed by Vucetic & Dobry (1991) at medium strains but generally rise above them at higher strains. In addition, the difference between the recommended curves and the corresponding Vucetic and Dobry (1991) curves becomes increasingly greater with increasing PI. The recommended curve for $PI = 0$ soils, however, plots close to the Seed *et al*. (1986) mean curve for sand (see Figure 3.11).

Shown in Figure 3.16 are the recommended damping curves for the Ashley Formation soils with $PI = 50$ and the stiff Upland soils with $PI = 30$. Similar to the curves for Pleistocene-age soils, the recommended curve for the Ashley Formation soils with $PI = 50$ follows the Vucetic & Dobry (1991) curve for $PI = 50$ at low to medium strains, but rapidly increases above it with increasing strain. The recommended curve for stiff Upland soils with $PI = 30$ generally follows the Vucetic and Dobry (1991) curve for $PI = 0$ and lies below the Seed *et al.* (1986) mean curve for sand at most strain levels (see Figure 3.10).

Presented in Figure 3.17 are the recommended damping curves for Tertiary- age soils at SRS with $PI = 0$ to 50, except the stiff Upland soils. The recommended curves lie generally lower than the corresponding Vucetic and Dobry (1991) curves at small to medium strains, but rapidly increase close to or above them with increasing shear strain. Furthermore, the
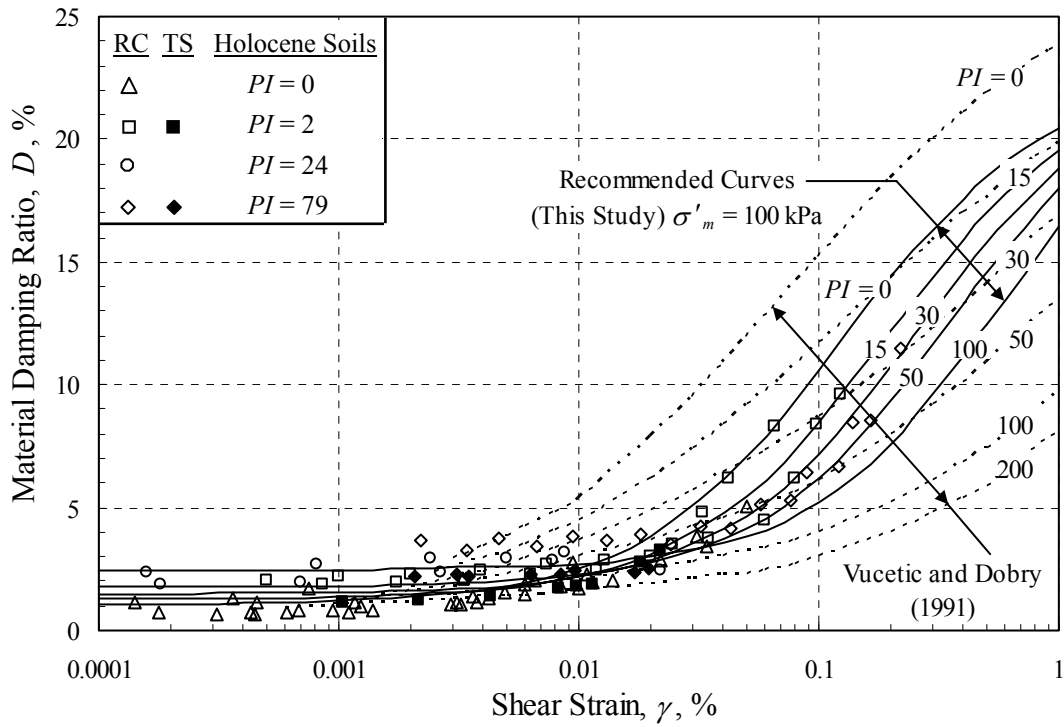
Figure 3.14 - Comparison of compiled data and recommended D - log γ curves for Holocene-age soils with curves proposed by Vucetic and Dobry (1991).
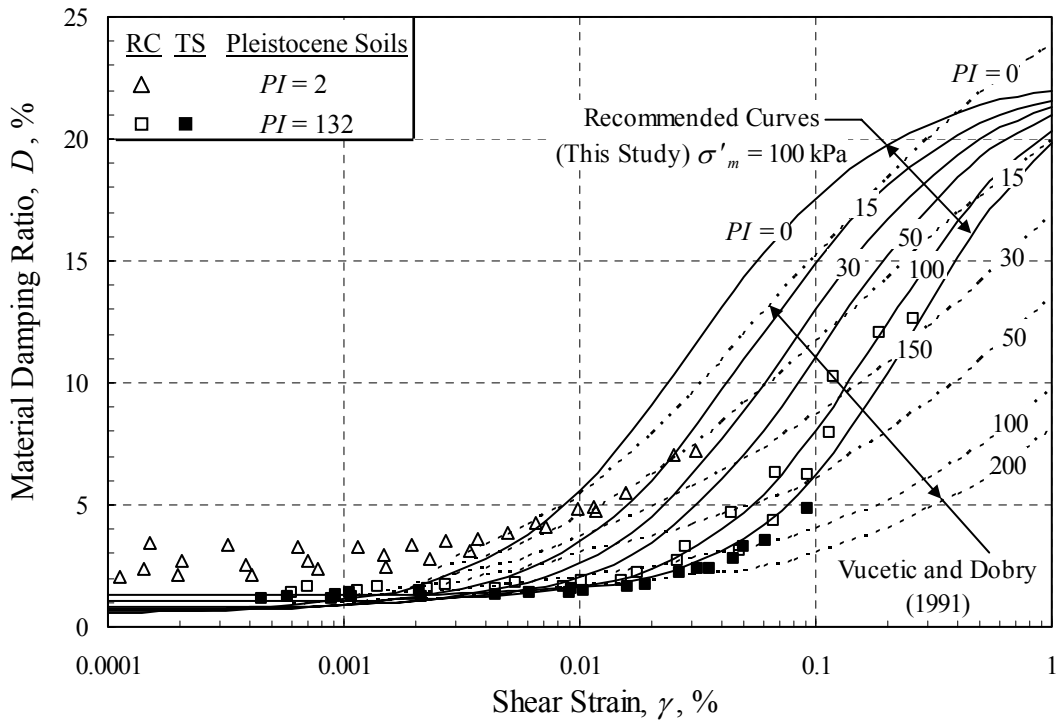
Figure 3.15 - Comparison of compiled data and recommended D - log γ curves for Pleistocene-age soils with curves proposed by Vucetic and Dobry (1991).
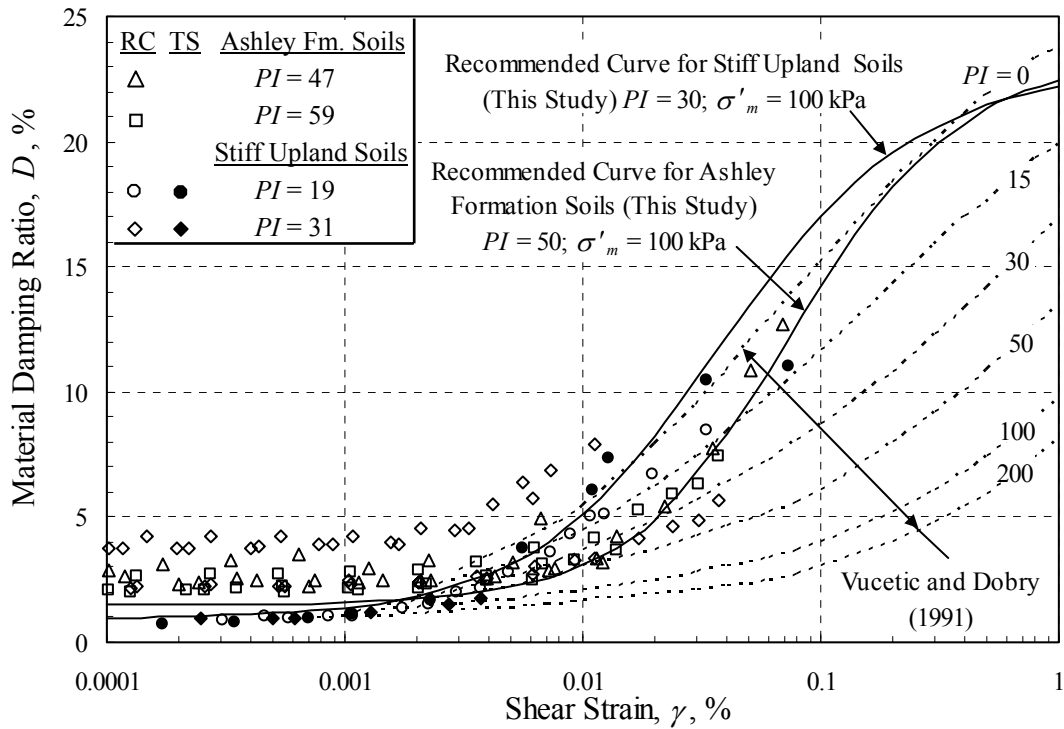
Figure 3.16 - Comparison of compiled data and recommended D - log γ curves for the Tertiary-age Ashley Formation and stiff Upland soils with curves proposed by Vucetic and Dobry (1991).
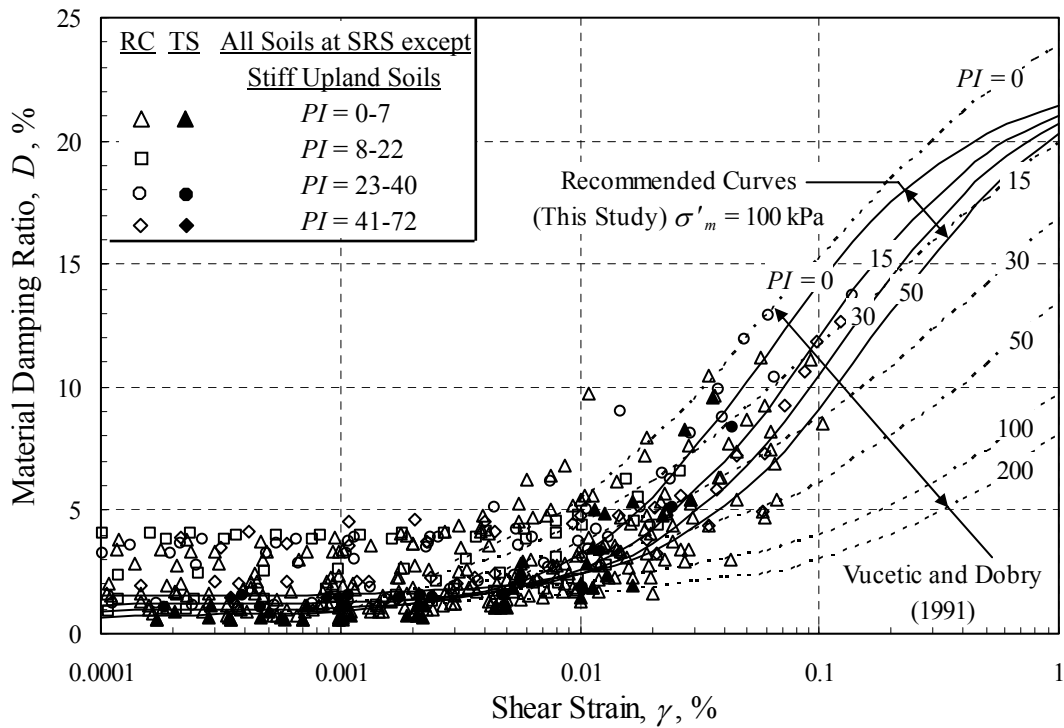
Figure 3.17 - Comparison of compiled data and recommended D - log γ curves for all Tertiary-age soils at SRS except the stiff Upland soils with curves proposed by Vucetic and Dobry (1991).

55
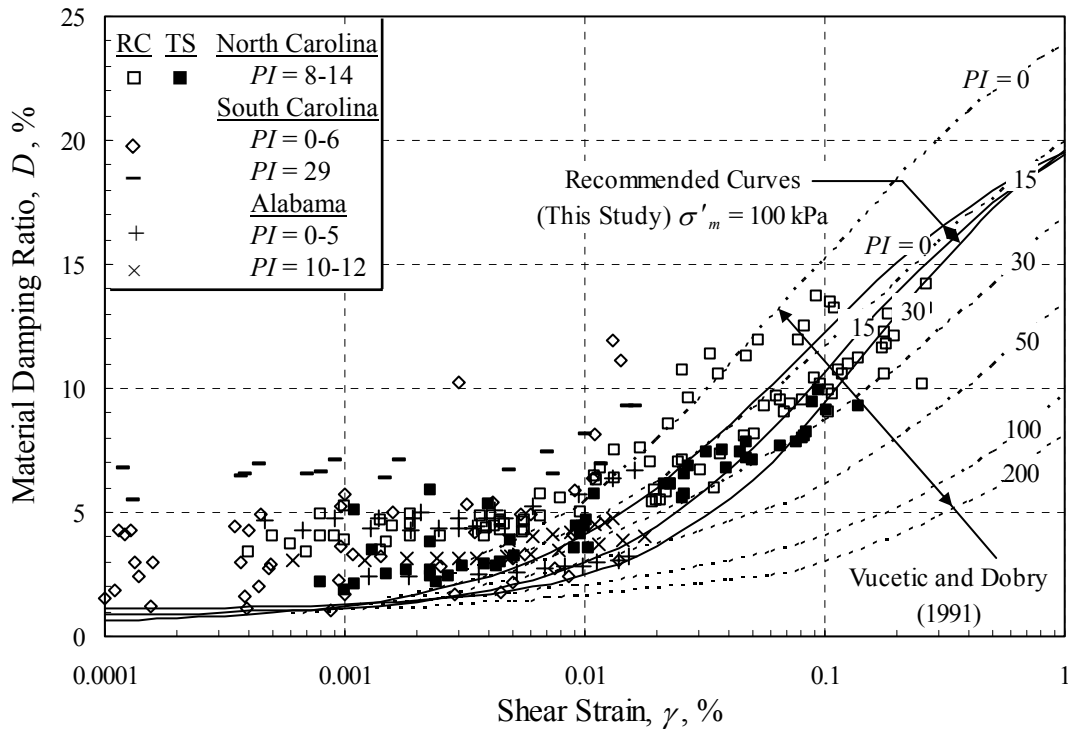
Figure 3.18 - Comparison of compiled data and recommended D - log γ curves for Piedmont residual soils and saprolites with curves proposed by Vucetic and Dobry (1991).

differences between the recommended curves and the corresponding Vucetic and Dobry (1991) curves become greater with increasing shear strain and soil plasticity. Just like the G/G_{max} predicting curves, somewhat improved predictions can be obtained if the specific formation at SRS is known, as noted in Table 3.3.

Presented in Figure 3.18 are the recommended damping curves for Piedmont residual soils and saprolites. The recommended curve for $PI = 0$ lies below the Vucetic and Dobry (1991) curve for $PI = 0$. However, it is still within the lower range proposed by Seed *et al.* (1986) for sand. The recommended curves for $PI = 15$ and 30 also plot lower than the corresponding Vucetic and Dobry (1991) curves at medium strain, but rise close to or above them at greater strains.

3.5 SUMMARY

In this chapter, procedures for estimating normalized shear modulus and material damping ratio of South Carolina soils were developed using existing Resonant Column and Torsional Shear test data for 122 samples and assuming a modified hyperbolic model. The recommended procedures can be summarized in the following eight steps:

1. Identify the major geologic units beneath the site in question. This involves determining the age (e.g., Holocene, Pleistocene, Tertiary) and/or formation (e.g., Ashley, Tobacco Road, Dry Branch) of each soil/rock layer.

2. From available subsurface data, develop profiles of soil type, average *PI*, and soil density. Subdivide major geologic units to reflect significant changes in *PI* and soil density. Also, identify the depth of the ground water table, noting any seasonal fluctuations and artesian pressures.

3. Assuming reasonable values of K'_0, calculate the average σ'_m and determine the corresponding ±50 % range of the σ'_m for each major geologic unit.

4. For each major geologic unit, calculate σ'_m for each layer within it. If the values of σ'_m for each layer is within ±50 % range of that geologic unit determined in Step 3, then the average σ'_m of the geologic unit is assigned to all layers within it. Otherwise, the major geologic unit needs to be subdivided and more than one average value of σ'_m should be used for the geologic unit to ensure the actual σ'_m of each layer is within ±50 % range of the assigned value.

5. Select the appropriate values of γ_{r1}, α, *k* and D_{min1} from Table 3.3 for each layer according to the geologic unit and *PI*. These values may be picked by rounding to the nearest listed *PI* value, or by interpolating between listed *PI* values.

6. Using Equations 3.3 and 3.7, convert the values of γ_{r1} and D_{min1} obtained in Step 5 to values of γ_r and D_{min} that correspond to the average σ'_m values assigned in Step 4.

7. Determine the design G/G_{max} curve for each layer by substituting γ_r and α into Equation 3.2.

8. Determine the design *D* curve for each layer by substituting Equation 3.8, G/G_{max} and D_{min} into Equation 3.5.

The design curves determined in Steps 7 and 8 were considered mean curves based on the available data. Generally, the design curves model the data well at small to medium strains. At high strains, the curves appeared to slightly under predict G/G_{max} and over predict *D* in some cases. Thus, a range of possible curves should be considered in the design. The calculated values of *COV* for Ln (γ_{r1}) were about 12 % for all Tertiary-age soils at SRS, except stiff Upland soils and about 15 % for Piedmont residual soils and saprolites. The *COV* values provided an indication of the uncertainty of the design curves. More data are needed before *COV* values can be calculated for the other geologic units.

Greater care should be exercised with using the curves for Pleistocene-age and Tertiary-age soils in the Charleston area, because they were determined using only four test specimens. More data are needed from all areas of the state, particularly from the Lower Coastal Plain area, to further validate the recommended curves.

In general, the Holocene soils exhibited more linearity than the older soils with similar *PI*. The recommended G/G_{max} curve for Holocene soils with *PI* = 0 follows the Seed *et al.* (1986) upper range curve for sand, the Idriss (1990) curve for sand, and the Stokoe *et al.* (1999) curve for sand. On the other hand, the recommended G/G_{max} curves for the older soils with *PI* = 0 generally follow the Seed *et al.* (1986) mean or lower range curve for sand and the Vucetic and Dobry (1991) curve for *PI* = 0 soils. The recommended *D* curve for Holocene soils with *PI* = 0 follows the Seed *et al.* (1986) lower range curve for sand and the Idriss (1990) curve for sand and clay. The recommended *D* curves for the older soils with *PI* = 0 generally follow the Seed *et al.* (1986) mean curve for sand and the Vucetic and Dobry (1991) curve for *PI* = 0 soils.

CHAPTER 4

APPLICATION OF THE RECOMMENDED PROCEDURES FOR
ESTIMATING THE DYNAMIC PROPERTIES OF SOUTH CAROLINA SOILS

To illustrate the application of the procedures recommended in Chapters 2 and 3 for estimating the dynamic properties of South Carolina soils, an example site from the geotechnical investigations for the new Cooper River Bridge, South Carolina, is considered in this chapter.

4.1 NEW COOPER RIVER BRIDGE AND EXAMPLE SITE

When completed, the new Cooper River Bridge will be North America's longest cable-stay span bridge, connecting the City of Charleston and the Town of Mount Pleasant (http://www.scdot.org). It is being built to replace the existing Grace Memorial and Silas N. Pearman bridges, which were completed in 1929 and 1966, respectively. Geotechnical investigations for the new bridge involved numerous field tests, including SPTs, CPTs and V_s measurements.

The example site is the cone sounding designated as DS-1, which is located near the edge of the Cooper River on the Mount Pleasant side (S&ME, 2000). The ground surface elevation at DS-1 is 2.9 m above mean sea level. Presented in Figure 4.1 are the seismic CPT measurements made at DS-1. Cone tip resistances are shown in Figure 4.1(a). Higher tip resistances indicate denser or stiffer soil. Cone friction ratios, defined as the sleeve resistance divided by the tip resistance, are shown in Figure 4.1(b). Low friction ratios (say < 0.5 %) indicate little or no silt and clay (fines). High friction ratios (say > 1.5 %) indicate significant fines. Pore pressure measurements are shown in Figure 4.1(c). They depend on the soil-cone behavior and the ground water table location. The ground water table lies near the ground surface at a depth of about 0.5 m. Values of V_s are shown in 4.1(d), and are a direct measure of small-strain soil stiffness.

For site response analysis, the profile of V_s and the variations of G/G_{max} and D with shear strain for each soil layer are needed. The step-by-step process for selecting these dynamic soil properties is described in the following sections.
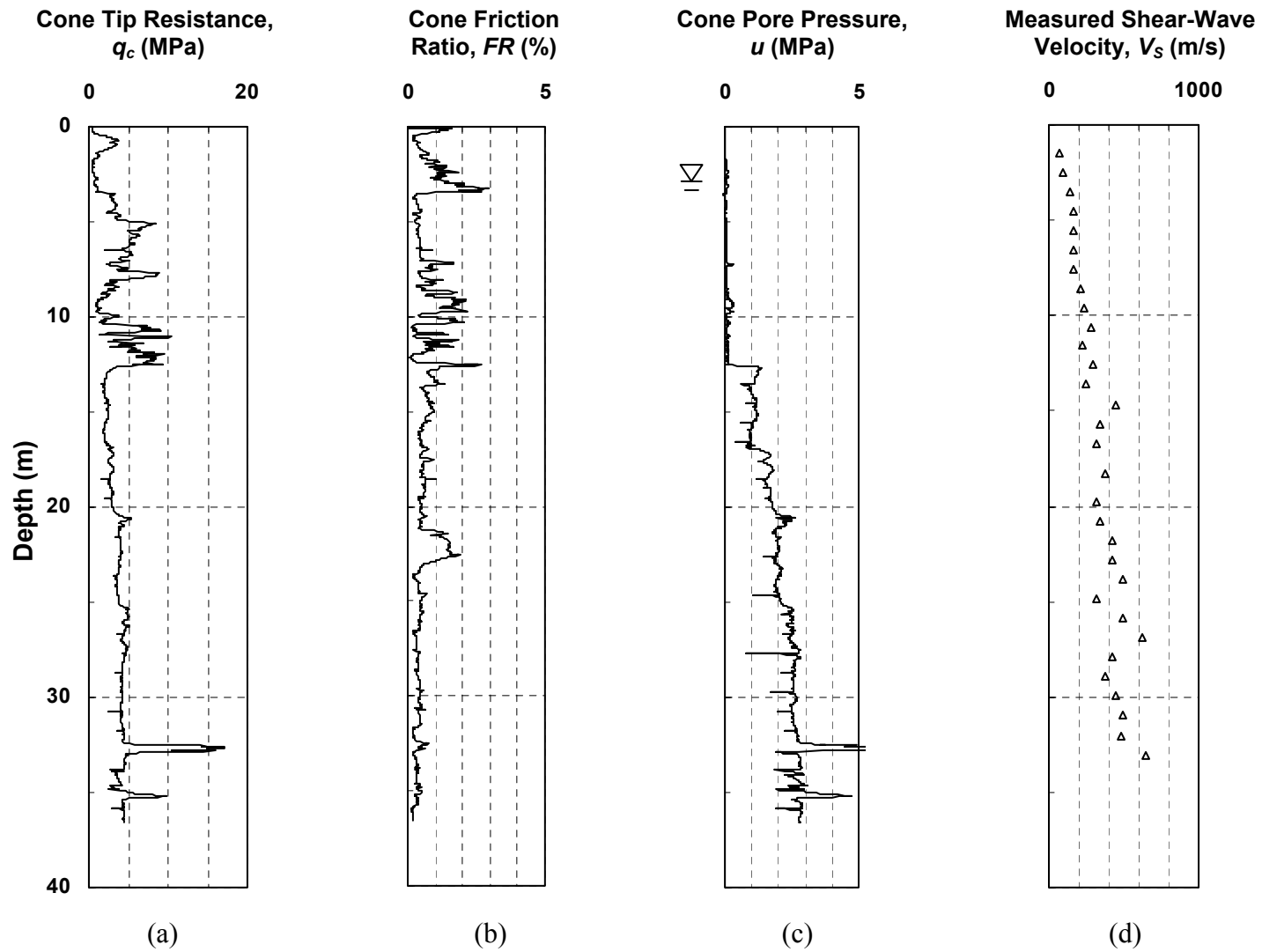
Figure 4.1 Seismic CPT measurements from the DS-1 investigation site, new Cooper River Bridge (S&ME, 2000).

4.2 PREDICTED SHEAR-WAVE VELOCITY FROM CPT DATA

Although V_s measurements are available at DS-1 and can be used directly for site response analysis, values of V_s are predicted from CPT data to illustrate the procedure. Based on the findings in Chapter 2, V_s can be estimated from CPT measurements in all soil types using the following equation (Equation 2.9):

$$V_s = 4.63 q_c^{0.342} I_c^{0.688} Z^{0.092} ASF \tag{4.1}$$

where V_s is the predicted shear-wave velocity in m/s, q_c is the cone tip resistance in kPa, I_c is the soil behavior type index, Z is the depth in m, and ASF is an age scaling factor. The values of q_c and Z are measured directly during CPT testing, and no special corrections are needed for them. On the other hand, additional information and calculation are required for ASF and I_c.

4.2.1 Age Scaling Factor

Shown in Figure 4.2 are the CPT measurements and major geologic units at the DS-1 site. The geologic units are inferred from the geologic map by Weems and Lemon (1993) and the CPT measurements. The Tertiary-age Ashley Formation, locally known as the "Cooper Marl," is characterized by: 1) fairly uniform cone tip resistances that do not project to 0.0 MPa at the ground surface, as observed in Figure 4.2(a); 2) fairly uniform friction ratios, as seen in Figure 4.2(b); and 3) high cone pore pressures, as observed in Figure 4.2(c). In the Holocene- and Pleistocene-age sediments, particularly the granular sediments, cone pore pressures are typically much lower than in the Ashley Formation and often follow the static pore-water pressure line (= unit weight of water multiplied by depth below the ground water table), as seen in Figure 4.2(c). One characteristic that can sometimes be used to distinguish between Holocene- and Pleistocene-age soils in uniform clay layers below the ground water table is the trend of cone tip resistances. The profile of cone tip resistance in saturated Holocene-age clays often projects to a tip resistance near 0.0 MPa at the ground surface, as observed in the clayey layer between 2 m and 3.5 m. In Pleistocene-age clays, however, the profile of cone tip resistance often projects back to a value greater than 0.0 MPa at zero depth, but less than the projected value for the Ashley Formation.

From Table 2.5, when using Equation 4.1 in the Charleston area, appropriate values of ASF are: 1.00 for Holocene-age soils, 1.23 for Pleistocene-age soils, and 2.29 for the Tertiary-age Ashley Formation.
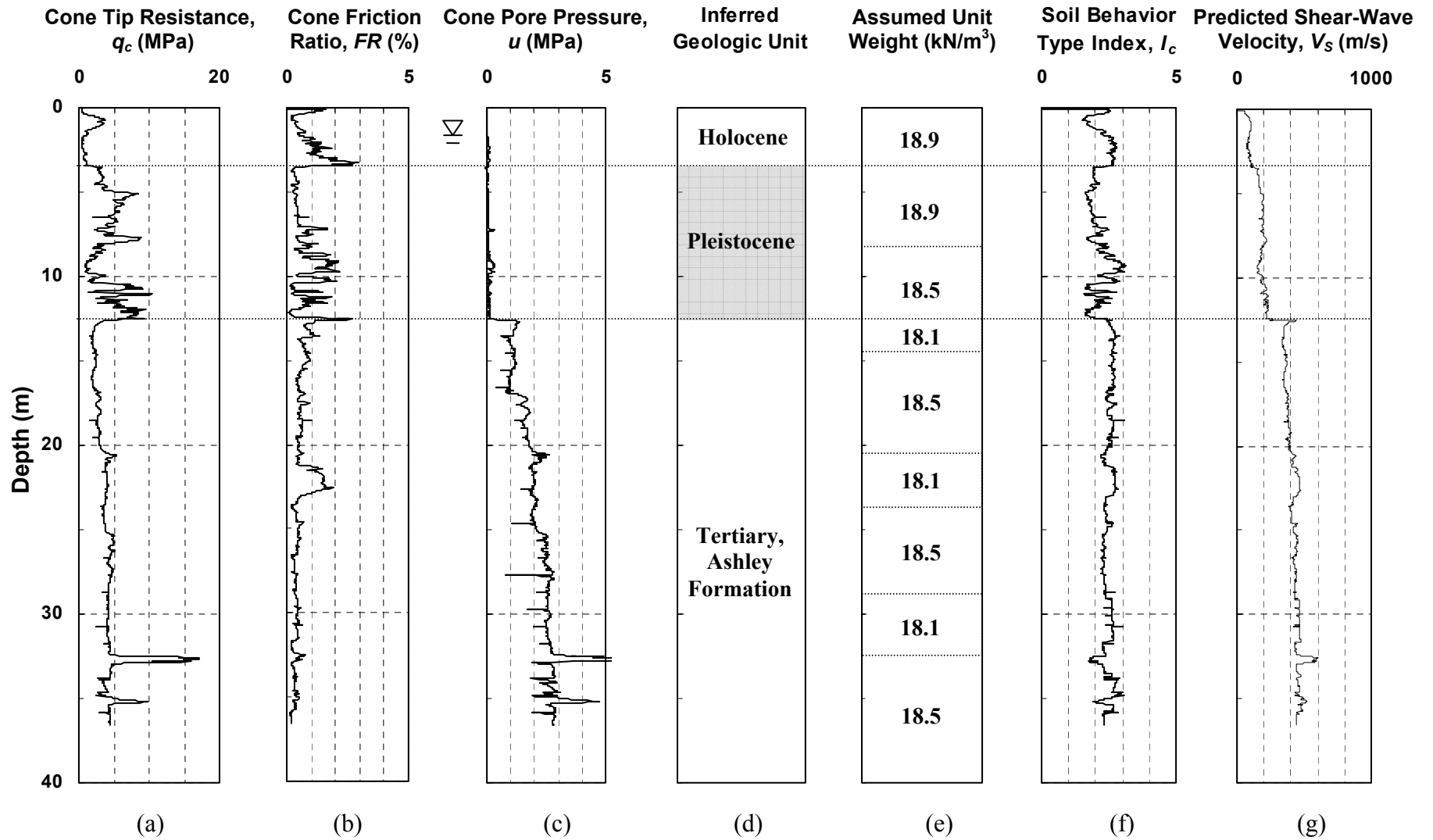
Figure 4.2 Predicted V_s from CPT measurements at DS-1.

4.2.2 Soil Behavior Type Index

As discussed in Section 2.1.3, the soil behavior type index, I_c, is calculated using the following equation (Equation 2.6):

$$I_c = \left[(3.47 - \log Q)^2 + (1.22 + \log F)^2\right]^{0.5} \tag{4.2}$$

where

$$Q = \frac{q_c - \sigma_v}{P_a}\left(\frac{P_a}{\sigma'_v}\right)^n \tag{4.3}$$

$$F = \frac{f_s}{q_c - \sigma_v} \times 100\% \tag{4.4}$$

and σ_v and σ'_v are total and effective vertical pressures, respectively, P_a is a reference pressure of 100 kPa, and f_s is sleeve resistance. The units of $q_c, f_s, \sigma_v, \sigma'_v$ and P_a are all the same.

The values of n and I_c are determined through an iterative procedure. The iterative procedure begins by assuming $n = 1.0$ and calculating I_c. If the calculated I_c is greater than 2.6, then this is the final value of I_c. Otherwise, I_c is recalculated using $n = 0.5$. If the recalculated I_c is less than 2.6, then I_c based on $n = 0.5$ is the final value. However, if the recalculated I_c is greater than 2.6, I_c is again recalculated using $n = 0.7$ for the final value.

To illustrate this iterative procedure, CPT measurements from DS-1 at the depth of 4.99 m are considered. The cone measurements at this depth are: $q_c = 5545$ kPa, and $f_s = 14$ kPa. Values of σ_v and σ'_v at a depth of 4.99 m are about 94 kPa and 50 kPa, respectively, assuming the unit weights listed in Figure 4.2(e). The assumed unit weights are based on penetration measurements, as well as soil descriptions given in the boring logs. Assuming $n = 1.0$, the computed values of Q, F and I_c are 109, 0.26 % and 1.56, respectively. Because I_c is less than 2.6, Q and I_c are recalculated assuming $n = 0.5$. For $n = 0.5$, the computed Q is 77 and I_c is 1.70. The I_c value of 1.70 is the final value because it is less than 2.6 when n of 0.5 is assumed. Final calculated values of I_c for the entire DS-1 CPT profile are plotted in Figure 4.2(f).

4.2.3 Predicted and Design V_s

Using Equation 4.1, the predicted V_s at the depth of 4.99 m is calculated as follows:

$$V_s = 4.63(5545)^{0.342}(1.70)^{0.688}(4.99)^{0.092}(1.23) = 181\,\text{m/s} \tag{4.5}$$

The calculation shown in Equation 4.5 can be repeated for all depths of the DS-1 CPT profile to generate the predicted V_s profile shown in Figure 4.2(g).

A comparison of the predicted and measured V_s profiles is presented in Figure 4.3. Some of the scatter observed in the measured V_s profile could be the result of difficult picks of the shear-wave arrivals, particularly at the greater depths where the source-to-receiver distances are fairly large in seismic cone testing. On the other hand, some of the scatter in V_s measurements in the Ashley Formation could be due to the variation in carbonate content. Nevertheless, both V_s profiles agree reasonably well, validating the accuracy of Equation 4.1 and age scaling factors.

Also plotted in Figure 4.3 is the base V_s profile selected for input into site response analysis. The base input, or design, V_s profile is obtained as follows: For each layer, average values for the measured V_s profile and predicted V_s profile are calculated first. Then, the mean value of these two averages is taken as the base design V_s for the layer. The resulting base design V_s profile reflects major changes in the stratigraphy and provides average values for each layer (see Figure 4.2).

Tabulated values of the base design V_s profile are given in Table 4.1. Below a depth of 36.5 m, values of V_s are based on downhole seismic measurements near DS-1 to a depth of about 100 m (S&ME, 2000) and estimates used in previous studies (Wheeler and Cramer, 2000; URS et $al.$, 2001). The design V_s profile extends to a depth of 808 m where the top of Pre-Cretaceous basement bedrock is assumed to be.

The base design V_s profile is used to begin the site response analysis. It is suggested that variation to the base design V_s profile also be considered in the analysis, particularly variations that bound the measured and predicted V_s values.

4.3   PREDICTED G/G_{max} CURVE FROM SITE CHARACTERISTICS

As discussed in Chapter 3, the variation of G/G_{max} with shear strain can be predicted using the following modified hyperbolic model (Equation 3.2):

$$G/G_{\max} = \frac{1}{1+\left(\dfrac{\gamma}{\gamma_r}\right)^{\alpha}}$$

(4.6)

where γ is the shear strain, γ_r is the reference strain, and α is the curvature coefficient. Values of α and γ_r at a mean effective confining pressure, σ'_m, of 100 kPa are selected from Table 3.3 based on the geology and PI of the soil at the depth in question.
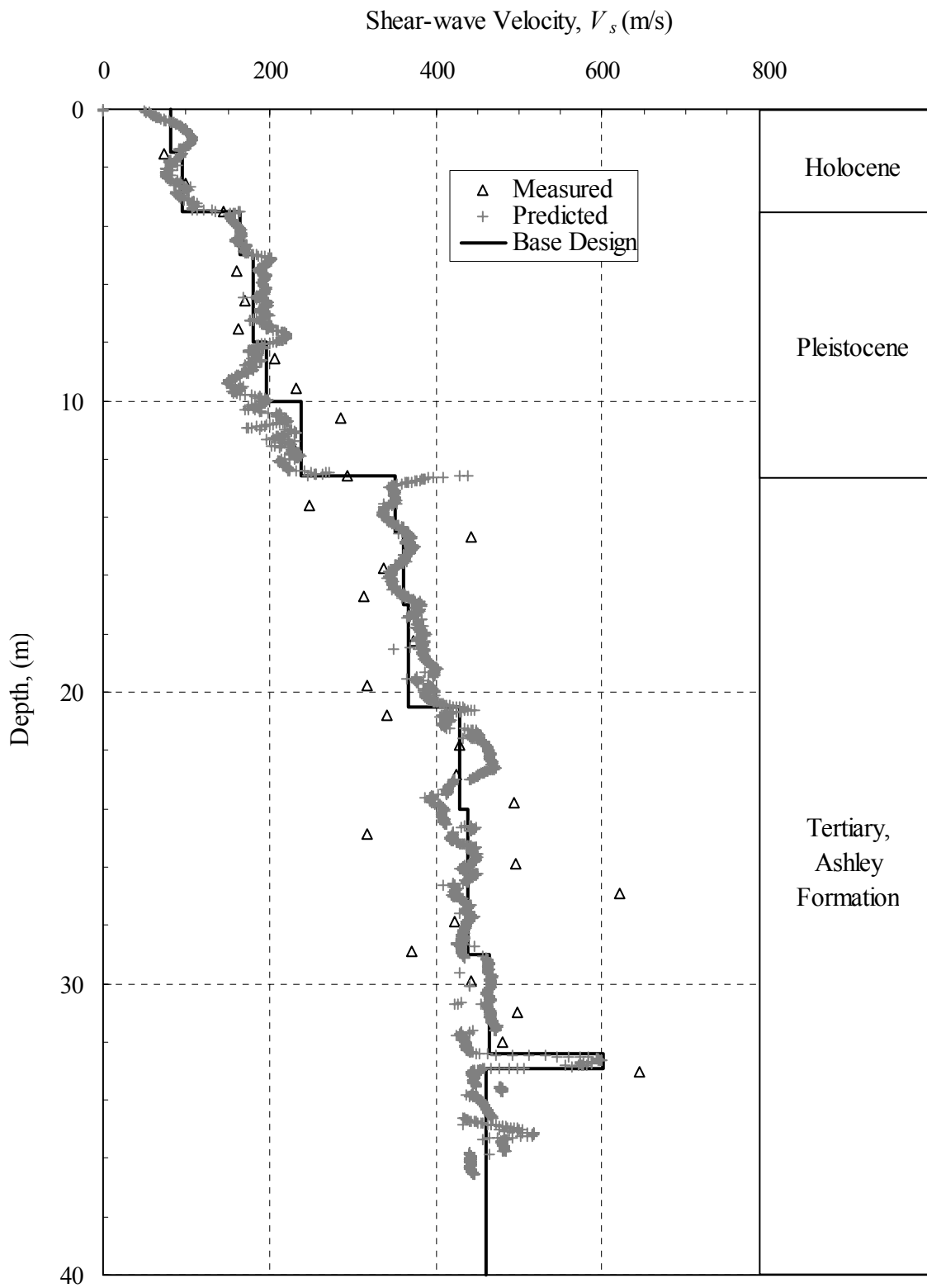
Figure 4.3. Comparison of measured and predicted V_s profiles for the DS-1 site.

Table 4.1 – Generalized soil/rock model for the DS-1 site, new Cooper River Bridge.

Layer No.	Thick-ness (m)	Bottom of Layer Depth (m)	Base Design V_s (m/s)	Total Unit Weight (kN/m³)	USCS Soil Type	Geology	PI	Average σ'_m (kPa)
1	1.5	1.5	81	18.9	SP-SC	Holocene	15	15
2	2	3.5	96	18.9	CH	Holocene	70	
3	1.5	5	165	18.9	SP-SC	Pleistocene	15	
4	3	8	181	18.9	SP-SC	Pleistocene	15	50
5	2	10	197	18.5	SC-SM	Pleistocene	15	
6	2.6	12.6	238	18.5	SC-SM	Pleistocene	15	
7	1.9	14.5	352	18.1	CH	Ashley Fm.	50	
8	2.5	17	362	18.5	SC	Ashley Fm.	30	
9	3.5	20.5	366	18.5	SC	Ashley Fm.	30	
10	3.5	24	428	18.1	MH	Ashley Fm.	50	
11	2.5	26.5	439	18.5	ML	Ashley Fm.	30	150
12	2.5	29	439	18.5	ML	Ashley Fm.	30	
13	3.4	32.4	466	18.1	MH	Ashley Fm.	50	
14	0.5	32.9	561	18.5	ML	Ashley Fm.	30	
15	3.6	36.5	463	18.5	ML	Ashley Fm.	30	
16	2.5	39	463	18.5	ML	Ashley Fm.	30	
17	2.5	41.5	463	18.5	ML	Ashley Fm.	30	
18	2.5	44	463	18.5	ML	Ashley Fm.	30	
19	5	49	463	18.1	CH	Ashley Fm.	50	
20	5	54	463	18.1	CH	Ashley Fm.	50	
21	6	60	540	18.1	CH	Ashley Fm.	50	400
22	10	70	655	18.5	CL,ML	Ashley Fm.	30	
23	10	80	655	18.5	SC-SM	Ashley Fm.	30	
24	10	90	762	18.9	CL,ML	Ashley Fm.	30	
25	10	100	762	18.9	SM,ML	Ashley Fm.	30	
26	20	120	762	19.6	Limestone	SRS All*	15	
27	20	140	777	19.6	Limestone	SRS All*	15	900
28	40	180	808	19.6	Limestone	SRS All*	15	
29	40	220	839	21.2	Silt, Sand	SRS All*	15	
30	70	290	881	22.5	Clayey Silt	SRS All*	30	
31	80	370	939	22.5	Clayey Silt	SRS All*	30	2500
32	80	450	1000	22.5	Clayey Silt	SRS All*	30	
33	178	528	1100	22.5	Sand	SRS All*	15	5000
34	180	808	1240	22.5	Sand	SRS All*	15	
35	Base	--	2900	22.5	--	Pre-Cretaceous Rock	--	--

* All soils at SRS except stiff Upland soils.

The inferred geology and approximate values of *PI* and σ'_m for each soil/rock layer beneath DS-1 are listed in Table 4.1. Values of *PI* are based on USCS soil types reported in the logs for nearby boreholes and are rounded to the nearest values listed in Table 3.3. Values of σ'_m are calculated assuming a coefficient of effective earth pressures at rest, K'_0, of 0.5 for all geologic units. Ideally, σ'_m should be calculated for each layer. However, this would mean having a unique curve for each layer, requiring more data entry time. Stokoe *et al.* (1995) suggested that σ'_m should be within ±50 % of the actual value. The approach used in this example is to calculate σ'_m at the center of each major geologic unit and compare that calculated value with the σ'_m value calculated for each layer within the unit. If the σ'_m for each layer is within ±50 % range of the calculated value for the geologic unit, then the σ'_m at the center of the major geologic unit is assigned to all layers within it. Otherwise, the geologic unit is subdivided and different σ'_m values are used for each subgroup. For example, two σ'_m values are used for the Ashley Formation unit because the unit is fairly thick and σ'_m values of layers change significantly through the unit (see Table 4.1).

To illustrate the procedure for selecting the G/G_{max} design curve, Layer 1 in Table 4.1 is used as an example. Layer 1 is 1.5 m thick and Holocene in age. Soil in Layer 1 exhibits *PI* values around 15. Thus, from Table 3.3, $\gamma_{r1} = 0.114$, $\alpha = 0.96$ and $k = 0.202$. For a σ'_m of 15 kPa, the average value for the Holocene unit, γ_r is calculated as (Equation 3.3):

$$\gamma_r = 0.114 \left(\frac{15 kPa}{100 kPa} \right)^{0.202} = 0.078 \tag{4.7}$$

Substituting α and γ_r into Equation 4.6 leads to the following equation:

$$G/G_{max} = \frac{1}{1 + \left(\dfrac{\gamma}{0.078} \right)^{0.96}} \tag{4.8}$$

Equation 4.8 defines the G/G_{max} design curve for Layer 1 and is plotted in Figure 4.4(a).

The above procedure for selecting G/G_{max} design curve for Layer 1 is repeated for Layers 2 through 34. The resulting base design curves for these layers are plotted in Figures 4.4(a), 4.5(a) and 4.6(a). Because no G/G_{max} test data are available for geologic units beneath the Ashley Formation in Charleston, curves for similar units at SRS are assumed. The variables defining the G/G_{max} base design curves are summarized in Table 4.2.

It should be pointed out that the G/G_{max} base design curves presented here are based on best-estimate values of available laboratory data and are considered as mean curves only. To accommodate uncertainty in material properties and design at different levels of risk, the base design curves can be varied using the corresponding *COV* values of Ln (γ_{r1}) (see Table 3.3).
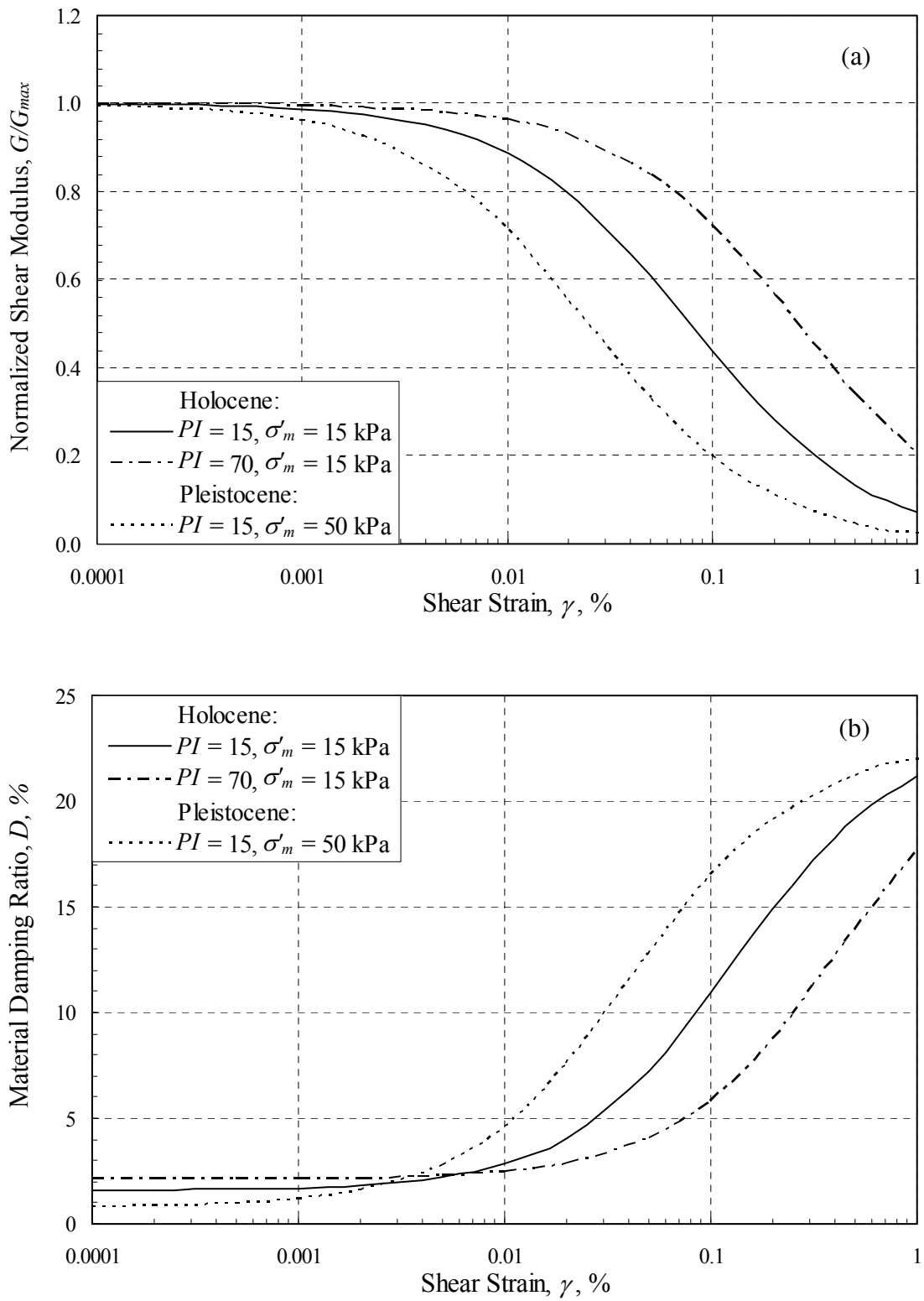
Figure 4.4. Base design (a) normalized shear modulus and (b) material damping ratio curves for the Holocene and Pleistocene soils at the DS-1 site.
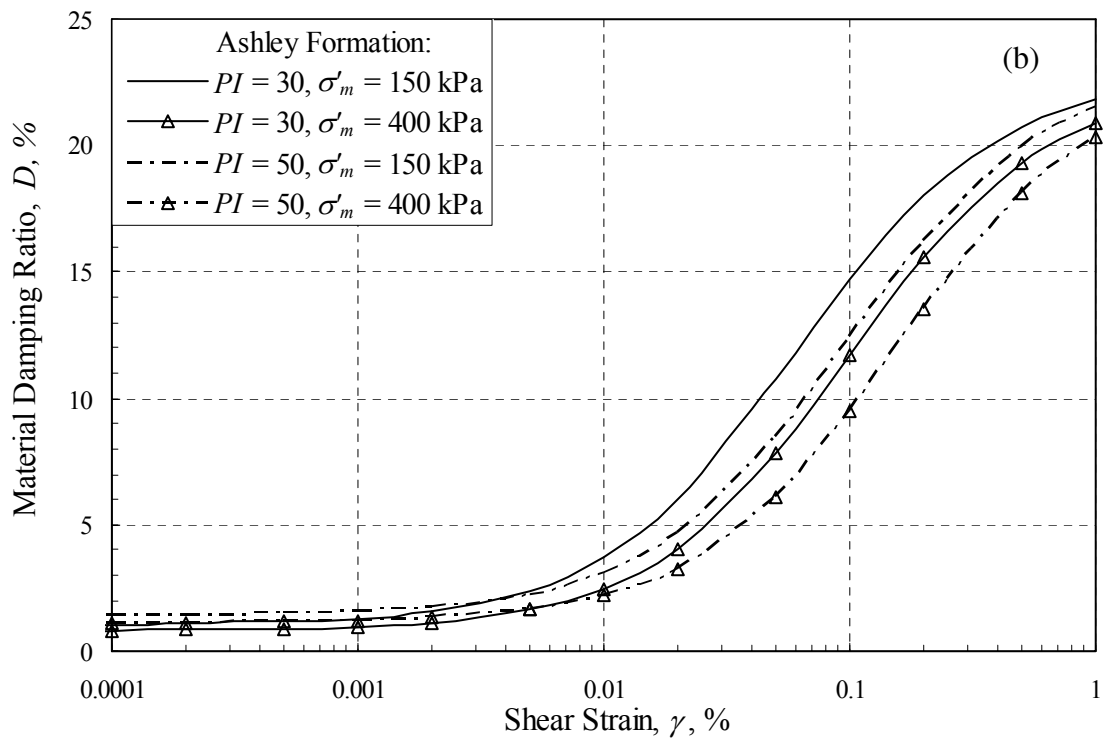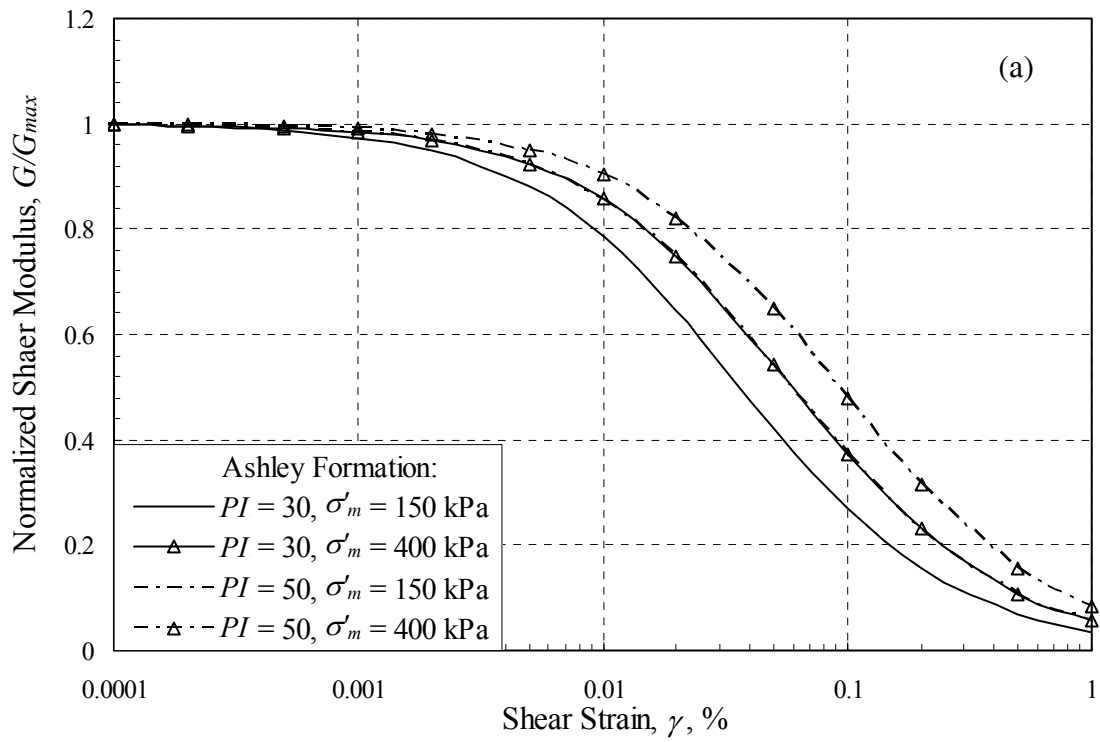
Figure 4.5. Base design (a) normalized shear modulus and (b) material damping ratio curves for the Ashley Formation at the DS-1 site.
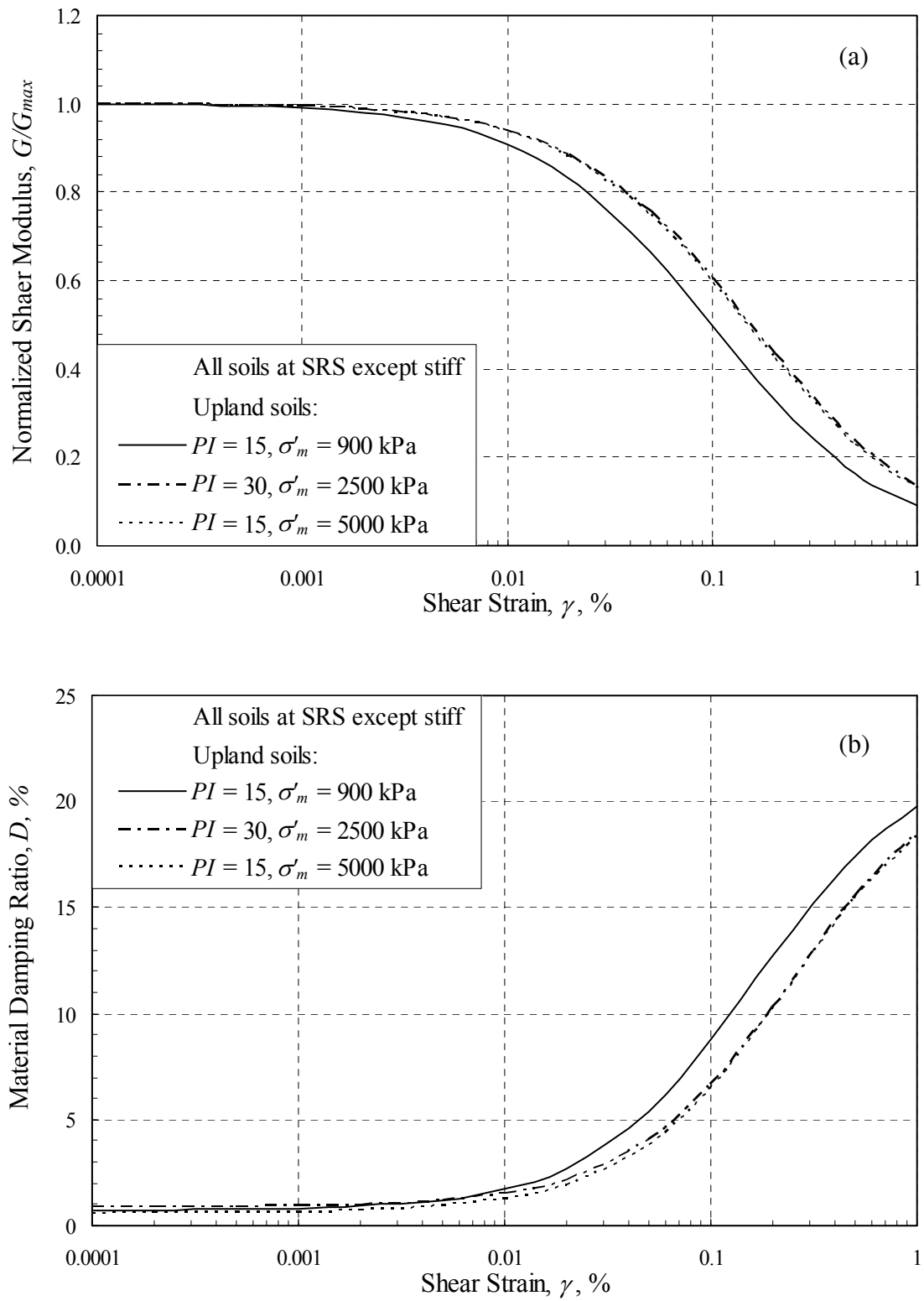
Figure 4.6. Base design (a) normalized shear modulus and (b) material damping ratio curves for soils beneath the Ashley Formation at the DS-1 site.

Table 4.2. Base design values of γ_r, α, k, and D_{min} for the DS-1 site.

Geologic Age (Formation)	Variable	Soil Plasticity Index, PI				
		0	15	30	50	70
Holocene	γ_{r1}, %		0.114			0.267
	α		0.96			0.99
	k		0.202			0.019
	D_{min1}, %		1.29			2.06
	$\gamma_{r\ 15\ kPa}$, %		0.078			0.257
	$D_{min\ 15\ kPa}$, %		1.57			2.10
Pleistocene (Wando)	γ_{r1}, %		0.032			
	α		1.02			
	k		0.402			
	D_{min1}, %		0.66			
	$\gamma_{r\ 50\ kPa}$, %		0.025			
	$D_{min\ 50\ kPa}$, %		0.76			
Tertiary (Ashley)	γ_{r1}, %			0.030	0.049	
	α			1.10	1.15	
	k			0.497	0.455	
	D_{min1}, %			1.14	1.52	
	$\gamma_{r\ 150\ kPa}$, %			0.037	0.059	
	$D_{min\ 150\ kPa}$, %			1.03	1.39	
	$\gamma_{r\ 400\ kPa}$, %			0.060	0.092	
	$D_{min\ 400\ kPa}$, %			0.81	1.11	
Tertiary and Cretaceous (All soils at SRS except stiff Upland soils)	γ_{r1}, %		0.058	0.079		
	α		1.00	1.00		
	k		0.240	0.208		
	D_{min1}, %		0.94	1.19		
	$\gamma_{r\ 900\ kPa}$, %		0.098			
	$D_{min\ 900\ kPa}$, %		0.72			
	$\gamma_{r\ 2500\ kPa}$, %			0.154		
	$D_{min\ 2500\ kPa}$, %			0.85		
	$\gamma_{r\ 5000\ kPa}$, %		0.149			
	$D_{min\ 5000\ kPa}$, %		0.59			

4.4   PREDICTED DAMPING FROM SITE CHARACTERISTICS

From Chapter 3, the material damping can be predicted by (Equation 3.5):

$$D = f(G/G_{\max}) + D_{\min} \tag{4.9}$$

where

$$f(G/G_{\max}) = 12.2(G/G_{\max})^2 - 34.2(G/G_{\max}) + 22.0 \tag{4.10}$$

The value of D_{min} at σ'_m of 100 kPa, D_{min1}, is selected from Table 3.3 according to geology and *PI* of the considered soil.

Considering Layer 1 in the generalized model for the DS-1 site (see Table 4.1), the value of D_{min1} listed in Table 3.3 for Holocene soil with $PI = 15$ and $\sigma'_m = 100$ kPa is 1.29. This value is adjusted to a σ'_m of 15 kPa by (Equation 3.7):

$$D_{min} = 1.29 \left(\frac{15kPa}{100kPa} \right)^{-0.202/2} = 1.57 \tag{4.11}$$

Substituting D_{min} of 1.57 and Equation 4.8 into Equation 4.9 leads to the following predictive equation:

$$D = 12.2 \left(\frac{1}{1 + \left(\dfrac{\gamma}{0.078} \right)^{0.96}} \right)^2 - 34.2 \left(\frac{1}{1 + \left(\dfrac{\gamma}{0.078} \right)^{0.96}} \right) + 23.57 \tag{4.12}$$

Equation 4.12 defines the damping design curve for Layer 1 and is plotted in Figure 4.4(b).

The above procedure for selecting the damping design curve for Layer 1 is repeated for Layers 2 through 34. The resulting damping design curves are plotted in Figures 4.4(b), 4.5(b) and 4.6(b). Because no material damping test data are available for geologic units beneath the Ashley Formation in Charleston, curves for similar units at SRS are assumed. The variables defining the damping design curves are summarized in Table 4.2.

Due to the scarcity of TS test results, the uncertainty in D_{min} is not characterized in this study. It is reasonable to assume that the uncertainty in D_{min} is similar to or even higher than that of γ_r. However, this uncertainty is only important in the small-strain range. In the medium- and high-strain ranges, the contribution of D_{min} for total damping is not significant.

4.5 SUMMARY

Procedures described in Chapter 2 and 3 for estimating the dynamic properties of South Carolina soils were applied in this chapter to the DS-1 site of the new Cooper River Bridge project. Predicted values of V_s compare well with V_s values measured at DS-1 by the seismic CPT. A base design V_s profile for DS-1 was presented in Figure 4.3. This base design V_s profile was based on values measured by the seismic CPT test and results predicted by the CPT-V_s equation recommended in Chapter 2 for all soil types. It was suggested variations to the base design V_s profile, particularly variations that bound the measured and predicted V_s values, also be considered in the site response analysis.

Base design G/G_{max} and D curves for each layer beneath the DS-1 site were presented in Figures 4.4, 4.5 and 4.6. These curves were based on the geology, PI and σ'_m information summarized in Table 4.1. Confining pressures for each layer were within ±50 % of the assigned value used to establish these curves, as suggested by Stokoe *et al*. (1995). Variations to the base design curves should also be considered in the site response analysis to account for the uncertainty in dynamic material properties.

CHAPTER 5

SUMMARY AND RECOMMENDATIONS

5.1 SUMMARY

Presented in this report are guidelines for estimating the dynamic properties of South Carolina soils for ground response analysis. The guidelines include recommended procedures for estimating the field V_S from penetration measurements, as well as the normalized shear modulus and material damping ratio curves from site characteristics.

The recommended CPT-V_S and SPT-V_S regression equations for Holocene-age soils are listed in Tables 2.4 and 2.6, respectively. Recommended age scaling factors were 1.2 to 1.3 for Pleistocene-age soils. For Tertiary-age soils, recommended age scaling factors ranged from 1.4 to 2.3 and appeared to depend on the amount of carbonate in the soil. Residual standard deviations associated with the recommended regression equations were about 15 m/s to 25 m/s for the Holocene equations, 40 m/s to 50 m/s for the Pleistocene equations, and 20 m/s to 60 m/s for the Tertiary equations. The equations and age scaling factors were based on previous studies and 123 penetration-velocity data pairs from South Carolina's Coastal Plain. Greater care should be exercised with using the recommended equations outside the range of the compiled V_S data noted in Tables 2.5 and 2.7.

Normalized shear modulus, G/G_{max}, and material damping ratio, D, of South Carolina soils were investigated using existing Resonant Column and Torsional Shear test data. These dynamic soil properties were evaluated with respect to the most important influencing factors identified in the literature—strain amplitude, confining pressure, and plasticity index. In addition, geology was used to group the data. The recommended G/G_{max} base design curves were defined by the modified hyperbolic model given in Equation 3.2 and the curve-fitting parameters listed in Table 3.3. In general, the recommended G/G_{max} base design curve for Holocene soils with $PI = 0$ followed the Seed *et al.* (1986) upper range curve for sand, the Idriss (1990) curve for sand, and the Stokoe *et al.* (1999) curve for sand. On the other hand, the recommended base design curves for the older soils with $PI = 0$ generally followed the Seed *et al.* (1986) mean or lower range curves for sand and the Vucetic and Dobry (1991) curve for $PI = 0$ soil. The recommended base design curves modeled the compiled data well at small to medium strains. At high strains, the recommended base design curves appeared to slightly under

predict the G/G_{max} data in some cases. When applying the curves in design, the uncertainty in soil properties should be taken into account by considering a range of possible curves.

The recommended D base design curves were expressed in terms of D_{min} and $f(G/G_{max})$. Equations 3.6 and 3.7 were suggested for estimating D_{min}, and were established using Torsional Shear data only. The best-fit equation for $f(G/G_{max})$ was given by Equation 3.8. In general, the recommended D base design curve for Holocene soils with $PI = 0$ follow the Seed *et al.* (1986) lower range curve for sand and the Idriss (1990) curve for sand and clay. The recommended base design curves for the older soils with $PI = 0$ generally followed the Seed *et al.* (1986) mean curve for sand and the Vucetic and Dobry (1991) curve for $PI = 0$ soil. Use of the recommended D and G/G_{max} base design curves developed in this report is encouraged over the earlier general curves because they provided better fits to the data from South Carolina.

5.2 RECOMMENDATIONS FOR FUTURE STUDIES

The following future studies are recommended:

1. The database of dynamic properties (i.e., V_S, G/G_{max}, and D) of South Carolina soils compiled for this study should be updated and expanded to include new data that is being generated each day. The South Carolina Department of Transportation is currently involved in several large construction projects across the state that included significant geotechnical investigations. The results of these geotechnical investigations should be cataloged and preserved. Such a database would be a valuable resource for the Department of Transportation, the State of South Carolina, and other organizations working in the State to reduce seismic hazards and improve construction practices.

2. Additional study is needed to better characterize the age scaling factors associated with the CPT-V_S and SPT-V_S equations for older soils, particularly soils in the Piedmont physiographic province. The residual soils and saprolites of the Piedmont may display characteristics quite different from the Coastal Plain sediments analyzed in this study. Also, the SPT data from Tertiary sediments available for this study were limited, making the age scaling factors for the SPT-V_S equations tentative until additional data can be analyzed.

3. More data are needed to better establish some of the G/G_{max} and D curves. The availability of high-quality low- to high-strain data is severely lacking for all areas of the State, except the SRS area. Additional data is particularly needed from the Charleston and other Lower Coastal Plain areas. More Torsional Shear tests, or similar laboratory measurements, for D at low frequency are needed to match the frequency characteristics of possible ground motion. The effect of PI on D_{min} needs to be better quantified in all soil types and geologic units. Also, more testing is needed to better quantify D at high stains.

4. Additional study is needed to quantify the effects of overconsolidation ratio, fines content, grain characteristics, microstructure of the soil, and other factors on the G/G_{max} and D curves. In this study, the effect of overconsolidation was implicitly included in the grouping of the data by geologic unit. The accuracy of the recommended curves may be improved if the effect of overconsolidation could be explicitly considered. Also, a consideration for fine content and microstructure of the soil could lead to more fully understanding of the mechanism through which PI or soil type affect the soil dynamic behavior. The necessity of such a consideration is justified by the fact that sometimes soils do not follow the trend of increasing linearity with increasing PI.

5. Additional work is needed to quantify the uncertainty of the recommended curves. In this report, the uncertainty concerning the compiled data was expressed in terms of COV for log γ_{r1} for soils at SRS and in the Piedmont. The model uncertainties associated with G/G_{max} and D were not considered. That is, it was assumed the actual soil behavior would follow a modified hyperbolic model. However, this assumption was less robust at high strains, as noted in Chapter 3, and this part of the uncertainty cannot be accounted for by COV for log γ_{r1}.

APPENDIX A

REFERENCES

Amick, P., and Gelinas, R. (1991). "The Search for Evidence of Large Prehistoric Earthquakes along the Atlantic Seaboard," *Science*, Vol. 251, 655-658.

Andrus, R. D., and Stokoe, K. H., II (2000). "Liquefaction Resistance of Soils from Shear-Wave Velocity," *Journal of Geotechnical and Geoenvironmental Engineering,* ASCE, Vol. 126, No. 11, 1015-1025.

Andrus, R. D., Stokoe, K. H., II, and Chung, R. M. (1999). "Draft Guidelines for Evaluation Liquefaction Resistance Using Shear Wave Velocity Measurements and Simplified Procedures," *NISTIR 6277,* National Institute of Standards and Technology, Gaithersburg, MD.

Assimaki, D., Kausel, E., and Whittle, A. (2000). "Model for Dynamic Shear Modulus and Damping for Granular Soils," *Journal of Geotechnical and Geoenvironmental Engineering*, ASCE, Vol. 126, No. 10, 859-869.

Baldi, G., Bellotti, R., Ghionna, V., Jamiolkowski, M., and Lo Presti, D. C. F. (1989). "Modulus of Sands from CPTs and DMTs," *Proceedings, 12th International Conference on Soil Mechanics and Foundation Engineering,* Vol. 1, Rio de Janeiro, Balkema, Rotterdam, 165-170.

Borden, R. H., Shao, L., and Gupta, A. (1994). "Construction related vibrations," *Rep. No. FHWA/NC/94-007*, Fed. Hwy. Admin., Washington, D.C.

Borden, R. H., Shao, L., and Gupta, A. (1996). "Dynamic Properties of Piedmont Residual Soils," *Journal of Geotechnical Engineering*, ASCE, Vol. 122, No. 10, 813-821.

Campanella, R. G., and Stewart, W. P. (1982). "Seismic Cone Analysis Using Digital Signal Processing for Dynamic Site Characterization," *Canadian Geotechnical Journal*, Vol. 29, 477-486.

Darendeli, M. B., (2001). "Development of a New Family of Normalized Modulus Reduction and Material Damping Curves," *Ph.D. Dissertation,* The University of Texas at Austin, Austin, TX.

EPRI (1993). "Guidelines for Determining Design Basis Ground Motions," *Final Report*, TR-102293, Electric Power Research Institute, Palo Alto, CA.

Ellis, B. S. (2003). "Regression Equations for Estimating Shear-Wave Velocity in South Carolina Sediments Using Penetration Test Data," *M.S. Thesis*, Clemson University, Clemson, SC.

Fear, C. E., and Robertson, P. K. (1995). "Estimating the Undrained Strength of Sand: A Theoretical Framework," *Canadian Geotechnical Journal,* Vol. 32, 859-870.

FEMA (2000). "HAZUS®99 Estimated Annualized Earthquake Losses for the United States," *FEMA 366*, Federal Emergency Management Agency, Washington, D.C.

Frankel, A. D., Mueller, C. S., Barnhard, T. P., Leyendecker, E. V., Wesson, R. L., Harmsen, S. C., Klein, F. W., Perkins, D. M., and Dickman, N. C. (2000). "USGS National Seismic Hazard Maps," *Earthquake Spectra*, EERI, Vol. 16, No. 1, 1-19.

Fugro-McClelland (Southwest), Inc. (1992). *Report 0401-1098*, test report for S&ME, Inc.

Geovision (2000). "Cooper River Bridge Borehole Velocities, Boreholes MP-2 and MP-5," *Report 0338-01*, report to S&ME, Inc., Corona, CA

Hardin, B. O., and Drnevich, V. P. (1972a). "Shear Modulus and Damping in Soils: Measurement and Parameter Effects," *Journal of Soil Mechanics and Foundation Engineering Division,* ASCE, Vol. 98, No. SM6, 603-624.

Hardin, B. O., and Drnevich, V. P. (1972b). "Shear Modulus and Damping in Soils: Design Equations and Curves," *Journal of Soil Mechanics and Foundation Engineering Division*, ASCE, Vol. 98, No. SM7, 667-692.

Hegazy, Y. A., and Mayne, P. W. (1995). "Statistical Correlations between V_s and Cone Penetration Data for Different Soil Types," *Proceedings of the International Symposium on Cone Penetration Testing, CPT '95,* Linkoping, Sweden, Vol. 2, Swedish Geotechnical Society, 173-178.

Hoyos, L., Jr., and Macari E. J. (1999). "Influence of In Situ Factors on Dynamic Response of Piedmont Residual Soils," *Journal of Geotechnical and Geoenvironmental Engineering*, ASCE, Vol. 125, No. 4, 271-279.

Hu, K., Gassman, S. L., and Talwani, P. (2002). "In-situ Properties of Soils at Paleoliquefaction Sites in the South Carolina Coastal Plain," *Seismological Research Letters*, Vol. 73, No. 6, November/December, 964-978.

Hwang, S. K. (1997). "Dynamic Properties of Natural Soils," *Ph.D. Dissertation,* The University of Texas at Austin, Austin, TX.

Idriss, I. M. (1990). "Response of Soft Soil Sites during Earthquake," *Proceedings of the H. Bolton Seed Memorial Symposium,* Vol. 2, 273-289.

Ishibashi, I., and Zhang, X. J. (1993). "Unified Dynamic Shear Moduli and Damping Ratios of Sand and Clay," *Soils and Foundations,* Japanese Society of Soil Mechanics and Foundation Engineering, Vol. 33, No. 1, 182-191.

Ishihara, K. (1996). *Soil Behavior in Earthquake Geotechnics*, Oxford University Press, New York, NY.

Iwasaki, T., Tatsuoka, F., and Takagi, Y. (1978). "Shear Moduli of Sands under Cyclic Torsional Shear Loading," *Soils and Foundations,* Japanese Society of Soil Mechanics and Foundation Engineering, Vol. 18, No. 1, 39-56.

Kim, D.-S. and Choo, Y. (2001). "Deformation Characteristics of Hydraulic-filled Cohesionless Soils in Korea," *Proceedings, 4th International Conference on Recent Advances in Geotechnical Earthquake Engineering and Soil Dynamics And Symposium in Honor of Prof. W. D. Liam Finn,* Edited by S. Prakash, San Diego, California, Paper No. 2.20.

Kokusho, T., Yoshida, Y., and Esashi, Y. (1982). "Dynamic Properties of Soft Clay for Wide Strain Range," *Soils and Foundations,* Japanese Geotechnical Society, Vol. 22, No. 4, 1-18.

Lanzo, G., and Vucetic, M. (1999). "Effect of Soil Plasticity on Damping Ratio at Small Cyclic Strains," *Soils and Foundations,* Japanese Geotechnical Society, Vol. 39, No. 4, 131-141.

Lee M. K. W. and Finn W. D. L. (1978). "DESRA-2, Dynamic Effective Stress Response Analysis of Soil Deposits with Energy Transmitting Boundary Including Assessment of Liquefaction Potential," *Soil Mechanics Series No. 38,* University of British Columbia, Vancouver, Canada.

Lee, R. C. (1996). "Investigations of Nonlinear Dynamic Soil Properties at the Savannah River Site (U)," WSRC-TR-96-0062, Westinghouse Savannah River Company, Aiken, SC.

Liao, S. S. C., and Whitman, R. V. (1986). "Overburden Correction Factors for SPT in Sands," *Journal of Geotechnical Engineering,* ASCE, Vol. 112, No. 3, 373-377.

Lunne, T., Robertson, P. K., and Powell, J. J. M. (1997). *Cone Penetration Testing in Geotechnical Practice,* E & FN Spon, Routledge, 352 p.

Mayne, P. W., and Rix, J. G. (1995). "Correlations between Shear Wave Velocity and Cone Tip Resistance in Natural Clays," *Soils and Foundations,* Japanese Society of Soil Mechanics and Foundation Engineering, Vol. 35, No. 2, 107-110.

Ni, S.-H. (1987). "Dynamic Properties of Sand under True Triaxial Stress States from Resonant Column/Torsional Shear Tests," *Ph.D. Dissertation,* The University of Texas at Austin, Austin, TX.

Obermeier, S. F., Gohn, G. S., Weems, R. E., Gelinas, R. L., and Rubin, M. (1985). "Geologic Evidence for Recurrent Moderate to Large Earthquakes near Charleston, South Carolina," *Science*, Vol. 227, 408-411.

Ohta, Y., and Goto, N. (1978). "Empirical Shear Wave Velocity Equations in Terms of Characteristic Soil Indexes," *Earthquake Engineering and Structural Dynamics*, Vol. 6, 167-187.

Pantel, N. S. (1981). "Generation and Attenuation of Seismic Waves in Downhole Testing," *Geotechnical Engineering Thesis GT81-1,* Department of Civil Engineering, The University of Texas at Austin, Austin, TX, 411 p.

Piratheepan, P., and Andrus, R. D. (2002). "Estimating Shear-Wave Velocity from SPT and CPT Data," final report to U.S. Geological Survey, Award Number 01HQR0007, Clemson University, Clemson, SC.

Pyke, R. M. (1993). "Modeling of Dynamic Soil Properties," Appendix 7.A in *Guidelines for Determining Design Bases Ground Motions*, Electric Power Research Institute, J. F. Schneider EPRI Project Manager, 7.A-1-7.A-90.

Rix, G. J., and Stokoe, K. H., II (1991). "Correlation of Initial Tangent Modulus and Cone Penetration Resistance," *Proceedings of the First International Symposium on Calibration Chamber Testing/ ISOCCT1,* Postdam, New York, Edited by An-bin Huang, 351-362.

Robertson, P. K. (1990). "Soil Classification Using the Cone Penetration Test," *Canadian Geotechnical Journal,* Vol. 27, No. 1, 151-158.

Robertson, P. K., Woeller, D. J., and Fin, W. D. L. (1992). "Seismic CPT for Evaluating Liquefaction Potential," *Canadian Geotechnical Journal,* Vol. 29, 686-695.

Robertson, P. K., and Wride (Fear), C. E. (1998). "Cyclic Liquefaction and Its Evaluation Based on the SPT and CPT," *Proceedings of the National Center for Earthquake Engineering Research (NCEER) Workshop on Evaluation of Liquefaction Resistance of Soils*, Salt Lake City, Utah, January 1996, Edited by T. L. Youd and I. M. Idriss, NCEER Report NCEER-97-0022, 41-87.

Rollins, K. M., Evans, M. D., Diehl, N. B., and Daily, W. D., III (1998). "Shear Modulus and Damping Relationships for Gravels," *Journal of the Geotechnical and Geoenvironmental Engineering,* ASCE, Vol. 124, No. 5, 396-405.

S&ME (1993-2000). Various unpublished project reports by S&ME, Inc. from 1993-2000, Mount Pleasant, SC. (Project numbers listed in Table C.1)

S&ME. (1993). *Seismic Soil Pile Interaction Analyses - Mark Clark Expressway/Stono River Crossings, Charleston, South Carolina*, Mount Pleasant, SC.

S&ME. (1998). *Second Report of Seismic Analysis - Daniel Island terminal, Charleston, South Carolina, S&ME Job No. 1131-97-741*, Mount Pleasant, SC.

S&ME (2000). *Phase II Geotechnical Data Summary Report - Cooper River Bridge Replacement Project, Charleston, South Carolina, S&ME Job No. 1131-99-876*, Mount Pleasant, SC.

Seed, H. B., and Idriss, I. M. (1970). "Soil Moduli and Damping Factors for Dynamic Response Analysis," *Report EERC 70-10,* Earthquake Engineering Research Institute, Berkeley, CA.

Seed, H. B., and Idriss, I. M. (1982). "Ground Motions and Soil Liquefaction during Earthquakes," Earthquake Engineering Research Institute, Berkeley, CA, 134 p.

Seed, H. B., Wong, R. T., Idirss, I. M., and Tokimatsu, K. (1986). "Moduli and Damping Factors for Dynamic Analysis of Cohesionless Soils," *Journal of the Geotechnical Engineering Division,* ASCE, Vol. 112, No. 11, 1016-1031.

Skempton, A. K. (1986). "Standard Penetration Test Procedures and the Effects in Sands of Overburden Pressure, Relative Density, Particle Size, Aging, and Overconsolidation," *Geotechnique,* Vol. 36, No. 3, 425-477

Stokoe, K. H., II, Lee, S. H. H., and Knox, D. P. (1985). "Shear Moduli Measurements under True Triaxial Stresses," *Proceeding, Advances in the Art of Testing Under Cyclic Conditions,* ASCE, 166-185.

Stokoe, K. H., II, Hwang, S. K., Lee, N. J., and Andrus, R. D. (1994). "Effects of Various Parameters on the Stiffness and Damping of Soils at Small to Medium Strains," *Proceedings, International Symposium on Prefailure Deformation Characteristics of Geomaterials,* Vol. 2, Japanese Society of Soil Mechanics and Foundation Engineering, Sapporo, Japan, 785-816.

Stokoe, K. H., II, Hwang, S. K., Darendeli, M. B., and Lee, N. J. (1995). "Correlation Study of Nonlinear Dynamic Soils Properties," final report to Westinghouse Savannah River Company, The University of Texas at Austin, Austin, TX.

Stokoe, K. H., II, Moulin, B. S., and Darendeli, M. B. (1998). "Laboratory Evaluation of the Dynamic Properties of Intact Soil Specimens from Daniel Island Terminal, South Carolina," *Geotechnical Engineering Report GR98-2,* The University of Texas at Austin, Austin, TX.

Stokoe, K. H., II, Darendeli, M. B., Andrus, R. D., and Brown, L. T. (1999). "Dynamic Soil Properties: Laboratory, Field and Correlation Studies," *Proceedings, 2nd International Conference on Earthquake Geotechnical Engineering,* Vol. 3, Lisbon, Portugal, 811-845.

Sun, J. I., Goleskorkhi, R., and Seed, H. B. (1988). "Dynamic Moduli and Damping Ratios for Cohesive Soils," *Report UCB/EERC-88/15,* University of California at Berkeley, Berkeley, CA.

Sykora, D. W. (1987). "Examination of Existing Shear Wave Velocity and Shear Modulus Correlation in Soils," *Miscellaneous Paper GL-87-22,* U.S. Army Engineer Waterways Experiment Station, Vicksburg, MS.

Talwani, P., and Cox, J. (1985). "Paleoseismic Evidence for Recurrence of Earthquakes near Charleston, South Carolina," *Science,* Vol. 229, 379-381.

Talwani, P., and Schaeffer, W. T. (2001). "Recurrence Rates of Large Earthquakes in the South Caroline Coastal Plain Based on Liquefaction Data," *Journal of Geophysical Research,* Vol. 106, 6621-6642.

Talwani, P., Gassman, S. L., and Hu, K. (2002). "Magnitudes of Prehistoric Earthquakes from a Study of Paleoliquefaction Features," final report to the U.S. Geological Survey, Grant No. 00HQAG0032.

URS Corporation, Durham Technologies, Inc., ImageCat, Inc., Pacific Engineering & Analysis, and S&ME, Inc (2001). "Comprehensive Seismic Risk and Vulnerability Study for the State of South Carolina," final report to the South Carolina Emergency Preparedness Division, Columbia, SC.

USACE (1973). "Dynamic Test Report Sheets on Soil Samples for Richard B. Russell Dam," *Report EN-FS-77-84,* U. S. Army Corps of Engineers, Laboratory South Atlantic.

USACE (1979). "Design Memorandum 17, Richard B. Russell Dam and Lake, Savannah River, Georgia and South Carolina," Appendix VIII of Volume IV: *Earth Embankments,* U. S. Army Corps of Engineers, Savannah District.

Vucetic, M., and Dobry, R. (1991). "Dynamic Effect of Soil Plasticity on Cyclic Response," *Journal of Geotechnical Engineering,* ASCE, Vol. 117, No. 1, 89-107.

Vucetic, M., Lanzo, G., and Doroudian, M. (1998). "Damping at Small Strains in Cyclic Simple Shear Test," *Journal of Geotechnical and Geoenvironmental Engineering,* ASCE, Vol. 124, No. 7, 585-594.

Weems, R. E., and Lemon, E. M., Jr. (1993). "Geology of the Cainhoy, Charleston, Fort Moultrie, and North Charleston Quadrangles, Charleston and Berkley Counties, South Carolina," *U.S. Geological Survey Miscellaneous Investigation Map I-1935, scale 1:24,000*. Department of the Interior, U.S. Geological Survey, Reston, VA.

Wheeler, R. L., and Cramer, C. H. (2000). "Preliminary Estimate of the Amplification of Possible Earthquake Ground Motion at a Site in Charleston County, South Carolina," *U.S. Geological Survey Open-File Report 00-0484*.

Woods, R. D. (1994). *Geophysical Characterization of Site*, A. A. Balkema, Rotterdam, Netherlands.

WPC (1999-2002). Various unpublished project reports by WrightPadgettChristopher from 1999-2002, Mount Pleasant, SC. (Project numbers listed in Table C.1)

Wroth, C. P. (1988). "Penetration Testing – A More Rigorous Approach to Interpretation," *Proceedings, 1st International Symposium on Penetration Testing,* Penetration Testing 1988, ISOPT-1, Vol. 1, Orlando, Edited by J. D. Ruiter, 303-311.

WSRC (2000). "Commercial Light Water Reactor Tritium Extraction Facility Geotechncial Summary Report (U)," K-ESR-H-00010, Rev. 2., Westinghouse Savannah River Company, Aiken, SC.

Yoshida, Y., Ikemi, M., and Kokusho, T. (1988). "Empirical Formulas of SPT Blow Counts for Gravelly Soils," *Proceeding, 1st International Symposium on Penetration Testing,* Penetration Testing 1988, ISOPT-1, Vol. 2, Orlando, Edited by J. D. Ruiter, 381-387.

Youd, T. L., Idriss, I. M., Andrus, R. D., Arango, I., Castro, G., Christian, J. T., Dobry, R., Finn, W. D. L., Harder, L. F., Jr., Hynes, M. E., Ishihara, K., Koester, J. P., Liao, S. S. C., Marcuson, W. F., III, Martin, G. R., Mitchell, J. K., Moriwaki, Y., Power, M. S., Robertson, P. K., Seed, R. B., and Stokoe, K. H., II (2001). "Liquefaction Resistance of Soils: Summary Report from the 1996 NCEER and 1998 NCEER/NSF Workshops on Evaluation of Liquefaction Resistance of Soils," *Journal of Geotechnical and Geoenvironmental Engineering,* Vol. 127, No. 10, 817-833.

Zen, K., Umehara, Y., and Hamada, K. (1978). "Laboratory Tests and In Situ Seismic Survey on Vibratory Shear Modulus of Clayey Soils with Various Plasticities," *Proceedings, 5th Japanese Earthquake Engineering Symposium,* 721-728.

APPENDIX B

SYMBOLS AND NOTATION

The following symbols and notation are used in this report:

ASF	=	age scaling factor for penetration-velocity equations;
a	=	fitting parameter;
b	=	fitting parameter;
COV	=	coefficient of variation;
C_B	=	borehole diameter correction factor;
C_E	=	hammer correction for energy ratio (ER);
C_N	=	overburden stress correction factor for SPT;
C_Q	=	overburden stress correction factor for CPT;
C_R	=	rod length correction factor;
C_S	=	sampler liner correction factor;
C_u	=	coefficient of uniformity;
C_{VS}	=	overburden stress correction factor for V_S;
D	=	material damping ratio;
D_{min}	=	small-strain material damping ratio;
D_{min1}	=	small-strain material damping ratio at a mean effective confining pressure of 100 kPa;
D_{50}	=	median grain size;
ER	=	hammer energy ratio;
F	=	dimensionless cone sleeve friction;
FC	=	fines content;
FR	=	cone friction ratio ($= f_s/q_c$);
f_s	=	measured cone sleeve friction;
$f(G/G_{max})$	=	function of normalized shear modulus;
G	=	shear modulus;
G_{max}	=	small-strain shear modulus;
G/G_{max}	=	normalized shear modulus;
I_c	=	soil behavior type index;
j	=	number of samples;
k	=	an exponent used in determining γ_r and D_{min} at confining pressure other than 100 kPa;
K'_0	=	coefficient of earth pressures at rest;

LL	$=$	liquid limit;
M_w	$=$	moment magnitude;
W_D	$=$	energy dissipated in one cycle of loading;
W_S	$=$	maximum strain energy stored in one cycle of loading;
n	$=$	an exponent used in normalizing cone tip resistance;
N_j	$=$	measured SPT blow count in Japanese practice;
N_m	$=$	measured blow count in SPT;
N_{60}	$=$	equipment-corrected blow count;
$(N_1)_{60}$	$=$	equipment- and energy-corrected blow count;
OCR	$=$	overconsolidation ratio;
PI	$=$	plasticity index;
P_a	$=$	a reference stress of 100 kPa;
Q	$=$	dimensionless cone tip resistance;
q_c	$=$	measured cone tip resistance;
q_{c1N}	$=$	normalized cone tip resistance;
R^2	$=$	coefficient of multiple determination;
s	$=$	residual standard deviation;
u	$=$	measured cone pore pressure;
V_S	$=$	measured small-strain shear-wave velocity;
V_{S1}	$=$	stress-corrected shear-wave velocity;
Z	$=$	depth;
α	$=$	curvature coefficient of normalized shear modulus curve;
γ	$=$	shear strain;
γ_r	$=$	reference strain;
γ_{r1}	$=$	reference strain at a mean effective confining pressure of 100 kPa;
ρ	$=$	mass density of soil;
σ'_h	$=$	horizontal effective pressure;
σ'_m	$=$	mean effective confining pressure;
σ_v	$=$	total vertical or overburden stress;
σ'_v	$=$	effective vertical or overburden stress;
τ	$=$	shear stress; and
τ_{max}	$=$	maximum shear stress.

APPENDIX C

SUMMARY OF FIELD V_S, CPT AND SPT DATA FROM SOUTH CAROLINA COMPILED FOR THIS STUDY

A summary of the field V_S, CPT and SPT data compiled from South Carolina by Ellis (2003) for this study is presented in this appendix. Table C.1 is a summary of V_S and penetration data for the selected layers. Table C.2 is a summary of the characteristics of the selected layer.

Table C.1 – Summary of shear-wave velocity and penetration test data.

Clemson University ID (CUID)	Site Reference	Top of layer depth (m)	Thickness (m)	Water table depth (m)	V_S test type/ quality of time histories[+]	No. of values in V_S average	V_S (m/s)	V_{S1} (m/s)	σ'_v (kPa)	No. of values in q_C average	q_C (kPa)	q_{c1N}	f_s (kPa)	F (%)	F_R (%)	I_c	No. of values in N average	N	N_{60}	$(N_1)_{60}$
S&ME																				
S&ME 2	1131-99-526 (E-6)	9.60	4.00	1.22	SCPT/NA	4	449	438	111	222	3168	30.3	26.6	0.90	0.84	2.34	NA	NA	NA	NA
S&ME 2	1131-99-526 (E-6)	17.63	8.05	1.22	SCPT/NA	8	312	267	187	483	3441	23.1	33.3	1.11	0.98	2.51	NA	NA	NA	NA
S&ME 3	1131-99-526 (MS-9)	12.52	3.03	0.00	SCPT/NA	3	473	455	118	150	3068	28.2	37.3	1.33	1.22	2.46	3	14	17	17
S&ME 4	1131-99-526 (S-12)	3.51	3.01	0.61	SCPT/NA	4	185	225	47	174	8836	124.0	26.0	0.31	0.30	1.56	NA	NA	NA	NA
S&ME 4	1131-99-526 (S-12)	12.51	3.02	0.61	SCPT/NA	3	506	477	127	161	2806	24.8	16.0	0.62	0.57	2.35	NA	NA	NA	NA
S&ME 4	1131-99-526 (S-12)	16.55	9.06	0.61	SCPT/NA	9	381	331	179	534	3448	23.7	22.6	0.76	0.67	2.44	NA	NA	NA	NA
S&ME 5	1131-99-634 (DS1)	4.03	4.00	0.46	SCPT/NA	4	165	189	59	216	5073	65.2	23.8	0.51	0.50	1.91	3	9	8	11
S&ME 5	1131-99-634 (DS1)	13.08	3.14	0.46	SCPT/NA	3	342	318	134	169	2177	17.6	16.0	0.85	0.74	2.56	2	13	15	12
S&ME 5	1131-99-634 (DS1)	16.24	5.07	0.46	SCPT/NA	4	336	297	166	303	3066	23.3	16.2	0.61	0.54	2.39	3	17	21	18
S&ME 5	1131-99-634 (DS1)	21.30	11.22	0.46	SCPT/NA	11	455	371	225	698	4233	27.0	22.5	0.61	0.54	2.31	8	20	24	17
S&ME 6	1131-99-634 (MPE-5)	7.35	6.00	0.46	SCPT/NA	6	367	376	88	363	10565	112.5	36.8	0.56	0.53	1.70	NA	NA	NA	NA
S&ME 6	1131-99-634 (MPE-5)	15.21	3.02	0.46	SCPT/NA	3	329	302	142	174	2823	22.9	28.6	1.13	1.01	2.51	NA	NA	NA	NA
S&ME 7	1131-99-634 (C-27)	13.48	3.05	1.22	SCPT/NA	3	253	238	128	195	5724	50.1	27.6	0.82	0.73	2.08	NA	NA	NA	NA
S&ME 8	1131-98-725 (B-38)	8.52	3.99	2.44	SCPT/NA	4	357	352	104	169	2938	27.4	20.8	0.78	0.73	2.35	NA	NA	NA	NA
S&ME 8	1131-98-725 (B-38)	15.42	4.97	2.44	SCPT/NA	3	419	365	173	255	4980	37.1	29.6	0.65	0.60	2.20	NA	NA	NA	NA
S&ME 9	1131-98-725 (B-45)	4.58	3.00	1.83	SCPT/NA	3	160	177	68	123	888	12.6	14.8	2.43	1.96	2.94	NA	NA	NA	NA
S&ME 9	1131-98-725 (B-45)	10.57	2.90	1.83	SCPT/NA	3	402	385	119	138	3629	33.1	33.6	1.02	0.95	2.34	NA	NA	NA	NA
S&ME 9	1131-98-725 (B-45)	15.50	3.09	1.83	SCPT/NA	3	405	362	156	155	3963	31.7	29.6	0.82	0.75	2.30	NA	NA	NA	NA
S&ME 9	1131-98-725 (B-45)	18.57	11.00	1.83	SCPT/NA	11	520	434	208	553	5341	37.1	27.8	0.57	0.52	2.17	NA	NA	NA	NA
S&ME 10	1131-98-725 (B-51)	4.47	3.00	2.74	SCPT/NA	3	144	154	77	125	2029	23.2	15.3	0.78	0.74	2.40	NA	NA	NA	NA
S&ME 10	1131-98-725 (B-51)	14.45	3.98	2.74	SCPT/NA	3	444	390	165	187	4854	37.6	19.6	0.43	0.40	2.10	NA	NA	NA	NA
S&ME 10	1131-98-725 (B-51)	20.19	8.70	2.74	SCPT/NA	9	487	397	228	386	6174	40.9	16.8	0.28	0.26	2.01	NA	NA	NA	NA
S&ME 11	1131-98-725 (B-55)	6.53	7.97	3.05	SCPT/NA	8	138	135	108	369	1678	15.6	23.5	1.68	1.44	2.75	NA	NA	NA	NA
S&ME 11	1131-98-725 (B-55)	15.50	7.00	3.05	SCPT/NA	4	538	468	175	343	5408	40.9	28.1	0.55	0.51	2.12	NA	NA	NA	NA
S&ME 12	1131-99-876 (CHS-4)	3.83	3.04	1.83	SCPT/NA	3	236	258	70	146	12535	152.0	63.0	0.48	0.47	1.60	NA	NA	NA	NA
S&ME 12	1131-99-876 (CHS-4)	10.92	3.02	1.83	SCPT/NA	3	195	186	119	143	1506	11.9	33.7	2.78	2.29	2.98	NA	NA	NA	NA
S&ME 12	1131-99-876 (CHS-4)	17.44	7.00	1.83	SCPT/NA	7	386	335	179	374	3468	25.3	14.9	0.48	0.43	2.30	NA	NA	NA	NA
S&ME 12	1131-99-876 (CHS-4)	24.46	12.90	1.83	SCPT/NA	12	451	359	250	712	3941	20.8	19.0	0.57	0.48	2.44	NA	NA	NA	NA
S&ME 13	1131-99-876 (CHS-20)	5.47	3.00	1.83	SCPT/NA	3	170	185	70	136	2000	27.1	41.8	2.25	2.10	2.59	NA	NA	NA	NA
S&ME 13	1131-99-876 (CHS-20)	13.56	3.96	1.83	SCPT/NA	4	180	171	124	223	2881	22.5	53.1	2.12	1.90	2.66	NA	NA	NA	NA
S&ME 13	1131-99-876 (CHS-20)	22.54	15.14	1.83	SCPT/NA	14	475	387	230	861	3858	21.2	33.1	1.07	0.89	2.40	NA	NA	NA	NA
S&ME 14	1131-99-876 (CHS-24)	9.54	9.00	0.91	SCPT/NA	9	192	191	105	378	2744	25.3	49.3	2.23	1.96	2.66	NA	NA	NA	NA
S&ME 14	1131-99-876 (CHS-24)	18.46	12.00	0.91	SCPT/NA	12	477	411	182	608	3781	27.1	25.0	0.76	0.67	2.36	NA	NA	NA	NA

*Seismic Cone Penetration Test
NA - Not Available

[+]Quality of time histories
1 = Good
2 = Fair

Table C.1 – Summary of shear-wave velocity and penetration test data. (Cont'd)

	--Site Description--				---Shear-Wave Velocity and Penetration Data of the Selected Layer---															
Clemson University ID (CUID)	Site Reference	Top of layer depth (m)	Thickness (m)	Water table depth (m)	V_s test type/ quality of time histories[+]	No. of values in V_s average	V_s (m/s)	V_{s1} (m/s)	σ'_v (kPa)	No. of values in q_c average	q_C (kPa)	q_{c1N}	f_s (kPa)	F (%)	F_R (%)	I_c	No. of values in N average	N	N_{60}	$(N_1)_{60}$
S&ME 15	1131-99-876 (CHS-26)	18.38	18.05	0.00	SCPT/NA	15	422	352	204	857	4176	29.2	18.5	0.48	0.42	2.26	NA	NA	NA	NA
S&ME 16	1131-99-876 (ML-15)	4.90	10.00	0.91	SCPT/NA	10	132	148	69	520	725	10.1	14.1	2.56	1.94	3.05	10	0	0	0
S&ME 17	1131-99-876 (ML-16)	11.54	6.01	3.66	SCPT/NA	6	112	102	140	331	779	5.6	15.3	2.99	1.98	3.36	4	0	0	0
S&ME 18	1131-99-876 (ML-18)	11.35	8.00	4.57	SCPT/NA	8	99	89	155	526	802	5.3	17.9	3.52	2.29	3.42	5	0	0	0
S&ME 19	1131-99-876 (ML-22)	3.57	5.95	0.91	SCPT/NA	6	77	87	62	269	539	8.8	6.9	1.82	1.29	3.03	NA	NA	NA	NA
S&ME 19	1131-99-876 (ML-22)	13.63	2.92	0.91	SCPT/NA	3	304	287	125	146	1524	12.4	26.3	2.13	1.75	2.91	NA	NA	NA	NA
S&ME 20	1131-99-876 (ML-24)	7.50	6.50	0.91	SCPT/NA	6	85	90	79	320	583	7.9	10.2	2.56	1.73	3.19	NA	NA	NA	NA
University of South Carolina																				
USC 1	TEN-01	6.50	2.60	1.52	SCPT/NA	3	346	361	84	103	3270	36.6	6.5	0.19	0.18	2.01	3	NA	16	18
USC 2	TEN-02	6.50	2.60	1.52	SCPT/NA	3	366	381	84	114	2906	31.9	15.3	0.55	0.53	2.25	6	NA	11	13
USC 3	TEN-03	6.50	6.00	1.52	SCPT/NA	5	428	423	103	190	3578	35.5	5.8	0.17	0.16	2.00	2	NA	15	16
USC 6	TEN-06	2.50	3.00	2.29	SCPT/NA	3	153	179	55	130	3179	42.9	33.5	1.15	1.13	2.25	3	NA	11	15
USC 7	TEN-07	2.50	3.00	2.29	SCPT/NA	3	175	205	54	117	4408	62.9	45.7	1.00	0.99	2.10	2	NA	4	6
USC 8	TEN-08	2.50	3.00	2.32	SCPT/NA	3	160	187	56	118	4499	62.2	38.8	0.95	0.93	2.06	3	NA	6	9
USC 9	TEN-09	3.50	3.00	3.05	SCPT/NA	3	153	168	70	112	3869	49.8	31.5	0.88	0.84	2.18	2	NA	4	5
USC 10	TEN-10	3.50	4.00	3.05	SCPT/NA	4	156	168	75	114	3133	49.8	23.1	0.54	0.54	2.18	6	NA	4	5
USC 11-13	SAM-01 / 02 / 03	2.50	5.00	2.13	SCPT/NA	12	252	286	61	458	8627	109.0	43.3	0.49	0.48	1.76	NA	NA	NA	NA
USC 14-16	SAM-04 / 05 / 06	2.50	4.00	1.83	SCPT/NA	12	268	314	55	475	6367	86.3	35.5	0.56	0.55	1.83	12	NA	12	17
USC 14-16	SAM-04 / 05 / 06	6.50	5.00	1.83	SCPT/NA	5	154	156	97	75	1239	19.0	2.8	0.05	0.06	2.50	9	NA	2	3
USC 19-22	GAP-03 / 04 / 05	2.50	2.00	2.13	SCPT/NA	6	111	134	48	236	481	95.0	4.2	1.00	0.86	2.30	6	NA	1	2
USC 19-22	GAP-03 / 04 / 05	4.50	2.00	2.13	SCPT/NA	4	163	178	70	153	21750	260.0	56.2	0.31	0.30	1.32	4	NA	35	42
Wright Padgett Christopher																				
WPC 1	2001-122 (SCPT1)	3.35	3.00	2.80	SCPT/NA	3	175	194	67	NA	9100	107.8	51.0	0.57	0.56	1.74	NA	NA	NA	NA
WPC 2	2001-201 (SC2)	4.40	4.00	4.00	SCPT/NA	4	220	226	91	200	17616	184.6	109.7	0.64	0.64	1.58	NA	NA	NA	NA
WPC 3	2001-211 (SCPT4)	1.70	3.00	1.52	SCPT / 1	3	196	247	42	151	8879	138.3	83.6	1.24	1.20	1.85	NA	NA	NA	NA
WPC 5	1999-175 (SCPT1)	2.90	11.00	1.01	SCPT/NA	10	88	99	69	551	343	4.7	9.6	4.97	2.15	3.51	8	1	2	2
WPC 5	1999-175 (SCPT1)	24.90	10.00	1.01	SCPT/NA	10	433	351	233	500	3259	14.6	47.6	1.67	1.02	2.82	7	12	13	9
WPC 10	2000-363 (SCPT1)	6.60	9.00	2.29	SCPT/NA	5	215	213	112	451	3578	32.1	56.6	4.14	2.70	2.87	NA	NA	NA	NA
WPC 11	2000-344 (SC1)	3.82	3.00	3.10	SCPT/NA	3	257	277	74	150	7715	91.9	39.1	0.52	0.52	1.81	NA	NA	NA	NA
WPC 11	2000-344 (SC1)	10.82	3.00	3.10	SCPT/NA	3	200	185	137	151	2707	21.2	89.8	3.70	3.70	2.83	NA	NA	NA	NA
WPC 12	2000-344 (SC10)	7.42	3.00	4.20	SCPT/NA	3	234	232	100	151	12901	129.2	109.8	1.90	1.65	2.24	NA	NA	NA	NA
WPC 16	2000-344 (SC15)	6.40	4.00	3.00	SCPT/NA	4	197	197	101	201	10157	102.6	38.3	0.40	0.39	1.68	NA	NA	NA	NA
WPC 17	2000-344 (SC2)	6.40	4.00	3.20	SCPT/NA	4	195	193	103	201	10708	106.2	43.6	0.40	0.39	1.67	NA	NA	NA	NA
WPC 17	2000-344 (SC2)	11.40	4.00	3.20	SCPT/NA	4	244	221	148	201	2310	15.8	134.5	6.68	5.18	3.11	NA	NA	NA	NA

*Seismic Cone Penetration Test
NA - Not Available

[+]Quality of time histories
1 = Good
2 = Fair

Table C.1 – Summary of shear-wave velocity and penetration test data. (Cont'd)

Clemson University ID (CUID)	Site Reference	Top of layer depth (m)	Thickness (m)	Water table depth (m)	V_S test type/ quality of time histories[+]	No. of values in V_S average	V_S (m/s)	V_{S1} (m/s)	σ'_v (kPa)	No. of values in q_C average	q_C (kPa)	q_{c1N}	f_s (kPa)	F (%)	F_R (%)	I_c	No. of values in N average	N	N_{60}	$(N_1)_{60}$
WPC 18	2000-344 (SC3)	4.50	4.00	2.50	SCPT/NA	4	150	160	79	201	9898	112.0	50.0	0.55	0.54	1.72	NA	NA	NA	NA
WPC 18	2000-344 (SC3)	9.50	3.00	2.50	SCPT/NA	3	173	166	120	151	2928	25.2	120.0	5.17	3.95	2.89	NA	NA	NA	NA
WPC 19	2000-344 (SC4)	11.82	3.00	1.60	SCPT/NA	3	251	242	122	151	2166	17.9	72.0	3.94	2.96	2.90	NA	NA	NA	NA
WPC 20	2000-344 (SC5A)	3.82	5.00	2.10	SCPT/NA	5	194	210	75	NA	11500	130.4	49.0	0.43	0.43	1.61	4	18	18	21
WPC 21	2000-344 (SC5B)	3.82	7.00	2.40	SCPT/NA	7	199	208	86	351	9490	105.1	51.4	0.62	0.60	1.77	NA	NA	NA	NA
WPC 22	2000-344 (SC6)	2.72	3.00	1.20	SCPT/NA	3	160	192	48	151	3266	48.1	27.0	1.03	0.99	2.20	NA	NA	NA	NA
WPC 23	2000-344 (SC7)	3.82	3.00	1.70	SCPT/NA	3	60	72	48	150	280	4.8	11.2	6.24	3.38	3.51	3	2	1	2
WPC 24	2000-344 (SC8)	7.62	3.00	2.30	SCPT/NA	3	156	155	102	151	1838	21.1	16.8	1.50	1.12	2.64	NA	NA	NA	NA
WPC 24	2000-344 (SC8)	14.62	3.00	2.30	SCPT/NA	3	303	268	165	151	17156	140.2	311.7	2.17	2.11	2.03	NA	NA	NA	NA
WPC 25	2000-344 (SC9)	2.72	4.00	1.10	SCPT/NA	4	60	75	39	201	165	2.8	10.2	7.87	4.48	3.78	NA	NA	NA	NA
WPC 25	2000-344 (SC9)	17.72	3.00	1.10	SCPT/NA	3	241	217	151	151	3010	20.1	113.4	4.40	3.09	2.91	NA	NA	NA	NA
WPC 27	2001-239 (SC3)	10.40	4.00	2.00	SCPT/NA	4	212	200	129	201	2132	17.3	38.5	2.54	1.93	2.81	NA	NA	NA	NA
WPC 28	2001-187 (SCPT1)	2.02	3.00	1.22	SCPT/NA	3	207	259	42	151	6905	110.0	67.2	1.11	1.09	1.97	NA	NA	NA	NA
WPC 28	2001-187 (SCPT1)	6.02	3.00	1.22	SCPT/NA	3	213	227	78	151	4112	48.7	33.9	1.51	1.30	2.27	NA	NA	NA	NA
WPC 30	2001-163 (SCPT1)	4.35	3.00	2.29	SCPT/NA	3	175	191	72	150	1629	21.0	32.8	2.82	2.59	2.42	NA	NA	NA	NA
WPC 32	2001-172 (CPT1)	7.70	2.00	5.49	SCPT / 1	2	202	191	124	101	7820	68.3	72.7	2.70	1.94	2.57	NA	NA	NA	NA
WPC 33	2001-172 (SCPT1)	5.70	3.00	5.49	SCPT / 1	3	231	226	110	NA	16092	147.6	125.5	0.78	0.77	1.74	NA	NA	NA	NA
WPC 35	2001-218 (SCPT1)	1.70	2.00	1.98	SCPT / 1	2	216	272	41	101	5378	85.2	41.2	0.78	0.77	1.91	NA	NA	NA	NA
WPC 37	2001-165 (SCPT1)	1.70	2.00	1.52	SCPT/NA	2	180	232	37	101	3408	56.2	7.6	0.19	0.18	1.84	NA	NA	NA	NA
WPC 37	2001-165 (SCPT1)	5.70	3.00	1.52	SCPT/NA	3	141	151	78	151	836	10.8	16.1	2.35	1.68	2.97	NA	NA	NA	NA
WPC 38	CHS2-02-041 (SC1)	2.40	3.00	1.80	SCPT/NA	3	203	243	50	NA	12459	171.2	67.6	0.55	0.54	1.57	NA	NA	NA	NA
WPC 39	2001-317 (SC2)	16.45	4.00	2.29	SCPT/NA	4	348	299	186	NA	2860	17.8	58.9	2.32	2.06	2.77	NA	NA	NA	NA
WPC 40	2001-319 (SCPT1)	3.70	3.00	2.99	SCPT / 1	3	221	240	72	151	8157	97.2	25:1	0.31	0.31	1.65	NA	NA	NA	NA
WPC 40	2001-319 (SCPT1)	7.70	2.00	2.99	SCPT / 2	2	386	384	102	90	10394	102.3	230.2	2.32	2.28	2.18	NA	NA	NA	NA
WPC 41	2001-342 (SCPT1)	2.70	3.00	1.62	SCPT / 1	3	124	147	51	151	665	10.9	7.1	1.15	0.99	2.79	NA	NA	NA	NA
WPC 41	2001-342 (SCPT1)	5.70	2.00	1.62	SCPT / 1	2	242	260	74	100	3320	38.4	6.6	0.23	0.22	2.00	NA	NA	NA	NA
WPC 42	2001-343 (SCPT1)	3.78	2.93	2.74	SCPT / 2	3	72	80	66	147	570	8.2	5.3	1.19	0.95	2.97	NA	NA	NA	NA
WPC 42	2001-343 (SCPT1)	8.70	2.00	2.74	SCPT / 2	2	245	242	102	101	9074	90.0	27.4	0.31	0.30	1.70	NA	NA	NA	NA
WPC 42	2001-343 (SCPT1)	11.70	3.00	2.74	SCPT / 2	3	168	155	134	151	1108	8.3	22.0	2.52	1.97	3.14	NA	NA	NA	NA
WPC 43	2001-292 (SCPT1)	3.60	2.00	3.05	SCPT / 1	2	175	194	67	101	4107	50.9	27.5	0.89	0.85	2.10	NA	NA	NA	NA
WPC 43	2001-292 (SCPT1)	7.60	2.00	3.05	SCPT / 1	2	234	233	103	101	9914	97.2	61.8	0.68	0.67	1.83	NA	NA	NA	NA
WPC 44	2001-350 (SCPT1)	7.70	6.00	3.05	SCPT / 2	6	231	223	117	301	2008	18.5	6.5	0.34	0.31	2.36	NA	NA	NA	NA
WPC 45	2001-303 (SCPT8)	3.70	2.00	2.29	SCPT / 1	2	252	283	61	NA	19265	239.1	78.9	0.41	0.41	1.38	NA	NA	NA	NA
WPC 47	2001-339 (SCPT1)	1.65	1.95	1.52	SCPT/NA	2	158	205	36	101	4654	75.6	34.0	0.75	0.75	1.94	NA	NA	NA	NA

*Seismic Cone Penetration Test
NA - Not Available

[+]Quality of time histories
1 = Good
2 = Fair

Table C.1 – Summary of shear-wave velocity and penetration test data. (Cont'd)

Clemson University ID (CUID)	Site Reference	Top of layer depth (m)	Thickness (m)	Water table depth (m)	V_S test type/ quality of time histories[+]	No. of values in V_S average	V_S (m/s)	V_{S1} (m/s)	σ'_v (kPa)	No. of values in q_C average	q_C (kPa)	q_{c1N}	f_s (kPa)	F (%)	F_R (%)	I_c	No. of values in N average	N	N_{60}	$(N_1)_{60}$
WPC 47	2001-339 (SCPT1)	6.60	2.00	1.52	SCPT/NA	2	336	354	81	101	7118	79.9	11.7	0.16	0.15	1.70	NA	NA	NA	NA
WPC 48	CHS2-02-044 (SCPT8)	4.70	3.00	2.44	SCPT/NA	3	209	224	76	NA	4090	45.7	22.4	0.56	0.55	2.07	NA	NA	NA	NA
WPC 50	CHS2-02-059 (B-06)	4.00	2.00	3.66	SCPT/NA	2	185	199	75	101	2041	25.1	46.4	2.28	1.76	2.62	NA	NA	NA	NA
WPC 51	CHS2-02-073 (SC6)	3.00	3.00	1.49	SCPT/NA	3	169	201	53	151	5955	82.1	68.0	1.23	1.20	2.01	NA	NA	NA	NA
WPC 53	2001-235 (SC1)	1.41	3.00	1.50	SCPT / 2	3	195	248	40	NA	5319	83.0	41.2	0.78	0.77	1.91	NA	NA	NA	NA
WPC 53	2001-235 (SC1)	4.40	2.00	1.50	SCPT / 1	2	243	273	62	NA	10638	152.2	48.3	0.46	0.45	1.56	NA	NA	NA	NA
WPC 53	2001-235 (SC1)	13.40	3.00	1.50	SCPT / 1	3	201	186	139	NA	1277	11.5	31.3	3.07	2.45	3.03	NA	NA	NA	NA
WPC 54	CHS2-02-041 (SC2)	2.90	3.00	1.80	SCPT/NA	3	209	244	55	NA	6314	83.3	45.3	0.73	0.72	1.89	NA	NA	NA	NA
WPC 54	CHS2-02-041 (SC2)	8.90	3.00	1.80	SCPT/NA	3	199	194	110	NA	1109	11.8	28.7	3.14	2.59	3.02	NA	NA	NA	NA
WPC 54	CHS2-02-041 (SC2)	13.90	4.00	1.80	SCPT/NA	4	261	228	170	NA	2219	18.7	69.7	3.58	3.14	2.87	NA	NA	NA	NA
Westinghouse Savannah River Company																				
SRS 2	HTEF-C2	12.44	2.74	10.15	SCPT / 1	3	312	260	208	111	7608	52.4	140.2	1.93	1.87	2.31	NA	NA	NA	NA
SRS 3 & 8	HTEF-C3 & C8	13.38	2.74	10.94	SCPT / 1	6	325	267	221	221	6278	38.3	118.0	2.07	1.97	2.45	NA	NA	NA	NA
SRS 3 & 8	HTEF-C3 & C8	19.63	6.40	10.94	SCPT / 1	14	358	272	299	522	21740	125.6	141.9	0.70	0.68	1.81	NA	NA	NA	NA
SRS 5	HTEF-C5	12.28	3.66	11.52	SCPT / 1	4	328	269	226	145	2179	9.8	92.5	5.04	4.40	3.19	NA	NA	NA	NA
SRS 5	HTEF-C5	20.51	6.40	11.52	SCPT / 1	7	348	262	310	248	18295	103.3	73.4	0.41	0.40	1.69	NA	NA	NA	NA
SRS 6	HTEF-C6	22.59	6.25	13.44	SCPT / 1	6	326	239	343	251	20468	110.5	75.3	0.38	0.37	1.64	NA	NA	NA	NA
SRS 7	HTEF-C7	12.41	5.18	12.56	SCPT / 1	6	330	266	238	216	3398	15.7	98.8	3.57	3.23	2.95	NA	NA	NA	NA
SRS 7	HTEF-C7	21.40	5.33	21.40	SCPT / 1	4	362	271	320	217	21297	118.8	102.7	0.49	0.48	1.68	NA	NA	NA	NA
SRS 9	HTEF-C9	13.29	2.74	11.61	SCPT / 1	3	350	284	228	108	4160	19.1	133.5	3.59	3.35	2.85	2	12	13	9
SRS 9	HTEF-C9	18.32	5.94	11.61	SCPT / 1	234	333	253	299	234	14589	85.8	69.4	0.51	0.50	1.81	4	46	51	30
SRS 10	HTEF-C10	11.43	3.66	11.73	SCPT / 1	4	351	290	215	146	3664	19.0	100.5	3.18	2.95	2.82	NA	NA	NA	NA
SRS 10	HTEF-C10	20.57	5.49	11.73	SCPT / 1	5	308	233	308	213	16161	92.2	78.8	0.49	0.48	1.77	NA	NA	NA	NA
SRS 13	HTEF-C13	21.52	6.40	12.83	SCPT / 1	7	364	270	329	257	19307	106.4	72.0	0.38	0.37	1.66	NA	NA	NA	NA
SRS 17	HTEF-C17	21.40	5.49	12.34	SCPT / 1	217	343	256	320	217	15462	86.5	51.6	0.35	0.34	1.72	NA	NA	NA	NA

*Seismic Cone Penetration Test
NA - Not Available

[+]Quality of time histories
1 = Good
2 = Fair

Table C.2 – Summary of characteristics of the selected layer.

| --Site Description-- | | | --General Characteristics of the Selected Layer-- | | | | | | | | | |
Clemson University ID (CUID)	Site Reference	Top of layer depth (m)	Soil Type	Deposit Type	Geologic Formation	Goelogic Age[a]	Avg. Fines Content (%)	Avg. Gravel Content (%)	Avg. CU	Avg. D50 (mm)	Avg. LL (%)	Avg. PI (%)
S&ME												
S&ME 2	1131-99-526 (E-6)	9.60	NA	Deep Marine	Ashley	T (~30Ma)	NA	NA	NA	NA	NA	NA
S&ME 2	1131-99-526 (E-6)	17.63	NA	Deep Marine	Ashley	T (~30Ma)	NA	NA	NA	NA	NA	NA
S&ME 3	1131-99-526 (MS-9)	12.52	Silt with Sand (MH)	Deep Marine	Ashley	T (~30Ma)	NA	NA	NA	NA	NA	NA
S&ME 4	1131-99-526 (S-12)	3.51	NA	Beach to Barrier Island	NA	P? / H?	NA	NA	NA	NA	NA	NA
S&ME 4	1131-99-526 (S-12)	12.51	NA	Deep Marine	Ashley	T (~30Ma)	NA	NA	NA	NA	NA	NA
S&ME 4	1131-99-526 (S-12)	16.55	NA	Deep Marine	Ashley	T (~30Ma)	¡NA	NA	NA	NA	NA	NA
S&ME 5	1131-99-634 (DS1)	4.03	Clayey Sand (SC to SM)	Beach / Barrier Island	NA	P (60ka)?	20.0	0.0	NA	0.180	NA	NA
S&ME 5	1131-99-634 (DS1)	13.08	Clayey Sand (SC)	Deep Marine	Ashley	T (~30Ma)	32.0	0.8	NA	0.110	59.0	31.0
S&ME 5	1131-99-634 (DS1)	16.24	Sandy Clay (CH)	Deep Marine	Ashley	T (~30Ma)	80.0	0.0	NA	NA	77.7	42.9
S&ME 5	1131-99-634 (DS1)	21.30	Sandy Silt (MH to ML)	Deep Marine	Ashley	T (~30Ma)	71.8	0.0	NA	NA	62.6	26.1
S&ME 6	1131-99-634 (MPE-5)	7.35	NA	Barrier Island	Wando	P (100ka)?	NA	NA	NA	NA	NA	NA
S&ME 6	1131-99-634 (MPE-5)	15.21	NA	Deep Marine	Ashley	T (~30Ma)	NA	NA	NA	NA	NA	NA
S&ME 7	1131-99-634 (C-27)	13.48	NA	NA	Wando?	P (100ka)?	NA	NA	NA	NA	NA	NA
S&ME 8	1131-98-725 (B-38)	8.52	NA	Deep Marine	Ashley	T (~30Ma)	NA	NA	NA	NA	NA	NA
S&ME 8	1131-98-725 (B-38)	15.42	NA	Deep Marine	Ashley	T (~30Ma)	NA	NA	NA	NA	NA	NA
S&ME 9	1131-98-725 (B-45)	4.58	NA	Estuarine	Ten Mile Hill	P (200ka)	NA	NA	NA	NA	NA	NA
S&ME 9	1131-98-725 (B-45)	10.57	NA	Deep Marine	Ashley	T (~30Ma)	NA	NA	NA	NA	NA	NA
S&ME 9	1131-98-725 (B-45)	15.50	NA	Deep Marine	Ashley	T (~30Ma)	NA	NA	NA	NA	NA	NA
S&ME 9	1131-98-725 (B-45)	18.57	NA	Deep Marine	Ashley	T (~30Ma)	NA	NA	NA	NA	NA	NA
S&ME 10	1131-98-725 (B-51)	4.47	NA	Estuarine	Ten Mile Hill	P (200ka)	NA	NA	NA	NA	NA	NA
S&ME 10	1131-98-725 (B-51)	14.45	NA	Deep Marine	Ashley	T (~30Ma)	NA	NA	NA	NA	NA	NA
S&ME 10	1131-98-725 (B-51)	20.19	NA	Deep Marine	Ashley	T (~30Ma)	NA	NA	NA	NA	NA	NA
S&ME 11	1131-98-725 (B-55)	6.53	NA	Estuarine	Ten Mile Hill	P (200ka)?	NA	NA	NA	NA	NA	NA
S&ME 11	1131-98-725 (B-55)	15.50	NA	Deep Marine	Ashley	T (~30Ma)	NA	NA	NA	NA	NA	NA
S&ME 12	1131-99-876 (CHS-4)	3.83	NA	Barrier Island	Wando	P (100ka)	NA	NA	NA	NA	NA	NA
S&ME 12	1131-99-876 (CHS-4)	10.92	NA	Tidal Marsh / Estuarine	Wando?	P (100ka)?	NA	NA	NA	NA	NA	NA
S&ME 12	1131-99-876 (CHS-4)	17.44	NA	Deep Marine	Ashley	T (~30Ma)	NA	NA	NA	NA	NA	NA
S&ME 12	1131-99-876 (CHS-4)	24.46	NA	Deep Marine	Ashley	T (~30Ma)	NA	NA	NA	NA	NA	NA
S&ME 13	1131-99-876 (CHS-20)	5.47	NA	Tidal Marsh / Estuarine	Wando	P (100ka)	NA	NA	NA	NA	NA	NA
S&ME 13	1131-99-876 (CHS-20)	13.56	NA	Tidal Marsh / Estuarine	Wando?	P (100ka)?	NA	NA	NA	NA	NA	NA
S&ME 13	1131-99-876 (CHS-20)	22.54	NA	Deep Marine	Ashley	T (~30Ma)	NA	NA	NA	NA	NA	NA
S&ME 14	1131-99-876 (CHS-24)	9.54	NA	Tidal Marsh / Estuarine	Wando	P (100ka)	NA	NA	NA	NA	NA	NA
S&ME 14	1131-99-876 (CHS-24)	18.46	NA	Deep Marine	Ashley	T (~30Ma)	NA	NA	NA	NA	NA	NA

[a]Geologic Age

H - Holocene
P - Pleistocene
T - Tertiary

NP - Non-Plastic
* - Estimated from description in report
NA - Not Available

Table C.2 – Summary of characteristics of the selected layer. (Cont'd)

Clemson University ID (CUID)	Site Reference	Top of layer depth (m)	Soil Type	Deposit Type	Geologic Formation	Goelogic Agea	Avg. Fines Content (%)	Avg. Gravel Content (%)	Avg. CU	Avg. D50 (mm)	Avg. LL (%)	Avg. PI (%)
--Site Description--			**--General Characteristics of the Selected Layer--**									
S&ME 15	1131-99-876 (CHS-26)	18.38	NA	Deep Marine	Ashley	T (~30Ma)	NA	NA	NA	NA	NA	NA
S&ME 16	1131-99-876 (ML-15)	4.90	Sandy Organic Clay (OH)	Tidal Marsh / Estuarine	NA	H	47.2	NA	NA	NA	51.0	23.0
S&ME 17	1131-99-876 (ML-16)	11.54	Sandy Organic Clay (OH)	Tidal Marsh / Estuarine	NA	H	NA	NA	NA	NA	NA	NA
S&ME 18	1131-99-876 (ML-18)	11.35	Sandy Organic Clay (OH)	Tidal Marsh / Estuarine	NA	H	NA	NA	NA	NA	NA	NA
S&ME 19	1131-99-876 (ML-22)	3.57	NA	Tidal Marsh / Estuarine	NA	H	NA	NA	NA	NA	NA	NA
S&ME 19	1131-99-876 (ML-22)	13.63	NA	Deep Marine	Ashley	T (~30Ma)	NA	NA	NA	NA	NA	NA
S&ME 20	1131-99-876 (ML-24)	7.03	NA	Tidal Marsh / Estuarine	NA	H	NA	NA	NA	NA	NA	NA
USC												
USC 1	TEN-01	6.50	Sandy Clay (CH)	Deep Marine	Ashley	T (~30Ma)	NA	NA	NA	NA	NA	NA
USC 2	TEN-02	6.50	Clayey Sand to Sandy Clay (SC-CH)	Deep Marine	Ashley	T (~30Ma)	NA	NA	NA	NA	NA	NA
USC 3	TEN-03	7.00	Sandy Clay (CH)	Deep Marine	Ashley	T (~30Ma)	NA	NA	NA	NA	NA	NA
USC 6	TEN-06	2.50	Fine Sand (SP)	Barrier Island	Ten Mile Hill	P (200ka)	<5*	0.0*	2.73	0.190	NA	NA
USC 7	TEN-07	2.50	Fine Sand (SP)	Barrier Island	Ten Mile Hill	P (200ka)	<5*	0.0*	1.80	0.180	NA	NA
USC 8	TEN-08	2.50	Fine Sand (SP)	Barrier Island	Ten Mile Hill	P (200ka)	<5*	0.0*	1.71	0.170	NA	NA
USC 9	TEN-09	3.50	Fine Sand (SP)	Barrier Island?	Ten Mile Hill	P (200ka)	<5*	0.0*	1.85	0.160	NA	NA
USC 10	TEN-10	3.50	Fine Sand (SP)	Barrier Island?	Ten Mile Hill	P (200ka)	<5*	0.0*	1.88	0.170	NA	NA
USC 11-13	SAM-01 / 02 / 03	2.50	Fine Sand (SP)	Beach?	NA	P (200ka)	<5*	0.0*	1.86	0.170	NA	NA
USC 14-16	SAM-04 / 05 / 06	2.50	Fine Sand (SP)	Beach?	NA	P (200ka)	<5*	0.0*	1.83	0.200	NA	NA
USC 14-16	SAM-04 / 05 / 06	6.50	Clay	Marsh	NA	P (200ka)	NA	NA	NA	NA	NA	NA
USC 19-22	GAP-03 / 04 / 05	2.50	NA	Marsh	NA	H?	6.0*	0.0*	2.45	0.200	NA	NA
USC 19-22	GAP-03 / 04 / 05	4.50	Fine / Medium Sand (SP?)	Beach / Barrier Island?	NA	P (200ka)?	8.0*	0.0*	2.44	0.210	NA	NA
WPC												
WPC 1	2001-122 (SCPT1)	3.35	NA	Barrier Island	Wando	P (100ka)	NA	NA	NA	NA	NA	NA
WPC 2	2001-201 (SC2)	4.40	NA	NA	NA	NA	NA	NA	NA	NA	NA	NA
WPC 3	2001-211 (SCPT4)	1.70	NA	NA	NA	H?	NA	NA	NA	NA	NA	NA
WPC 5	1999-175 (SCPT1)	2.90	Silty Sandy Clay (CH-OH)	Tidal Marsh / Estuarine	NA	H	81.0	0.0	NA	0.013	142.0	56.0
WPC 5	1999-175 (SCPT1)	24.90	Clayey, Sandy Silt (ML)	Deep Marine	Ashley	T (~30Ma)	NA	NA	NA	NA	NA	NA
WPC 10	2000-363 (SCPT1)	6.60	NA	Estuarine	Wando	P (100ka)	NA	NA	NA	NA	NA	NA
WPC 11	2000-344 (SC1)	3.82	NA	Fluvial?	NA	H?	NA	NA	NA	NA	NA	NA
WPC 11	2000-344 (SC1)	10.82	NA	Tidal Marsh / Estuarine	NA	P?	NA	NA	NA	NA	NA	NA
WPC 12	2000-344 (SC10)	7.42	NA	Fluvial?	NA	H?	NA	NA	NA	NA	NA	NA
WPC 16	2000-344 (SC15)	6.40	NA	Fluvial?	NA	H?	NA	NA	NA	NA	NA	NA
WPC 17	2000-344 (SC2)	6.40	NA	Fluvial?	NA	H?	NA	NA	NA	NA	NA	NA
WPC 17	2000-344 (SC2)	11.40	NA	Tidal Marsh / Estuarine	NA	P?	NA	NA	NA	NA	NA	NA

a Geologic Age
H - Holocene
P - Pleistocene
T - Tertiary

NP - Non-Plastic
* - Estimated from description in report
NA - Not Available

Table C.2 – Summary of characteristics of the selected layer. (Cont'd)

Clemson University ID (CUID)	Site Reference	Top of layer depth (m)	Soil Type	Deposit Type	Geologic Formation	Goelogic Agea	Avg. Fines Content (%)	Avg. Gravel Content (%)	Avg. CU	Avg. D50 (mm)	Avg. LL (%)	Avg. PI (%)
	--Site Description--				--General Characteristics of the Selected Layer--							
WPC 18	2000-344 (SC3)	4.50	NA	Fluvial?	NA	H?	NA	NA	NA	NA	NA	NA
WPC 18	2000-344 (SC3)	9.50	NA	Tidal Marsh / Estuarine	NA	P?	NA	NA	NA	NA	NA	NA
WPC 19	2000-344 (SC4)	11.82	NA	Tidal Marsh / Estuarine	NA	P?	NA	NA	NA	NA	NA	NA
WPC 20	2000-344 (SC5A)	3.82	Silty Sand (SM)	Fluvial?	NA	H?	28.6	0.0	5.90	0.127	NA	NA
WPC 21	2000-344 (SC5B)	3.82	Silty Sand (SM)	Fluvial?	NA	H?	NA	NA	NA	NA	NA	NA
WPC 22	2000-344 (SC6)	2.72	Clayey Sand (SC)	Fluvial?	NA	H?	32.0	0.0	41.2	0.138	NA	NA
WPC 23	2000-344 (SC7)	3.82	Organic Clay (OH)	Tidal Marsh / Estuarine	NA	H?	NA	NA	NA	NA	NA	NA
WPC 24	2000-344 (SC8)	7.62	NA	Tidal Marsh / Estuarine	NA	H?	NA	NA	NA	NA	NA	NA
WPC 24	2000-344 (SC8)	14.62	NA	NA	NA	P?	NA	NA	NA	NA	NA	NA
WPC 25	2000-344 (SC9)	2.72	NA	Tidal Marsh / Estuarine	NA	H?	NA	NA	NA	NA	NA	NA
WPC 25	2000-344 (SC9)	17.72	NA	Tidal Marsh / Estuarine	NA	P?	NA	NA	NA	NA	NA	NA
WPC 27	2001-239 (SC3)	10.40	NA	Tidal Marsh / Estuarine	Wando	P (100ka)	NA	NA	NA	NA	NA	NA
WPC 28	2001-187 (SCPT1)	2.02	NA	Tidal Marsh / Estuarine	Wando	P (100ka)	NA	NA	NA	NA	NA	NA
WPC 28	2001-187 (SCPT1)	6.02	NA	NA	NA	P	NA	NA	NA	NA	NA	NA
WPC 30	2001-163 (SCPT1)	4.35	NA	Estuarine	NA	P (<700ka)	NA	NA	NA	NA	NA	NA
WPC 32	2001-172 (CPT1)	7.70	NA	Estuarine	NA	P?	NA	NA	NA	NA	NA	NA
WPC 33	2001-172 (SCPT1)	5.70	NA	Barrier Island?	NA	P?	NA	NA	NA	NA	NA	NA
WPC 35	2001-218 (SCPT1)	1.70	NA	NA	Ten Mile Hill	P (200ka)	NA	NA	NA	NA	NA	NA
WPC 37	2001-165 (SCPT1)	1.70	Silty Sand (SM)	Barrier Island?	Wando	P (100ka)	NA	NA	NA	NA	NA	NA
WPC 37	2001-165 (SCPT1)	5.70	NA	Estuarine	Wando	P (100ka)	NA	NA	NA	NA	NA	NA
WPC 38	CHS2-02-041 (SC1)	2.40	NA	Barrier Island	Wando	P (100ka)	NA	NA	NA	NA	NA	NA
WPC 39	2001-317 (SC2)	16.45	NA	Deep Marine	Ashley	T (~30Ma)	NA	NA	NA	NA	NA	NA
WPC 40	2001-319 (SCPT1)	3.70	NA	Fluvial?	NA	P (>1000ka)	NA	NA	NA	NA	NA	NA
WPC 40	2001-319 (SCPT1)	7.70	NA	NA	NA	T	NA	NA	NA	NA	NA	NA
WPC 41	2001-342 (SCPT1)	2.70	NA	Estuarine	Wando?	P (100ka)	NA	NA	NA	NA	NA	NA
WPC 41	2001-342 (SCPT1)	5.70	NA	NA	Wando?	P (100ka)	NA	NA	NA	NA	NA	NA
WPC 42	2001-343 (SCPT1)	3.78	NA	Tidal Marsh / Estuarine	NA	H	NA	NA	NA	NA	NA	NA
WPC 42	2001-343 (SCPT1)	8.70	NA	NA	Wando	P (100ka)	NA	NA	NA	NA	NA	NA
WPC 42	2001-343 (SCPT1)	11.70	NA	Estuarine	Wando	P (100ka)	NA	NA	NA	NA	NA	NA
WPC 43	2001-292 (SCPT1)	3.60	NA	Barrier Island	Ten Mile Hill	P (200ka)	NA	NA	NA	NA	NA	NA
WPC 43	2001-292 (SCPT1)	7.60	NA	NA	Ten Mile Hill	P (200ka)?	NA	NA	NA	NA	NA	NA
WPC 44	2001-350 (SCPT1)	7.70	NA	Deep Marine	Ashley	T (~30Ma)	NA	NA	NA	NA	NA	NA
WPC 45	2001-303 (SCPT8)	3.70	Sand (SP)	Barrier Island	Wando	P (100ka)	1.4	7.8	5.57	0.859	NA	NA
WPC 47	2001-339 (SCPT1)	1.65	NA	NA	NA	NA	NA	NA	NA	NA	NA	NA

[B]Geologic Age

H - Holocene
P - Pleistocene
T - Tertiary

NP - Non-Plastic
* - Estimated from description in report
NA - Not Available

Table C.2 – Summary of characteristics of the selected layer. (Cont'd)

Clemson University ID (CUID)	Site Reference	Top of layer depth (m)	Soil Type	Deposit Type	Geologic Formation	Goelogic Agea	Avg. Fines Content (%)	Avg. Gravel Content (%)	Avg. CU	Avg. D50 (mm)	Avg. LL (%)	Avg. PI (%)
			--Site Description-- / **--General Characteristics of the Selected Layer--**									
WPC 47	2001-339 (SCPT1)	6.60	NA	NA	NA	NA	NA	NA	NA	NA	NA	NA
WPC 48	CHS2-02-044 (SCPT8)	4.70	NA	NA	NA	NA	NA	NA	NA	NA	NA	NA
WPC 50	CHS2-02-059 (B-06)	4.00	NA	NA	Ten Mile Hill	P (200ka)	NA	NA	NA	NA	NA	NA
WPC 51	CHS2-02-073 (SC6)	3.00	NA	NA	Ten Mile Hill	P (200ka)	NA	NA	NA	NA	NA	NA
WPC 53	2001-235 (SC1)	1.41	NA	Barrier Island?	Wando	P (100ka)	NA	NA	NA	NA	NA	NA
WPC 53	2001-235 (SC1)	4.40	NA	Barrier Island?	Wando	P (100ka)	NA	NA	NA	NA	NA	NA
WPC 53	2001-235 (SC1)	13.40	NA	NA	NA	NA	NA	NA	NA	NA	NA	NA
WPC 54	CHS2-02-041 (SC2)	2.90	NA	Barrier Island	Wando	P (100ka)	NA	NA	NA	NA	NA	NA
WPC 54	CHS2-02-041 (SC2)	8.90	NA	Tidal Marsh / Estuarine	Wando?	P (100ka)?	NA	NA	NA	NA	NA	NA
WPC 54	CHS2-02-041 (SC2)	13.90	NA	Deep Marine	Ashley	T(~30Ma)	NA	NA	NA	NA	NA	NA
SRS												
SRS 2	HTEF-C2	12.44	NA	NA	Tobacco Road	T (~40Ma)	NA	NA	NA	NA	NA	NA
SRS 3 & 8	HTEF-C3 & C8	13.38	Silty Sand (SM)	NA	Dry Branch	T (~40Ma)	11.4	0.0	NA	0.190	41.0	14.0
SRS 3 & 8	HTEF-C3 & C8	19.63	Silty Sand (SM)	NA	Dry Branch	T (~40Ma)	NA	NA	NA	NA	NA	NA
SRS 5	HTEF-C5	12.28	NA	NA	Tobacco Road	T (~40Ma)	NA	NA	NA	NA	NA	NA
SRS 5	HTEF-C5	20.51	NA	NA	Dry Branch	T (~40Ma)	NA	NA	NA	NA	NA	NA
SRS 6	HTEF-C6	22.59	NA	NA	Dry Branch	T (~40Ma)	NA	NA	NA	NA	NA	NA
SRS 7	HTEF-C7	12.41	NA	NA	Tobacco Road	T (~40Ma)	NA	NA	NA	NA	NA	NA
SRS 7	HTEF-C7	21.40	NA	NA	Dry Branch	T (~40Ma)	NA	NA	NA	NA	NA	NA
SRS 9	HTEF-C9	13.29	Clayey Sand (SC)	NA	Dry Branch	T (~40Ma)	18.4	0.0	50.6	0.180	38.0	10.0
SRS 9	HTEF-C9	18.32	Poorly Graded Sand with Silt (SP-SM)	NA	Dry Branch?	T (~40Ma)?	9.6	0.0	4.90	0.380	NL	NP
SRS 10	HTEF-C10	11.43	NA	NA	Tobacco Road	T (~40Ma)	NA	NA	NA	NA	NA	NA
SRS 10	HTEF-C10	20.57	NA	NA	Dry Branch	T (~40Ma)	NA	NA	NA	NA	NA	NA
SRS 13	HTEF-C13	21.52	NA	NA	Dry Branch	T (~40Ma)	NA	NA	NA	NA	NA	NA
SRS 17	HTEF-C17	21.40	NA	NA	Dry Branch	T (~40Ma)	NA	NA	NA	NA	NA	NA

a Geologic Age

H - Holocene
P - Pleistocene
T - Tertiary

NP - Non-Plastic
* - Estimated from description in report
NA - Not Available

APPENDIX D

SELECTED PENETRATION-VELOCITY EQUATIONS FROM EARLIER STUDIES

A summary of selected penetration-velocity equations from earlier studies is presented in this appendix. Table D.1 is a summary of selected SPT-V_S equations proposed for Holocene sands. Table D.2 is a summary of selected CPT-V_S equations proposed for Holocene sands. Tables D.3 and D.4 are summaries of selected CPT-V_S equations proposed for Holocene clays and for all Holocene soils, respectively.

Table D.1 - Selected earlier SPT-V_S equations proposed for Holocene sands.

Reference	Original Equation	R^2	Type of Soil	Units	Assumptions for Adjustment	Adjusted Equation for Comparison
Ohta and Goto (1978)	$V_S = 74.7 N_j^{0.171} Z^{0.199}$ $V_S = 73.3 N_j^{0.171} Z^{0.199}$ $V_S = 78.1 N_j^{0.171} Z^{0.199}$ $V_S = 79.3 N_j^{0.171} Z^{0.199}$	N/A N/A N/A N/A	Fine Medium Coarse Sand & gravel	V_S in m/s Z in m	$N_j = 60/67(N_{60})$, as suggested by Seed et al. (1986)	$V_S = 73.3 N_{60}^{0.171} Z^{0.199}$ $V_S = 72.0 N_{60}^{0.171} Z^{0.199}$ $V_S = 76.6 N_{60}^{0.171} Z^{0.199}$ $V_S = 77.8 N_{60}^{0.171} Z^{0.199}$
Seed et al. (1986)	$G_{max} = 20{,}000 (N_1)_{60}^{1/3} (\sigma'_m)^{0.5}$	N/A	Granular soils	G_{max} & σ'_m in lb/ft² V_{S1} in m/s	$G_{max} = \rho V_S^2$; $\rho = 3.73$ lb-s²/ft²; $\sigma'_m = 0.65\sigma'_v$; $\sigma'_v = 2000$ lb/ft²	$V_{S1} = 134(N_1)_{60}^{0.167}$
Yoshida et al. (1988)	$V_S = 49 N_j^{0.25} \sigma'_v{}^{0.14}$ $V_S = 56 N_j^{0.25} \sigma'_v{}^{0.14}$	N/A	Fine Fine to coarse	V_S in m/s σ'_v in kPa	$N_j = 60/78(N_{60})$, as suggested by Lum & Yan (1994); $\sigma'_v = 100$ kPa	$V_{S1} = 87(N_1)_{60}^{0.25}$ $V_{S1} = 100(N_1)_{60}^{0.25}$
Fear and Robertson (1995)	$V_{S1} = 89.8(N_1)_{60}^{0.25}$ $V_{S1} = 113(N_1)_{60}^{0.25}$	N/A	Ottawa sand Alaska sand (FC = 30 %)	V_{S1} in m/s	None	$V_{S1} = 89.8(N_1)_{60}^{0.25}$ $V_{S1} = 113(N_1)_{60}^{0.25}$
Andrus and Stokoe (2000)	$V_{S1} = 93.2(N_1)_{60}^{0.231}$	N/A	FC < 10 % & non-plastic	V_{S1} in m/s	None	$V_{S1} = 93.2(N_1)_{60}^{0.231}$
Piratheepan and Andrus (2002)	$V_S = 66.7 N_{60}^{0.248} Z^{0.138}$ $V_S = 72.3 N_{60}^{0.228} Z^{0.152}$ $V_S = 72.9 N_{60}^{0.224} Z^{0.130}$ $V_{S1} = 95.5(N_1)_{60}^{0.226}$ $V_{S1} = 103(N_1)_{60}^{0.205}$ $V_{S1} = 102(N_1)_{60}^{0.205}$	0.823 0.951 0.788 0.688 0.878 0.719	FC<10 % FC=10-35 % FC<40 % FC<10 % FC=10-35 % FC<40 %	V_S and V_{S1} in m/s Z in m	None	$V_S = 66.7 N_{60}^{0.248} Z^{0.138}$ $V_S = 72.3 N_{60}^{0.228} Z^{0.152}$ $V_S = 72.9 N_{60}^{0.224} Z^{0.130}$ $V_{S1} = 95.5(N_1)_{60}^{0.226}$ $V_{S1} = 103(N_1)_{60}^{0.205}$ $V_{S1} = 102(N_1)_{60}^{0.205}$

Table D.2 - Selected earlier CPT-V_S equations proposed for Holocene sands.

Reference	Original Equation	R^2	Type of Soil	Units	Assumptions for Adjustment	Adjusted Equation for Comparison
Baldi et al. (1989)	$V_S = 277 q_c^{0.13} \sigma'_v{}^{0.27}$	N/A	Mainly silica sand	q_c and σ'_v in MPa V_{S1} and V_S in m/s	$\sigma'_v = 0.1$ MPa	$V_{S1} = 110 q_{c1N}^{0.13}$
Rix and Stokoe (1991)	$\dfrac{G_{max}}{q_c} = 1634 \left[\dfrac{q_c}{\sqrt{\sigma'_v}} \right]^{-0.75}$	N/A	Mainly silica sand	G_{max}, q_c and σ'_v in kPa V_{S1} in m/s	$G_{max} = \rho V_S^2$; $\rho = 3.73$ lb-s^2/ft^2; $\sigma'_v = 100$ kPa	$V_{S1} = 123 q_{c1N}^{0.125}$
Robertson et al. (1992)	$V_{S1} = 60.3 q_{c1}^{0.23}$	N/A	Mainly silica sand	q_c in bars V_{S1} in m/s	None	$V_{S1} = 60.3 q_{c1N}^{0.23}$
Fear and Robertson (1995)	$q_{c1} = \left(\dfrac{V_{S1}}{135} \right)^{4.35}$	N/A	Alaska sand (FC = 30 %)	q_{c1} in MPa V_{S1} in m/s	None	$V_{S1} = 79.5 q_{c1N}^{0.23}$
Hegazy and Mayne (1995)	$V_S = 13.18 q_c^{0.192} \sigma'_v{}^{0.179}$ $V_S = 12.02 q_c^{0.319} f_s^{-0.0466}$	0.684 0.574	Various sands (Age range not specified)	q_c, f_s and σ'_v in kPa V_{S1} and V_S in m/s	$\sigma'_v = 100$ kPa	$V_{S1} = 72.8 q_{c1N}^{0.192}$ $V_S = 12.02 q_c^{0.319} f_s^{-0.0466}$
Andrus et al. (1999)	$V_{S1} = 88.2 q_{c1N}^{0.154}$	N/A	FC < 10 % and non-plastic	V_{S1} in m/s	None	$V_{S1} = 88.2 q_{c1N}^{0.154}$
Piratheepan and Andrus (2002)	$V_{S1} = 77.4 q_{c1N}^{0.178}$ $V_{S1} = 55.3 q_{c1N}^{0.224} I_c^{0.235}$ $V_S = 26.3 q_c^{0.199} f_s^{0.003}$ $V_S = 25.3 q_c^{0.163} f_s^{0.029} Z^{0.155}$	0.597 0.625 0.606 0.740	Sandy soils with $I_c < 2.05$	q_c and f_s in kPa V_{S1} and V_S in m/s Z in m	None	$V_{S1} = 77.4 q_{c1N}^{0.178}$ $V_{S1} = 55.3 q_{c1N}^{0.224} I_c^{0.235}$ $V_S = 26.3 q_c^{0.199} f_s^{0.003}$ $V_S = 25.3 q_c^{0.163} f_s^{0.029} Z^{0.155}$

Table D.3 - Selected earlier CPT-V_S equations proposed for Holocene clays.

Reference	Original Equation	R^2	Type of Soil	Units	Assumptions for Adjustment	Adjusted Equation for Comparison
Hegazy and Mayne (1995)	$V_S = 3.18q_c^{0.549}f_s^{0.025}$	0.778	Various clays (Age range not specified)	q_c , and f_s in kPa V_S in m/s	$\sigma'_v = 100$ kPa	$V_S = 3.18q_c^{0.549}f_s^{0.025}$
Piratheepan and Andrus (2002)	$V_{S1} = 50.2q_{c1N}^{0.428}$ $V_{S1} = 2.9q_{c1N}^{0.665}I_c^{0.205}$ $V_S = 12.3q_c^{0.313}f_s^{0.084}$ $V_S = 0.274q_c^{0.628}f_s^{-0.004}I_c^{1.688}$ $V_S = 11.9q_c^{0.269}f_s^{0.108}Z^{0.127}$	0.822 0.878 0.892 0.941 0.905	Clayey soils with $I_c > 2.6$	q_c and f_s in kPa V_{S1} and V_S in m/s Z in m	None	$V_{S1} = 50.2q_{c1N}^{0.428}$ $V_{S1} = 2.9q_{c1N}^{0.665}I_c^{0.205}$ $V_S = 12.3q_c^{0.313}f_s^{0.084}$ $V_S = 0.274q_c^{0.628}f_s^{-0.004}I_c^{1.688}$ $V_S = 11.9q_c^{0.269}f_s^{0.108}Z^{0.127}$

Table D.4 - Selected earlier CPT-V_S equations proposed for all Holocene soils.

Reference	Original Equation	R^2	Type of Soil	Units	Assumptions for Adjustment	Adjusted Equation for Comparison
Hegazy and Mayne (1995)	$V_S = \left(10.1\log q_c - 11.4\right)^{1.67}(FR)^{0.3}$	0.695	All soils (Age range not specified)	q_c in kPa $FR =$ f_s/q_c*100 V_S in m/s	None	$V_S = \left(10.1\log q_c - 11.4\right)^{1.67}(FR)^{0.3}$
Piratheepan and Andrus (2002)	$V_{S1} = 100q_{c1N}^{0.133}$ $V_{S1} = 35.7q_{c1N}^{0.283}I_c^{0.574}$ $V_S = 55.8q_c^{0.076}f_s^{0.109}$ $V_S = 32.3q_c^{0.089}f_s^{0.121}D^{0.215}$ $V_S = 4.2.9q_c^{0.331}Z^{0.164}I_c^{0.721}$	0.519 0.673 0.617 0.733 0.716	All soils	q_c and f_s in kPa V_{S1} and V_S in m/s Z in m	None	$V_{S1} = 100q_{c1N}^{0.133}$ $V_{S1} = 35.7q_{c1N}^{0.283}I_c^{0.574}$ $V_S = 55.8q_c^{0.076}f_s^{0.109}$ $V_S = 32.3q_c^{0.089}f_s^{0.121}D^{0.215}$ $V_S = 4.2.9q_c^{0.331}Z^{0.164}I_c^{0.721}$

APPENDIX E

SUMMARY OF CPT-V_S AND SPT-V_S REGRESSION EQUATIONS DEVELOPED FOR THIS STUDY

A summary of the CPT-V_S and SPT-V_S regression equations developed by Ellis (2003) for this study is presented in this appendix. Tables E.1 through E.7 are the equations based on CPT-V_S data pairs. Tables E.8 through E.10 are the equations based on SPT-V_S data pairs. Examples calculations of the ages scaling factor and residual standard deviation are given in Table E.11

Table E.1 - Developed CPT-V_S regression equations based on measurements in all Holocene soil types and from South Carolina, California, Canada, and Japan.

Regression Equation for V_s[a] (m/s)	R^2	s (m/s)	No. of Data Pairs	Equation Number
$V_s=33.0q_c^{0.186}$	0.597	30	81	E.1
$V_s=40.8q_c^{0.119}f_s^{0.100}$	0.663	27	81	E.2
$V_s=10.5q_c^{0.191}(\sigma'_v)^{0.257}$	0.684	27	81	E.3
$V_s=2.65*I_c*q_c^{0.398}$	0.692	26	81	E.4
$V_s=5.13q_c^{0.343}I_c^{0.734}$	0.707	26	81	E.5
$V_s=3.03q_c^{0.406}f_s^{-0.036}I_c^{0.910}$	0.709	26	81	E.6
$V_s=2.34*I_c*q_c^{0.434}f_s^{-0.049}$	0.709	26	81	E.7
$V_s=2.18*I_c*q_c^{0.406}Z^{0.080}$	0.711	25	81	E.8
$V_s=30.1q_c^{0.120}f_s^{0.117}Z^{0.145}$	0.720	25	81	E.9
$V_s=4.63q_c^{0.342}I_c^{0.688}Z^{0.092}$	0.731	25	81	E.10
$V_s=7.08q_c^{0.289}f_s^{0.031}Z^{0.105}I_c^{0.535}$	0.732	25	81	E.11
$V_s=14.0q_c^{0.128}f_s^{0.094}(\sigma'_v)^{0.235}$	0.739	24	81	E.12
$V_s=3.57q_c^{0.314}I_c^{0.574}(\sigma'_v)^{0.168}$	0.741	24	81	E.13

[a] q_c, σ'_v, and f_s in kPa, Z in meters, and I_c dimensionless

Table E.2 - Developed CPT-V_S regression equations based on measurements in sandy and clayey Holocene soils and from South Carolina, California, Canada, and Japan.

Soil Type	Regression Equation for $V_s{}^a$ (m/s)	R^2	s (m/s)	No. of Data Pairs	Equation Number
$I_c < 2.05$ (Sands and sand mixtures)	$V_s=2.57*I_c*q_c{}^{0.400}$	0.413	23	33	E.14
	$V_s=25.1q_c{}^{0.206}f_s{}^{0.005}$	0.542	21	33	E.15
	$V_s=24.4q_c{}^{0.211}$	0.542	20	33	E.16
	$V_s=2.25*I_c*q_c{}^{0.393}Z^{0.131}$	0.564	20	33	E.17
	$V_s=11.9q_c{}^{0.272}I_c{}^{0.306}$	0.570	20	33	E.18
	$V_s=15.6q_c{}^{0.188}(\sigma'_v)^{0.157}$	0.624	19	33	E.19
	$V_s=18.6q_c{}^{0.144}f_s{}^{0.038}(\sigma'_v)^{0.175}$	0.636	19	33	E.20
	$V_s=5.88q_c{}^{0.273}I_c{}^{0.377}(\sigma'_v)^{0.154}$	0.644	19	33	E.21
	$V_s=0.878*I_c*q_c{}^{0.581}f_s{}^{-0.153}$	0.664	18	33	E.22
	$V_s=32.2q_c{}^{0.137}f_s{}^{0.051}Z^{0.141}$	0.682	18	33	E.23
	$V_s=0.330q_c{}^{0.687}f_s{}^{-0.196}I_c{}^{1.319}$	0.683	17	33	E.24
	$V_s=8.27q_c{}^{0.285}I_c{}^{0.406}Z^{0.122}$	0.684	17	33	E.25
$I_c > 2.60$ (Clays and clay mixtures)	$V_s=6.21q_c{}^{0.444}$	0.830	18	31	E.26
	$V_s=9.93q_c{}^{0.338}f_s{}^{0.078}$	0.841	18	31	E.27
	$V_s=9.72q_c{}^{0.333}f_s{}^{0.084}Z^{0.023}$	0.841	18	31	E.28
	$V_s=3.10q_c{}^{0.423}(\sigma'_v)^{0.180}$	0.852	17	31	E.29
	$V_s=5.39q_c{}^{0.284}f_s{}^{0.105}(\sigma'_v)^{0.203}$	0.871	17	31	E.30
	$V_s=0.924*I_c*q_c{}^{0.554}$	0.879	16	31	E.31
	$V_s=1.06*I_c*q_c{}^{0.526}f_s{}^{0.022}$	0.880	16	31	E.32
	$V_s=1.06*I_c*q_c{}^{0.551}Z^{-0.057}$	0.883	16	31	E.33
	$V_s=0.263q_c{}^{0.646}f_s{}^{-0.014}I_c{}^{1.603}$	0.886	16	31	E.34
	$V_s=0.332q_c{}^{0.618}I_c{}^{1.529}$	0.886	15	31	E.35
	$V_s=0.278q_c{}^{0.642}I_c{}^{1.701}(\sigma'_v)^{-0.040}$	0.886	16	31	E.36
	$V_s=0.208q_c{}^{0.654}I_c{}^{1.910}Z^{-0.108}$	0.899	15	31	E.37
	$V_s=0.0260q_c{}^{0.904}f_s{}^{-0.122}Z^{-0.188}I_c{}^{2.681}$	0.910	14	31	E.38

[a] q_c, σ'_v, and f_s in kPa, Z in meters, and I_c dimensionless

Table E.3 - Developed CPT-V_S regression equations based on stress-corrected measurements in Holocene soils and from South Carolina, California, Canada, and Japan.

Soil Type	Regression Equation for V_{s1}[a], (m/s)	R^2	s (m/s)	No. of Data Pairs	Equation Number
All soils	$V_{s1}=80.8q_{c1N}^{0.185}$	0.632	30	81	E.39
	$V_{s1}=71.8q_{c1N}^{0.217}F^{0.077}$	0.675	28	81	E.40
	$V_{s1}=37.2q_{c1N}^{0.291}I_c^{0.484}$	0.675	28	81	E.41
	$V_{s1}=50.3q_{c1N}^{0.258}F^{0.040}I_c^{0.258}$	0.677	28	81	E.42
$I_c < 2.05$ (Sands and sand mixtures)	$V_{s1}=76.8q_{c1N}^{0.186}$	0.474	22	33	E.43
	$V_{s1}=83.5q_{c1N}^{0.176}F^{0.051}$	0.508	21	33	E.44
	$V_{s1}=49.8q_{c1N}^{0.244}I_c^{0.299}$	0.510	21	33	E.45
	$V_{s1}=32.5q_{c1N}^{0.301}F^{-0.043}I_c^{0.543}$	0.510	22	33	E.46
$I_c > 2.60$ (Clays and clay mixtures)	$V_{s1}=48.9q_{c1N}^{0.412}$	0.758	21	31	E.47
	$V_{s1}=45.4q_{c1N}^{0.402}F^{0.109}$	0.781	20	31	E.48
	$V_{s1}=2.10q_{c1N}^{0.698}I_c^{2.218}$	0.822	18	31	E.49
	$V_{s1}=0.310q_{c1N}^{0.900}F^{-0.150}I_c^{3.629}$	0.836	18	31	E.50

[a] q_{c1N}, F and I_c dimensionless

Table E.4 - Selected CPT-V_S regression equations based on uncorrected measurements for Holocene soils with calculated age scaling factors for Pleistocene soils in the South Carolina Coastal Plain.

Soil Type	Regression Equation for $V_s{}^a$, (m/s)	Age Scaling Factors (*ASF*)	*s* (m/s)	No. of Data Pairs	Equation Number
$I_c < 2.05$	$V_s=8.27q_c{}^{0.285}I_c{}^{0.406}Z^{0.122}ASF$	1.33	46	23	E.51
	$V_s=5.88q_c{}^{0.273}I_c{}^{0.377}(\sigma'_v)^{0.154}ASF$	1.37	47	23	E.52
$I_c > 2.60$	$V_s=0.208q_c{}^{0.654}I_c{}^{1.910}Z^{-0.108}ASF$	1.16	40	17	E.53
	$V_s=0.278q_c{}^{0.642}I_c{}^{1.701}(\sigma'_v)^{-0.040}ASF$	1.11	41	17	E.54
All Soils	$V_s=4.63q_c{}^{0.342}I_c{}^{0.688}Z^{0.092}ASF$	1.22	37	53	E.55
	$V_s=3.57q_c{}^{0.314}I_c{}^{0.574}(\sigma'_v)^{0.168}ASF$	1.25	38	53	E.56

[a] q_c and σ'_v in kPa, Z in meters, and I_c dimensionless

Table E.5 - Selected CPT-V_S regression equations based on uncorrected measurements for Holocene soils with calculated age scaling factors for all Tertiary soils in the South Carolina Coastal Plain.

Soil Type	Regression Equation for $V_s{}^a$, (m/s)	Age Scaling Factors (*ASF*)	*s* (m/s)	No. of Data Pairs	Equation Number
$I_c < 2.05$	$V_s=8.27q_c{}^{0.285}I_c{}^{0.406}Z^{0.122}ASF$	1.60	94	11	E.57
	$V_s=5.88q_c{}^{0.273}I_c{}^{0.377}(\sigma'_v)^{0.154}\ ASF$	1.58	101	11	E.58
$I_c > 2.60$	$V_s=0.208q_c{}^{0.654}I_c{}^{1.910}Z^{-0.108}\ ASF$	1.63	73	8	E.59
	$V_s=0.278q_c{}^{0.642}I_c{}^{1.701}(\sigma'_v)^{-0.040}\ ASF$	1.52	62	8	E.60
All Soils	$V_s=4.63q_c{}^{0.342}I_c{}^{0.688}Z^{0.092}\ ASF$	2.00	106	45	E.61
	$V_s=3.57q_c{}^{0.314}I_c{}^{0.574}(\sigma'_v)^{0.168}\ ASF$	1.97	120	45	E.62

[a] q_c and σ'_v in kPa, D in meters, and I_c dimensionless

Table E.6 - Selected CPT-V_S regression equations based on uncorrected measurements for Holocene soils with calculated age scaling factors for Tertiary soils in the South Carolina Coastal Plain grouped by geologic formations.

I_c	Equation for Predicting V_s ^{a}, m/s	ASF	No. of Data Pairs	s^b m/s	Range of I_c	Equation Number
Ashley formation--Charleston						
< 2.05	$V_s=8.27q_c^{0.285}I_c^{0.406}Z^{0.122}ASF$	2.47	3	61	2.00-2.01	E.63
	$V_s=5.88q_c^{0.273}I_c^{0.377}(\sigma'_v)^{0.154}ASF$	2.53	3	60	2.00-2.01	E.64
> 2.60	$V_s=0.208q_c^{0.654}I_c^{1.910}Z^{-0.108}ASF$	1.87	4	66	2.77-2.91	E.65
	$V_s=0.278q_c^{0.642}I_c^{1.701}(\sigma'_v)^{-0.040}ASF$	1.70	4	59	2.77-2.91	E.66
All values	$V_s=4.63q_c^{0.342}I_c^{0.688}Z^{0.092}ASF$	2.27	30	64	2.00-2.91	E.67
	$V_s=3.57q_c^{0.314}I_c^{0.574}(\sigma'_v)^{0.168}ASF$	2.27	30	65	2.00-2.91	E.68
Tobacco Road formation--Savannah River Site						
< 2.05	$V_s=8.27q_c^{0.285}I_c^{0.406}Z^{0.122}ASF$	--	0	--^{b}	--	E.69
	$V_s=5.88q_c^{0.273}I_c^{0.377}(\sigma'_v)^{0.154}ASF$	--	0	--^{b}	--	E.70
> 2.60	$V_s=0.208q_c^{0.654}I_c^{1.910}Z^{-0.108}ASF$	1.42	3	31	2.82-3.19	E.71
	$V_s=0.278q_c^{0.642}I_c^{1.701}(\sigma'_v)^{-0.040}ASF$	1.37	3	34	2.82-3.19	E.72
All values	$V_s=4.63q_c^{0.342}I_c^{0.688}Z^{0.092}ASF$	1.65	4	48	2.31-3.19	E.73
	$V_s=3.57q_c^{0.314}I_c^{0.574}(\sigma'_v)^{0.168}ASF$	1.56	4	46	2.31-3.19	E.74
Dry Branch formation--Savannah River Site						
< 2.05	$V_s=8.27q_c^{0.285}I_c^{0.406}Z^{0.122}ASF$	1.38	8	19	1.64-1.81	E.75
	$V_s=5.88q_c^{0.273}I_c^{0.377}(\sigma'_v)^{0.154}ASF$	1.34	8	19	1.64-1.81	E.76
> 2.60	$V_s=0.208q_c^{0.654}I_c^{1.910}Z^{-0.108}ASF$	1.31	1	--^{b}	2.85	E.77
	$V_s=0.278q_c^{0.642}I_c^{1.701}(\sigma'_v)^{-0.040}ASF$	1.25	1	--^{b}	2.85	E.78
All values	$V_s=4.63q_c^{0.342}I_c^{0.688}Z^{0.092}ASF$	1.38	10	32	1.64-2.85	E.79
	$V_s=3.57q_c^{0.314}I_c^{0.574}(\sigma'_v)^{0.168}ASF$	1.28	10	34	1.64-2.85	E.80

^{a} q_c and σ'_v in kPa, Z in meters, and I_c dimensionless
^{b}At least 3 measurements needed to calculate residual standard deviation

Table E.7 - Selected CPT-V_S regression equations based on stress-corrected measurements for Holocene soils with calculated age scaling factors for Pleistocene and Tertiary soils in the South Carolina Coastal Plain grouped by geologic formations.

	Regression Equations for V_{s1}[a], (m/s)		ASF	No. of Data Pairs	s m/s	Eq. No.
Pleistocene-age soils						
$I_c < 2.05$		$V_{s1}=49.8q_{c1N}^{0.244}I_c^{0.299}ASF$	1.36	23	49	E.81
$I_c > 2.60$		$V_{s1}=2.10q_{c1N}^{0.698}I_c^{2.218}ASF$	1.19	17	37	E.82
All Values		$V_{s1}=37.2q_{c1N}^{0.291}I_c^{0.484}ASF$	1.28	53	39	E.83
Tertiary-age soils						
Ashley	$I_c < 2.05$	$V_{s1}=49.8q_{c1N}^{0.244}I_c^{0.299}ASF$	2.65	3	47	E.84
Ashley	$I_c > 2.60$	$V_{s1}=2.10q_{c1N}^{0.698}I_c^{2.218}ASF$	2.03	4	97	E.85
Ashley	All Values	$V_{s1}=37.2q_{c1N}^{0.291}I_c^{0.484}ASF$	2.46	30	57	E.86
Tobacco Road	$I_c < 2.05$	$V_{s1}=49.8q_{c1N}^{0.244}I_c^{0.299}ASF$	--	0	--[b]	E.87
Tobacco Road	$I_c > 2.60$	$V_{s1}=2.10q_{c1N}^{0.698}I_c^{2.218}ASF$	1.82	3	33	E.88
Tobacco Road	All Values	$V_{s1}=37.2q_{c1N}^{0.291}I_c^{0.484}ASF$	1.87	4	57	E.89
Dry Branch	$I_c < 2.05$	$V_{s1}=49.8q_{c1N}^{0.244}I_c^{0.299}ASF$	1.42	8	14	E.90
Dry Branch	$I_c > 2.60$	$V_{s1}=2.10q_{c1N}^{0.698}I_c^{2.218}ASF$	1.69	1	--[b]	E.91
Dry Branch	All Values	$V_{s1}=37.2q_{c1N}^{0.291}I_c^{0.484}ASF$	1.46	10	33	E.92

[a]q_{c1N} and I_c dimensionless
[b]At least 3 measurements needed to calculate residual standard deviation

Table E.8 - Selected SPT-V_S regression equations developed by Piratheepan and Andrus (2002) with reported s and R^2 values for Holocene soils from California, Japan and Canada grouped by fines content.

FC	Regression Equations for Predicting V_s or V_{s1}[a], (m/s)	R^2	s (m/s)	No. of Data Pairs	Equation Number
<10%	$V_s=66.7(N_{60})^{0.248}Z^{0.138}$	0.823	15	25	E.93
	$V_{s1}=95.5(N_1)_{60}^{0.226}$	0.688	18	28	E.94
10-35%	$V_s=72.3(N_{60})^{0.228}Z^{0.152}$	0.951	8	10	E.95
	$V_{s1}=103 (N_1)_{60}^{0.205}$	0.878	12	13	E.96
<40%	$V_s=72.9(N_{60})^{0.224}Z^{0.130}$	0.788	16	39	E.97
	$V_{s1}=102(N_1)_{60}^{0.205}$	0.719	17	45	E.98

[a]$(N_1)_{60}$ and N_{60} in blows/0.3 meter, and Z in meters

Table E.9 - Selected SPT-V_S regression equations developed by Piratheepan and Andrus (2002) for Holocene soils with calculated age scaling factors for Pleistocene soils in the South Carolina Coastal Plain.

FC	Regression Equations for Predicting V_s or V_{s1}[a], (m/s)	Pleistocene			Eq. No.
		ASF	No. of Data Pairs	s m/s	
<10%	$V_s=66.7(N_{60})^{0.248}Z^{0.138}ASF$	1.28	7	58	E.99
	$V_{s1}=95.5(N_1)_{60}^{0.226}ASF$	1.24	7	64	E.100
10-35%	$V_s=72.3(N_{60})^{0.228}Z^{0.152}ASF$	1.08	1	--[b]	E.101
	$V_{s1}=103(N_1)_{60}^{0.205}ASF$	1.11	1	--[b]	E.102
<40%	$V_s=72.9(N_{60})^{0.224}Z^{0.130}ASF$	1.23	8	50	E.103
	$V_{s1}=102(N_1)_{60}^{0.205}ASF$	1.21	8	56	E.104

[a]$(N_1)_{60}$ and N_{60} in blows/0.3 meter, and Z in meters
[b]At least 3 measurements needed to calculate residual standard deviation

Table E.10 - Selected SPT-V_S regression equations developed by Piratheepan and Andrus (2002) for Holocene soils with calculated age scaling factors for Tertiary soils in the South Carolina Coastal Plain.

FC	Regression Equations for Predicting V_s or V_{s1}[a], (m/s)	ASF	No. of Data Pairs	s m/s	Eq. No.
All Tertiary soils--South Carolina Coastal Plain					
10-35%	$V_s=72.3(N_{60})^{0.228}Z^{0.152}ASF$	1.56	3	118	E.105
	$V_{s1}=103.4(N_1)_{60}^{0.205}ASF$	1.61	3	92	E.106
<40%	$V_s=72.9(N_{60})^{0.224}Z^{0.130}ASF$	1.66	3	114	E.107
	$V_{s1}=101.8(N_1)_{60}^{0.205}ASF$	1.63	3	92	E.108
Ashley Soils--Charleston					
10-35%	$V_s=72.3(N_{60})^{0.228}Z^{0.152}ASF$	1.71	1	--[b]	E.109
	$V_{s1}=103(N_1)_{60}^{0.205}ASF$	1.84	1	--[b]	E.110
<40%	$V_s=72.9(N_{60})^{0.224}Z^{0.130}ASF$	1.82	1	--[b]	E.111
	$V_{s1}=102(N_1)_{60}^{0.205}ASF$	1.86	1	--[b]	E.112
Dry Branch--Savannah River Site					
10-35%	$V_s=72.3(N_{60})^{0.228}D^{0.152}ASF$	1.48	2	--[b]	E.113
	$V_{s1}=103(N_1)_{60}^{0.205}ASF$	1.50	2	--[b]	E.114
<40%	$V_s=72.9(N_{60})^{0.224}Z^{0.130}ASF$	1.59	2	--[b]	E.115
	$V_{s1}=102(N_1)_{60}^{0.205}ASF$	1.51	2	--[b]	E.116

[a]$(N_1)_{60}$ and N_{60} in blows/0.3 meter, and Z in meters
[b]At least 3 measurements needed to calculate residual standard deviation

Table E.11 – Example calculations of age scaling factor (*ASF*) and residual standard
deviation (*s*).

Measured V_{SI} (m/s)	I_c	q_{c1N}	Predicted V_{SI}[a] (m/s)	Column (1) / Column (4)	New Predicted V_{SI} Using *ASF*	Column (6) - Column (1)	[Column (7)]²
(1)	(2)	(3)	(4)	(5)	(6)	(7)	(8)
178	1.32	260.0	215	0.831	284	105	11079
283	1.38	239.1	214	1.325	283	-1	1
225	1.56	124.0	188	1.197	248	23	538
273	1.56	152.2	199	1.373	263	-10	109
243	1.57	171.2	207	1.174	273	30	923
258	1.60	152.0	201	1.281	266	8	64
240	1.65	97.2	180	1.337	237	-3	8
242	1.70	90.0	178	1.359	235	-7	47
376	1.70	112.5	190	1.979	251	-125	15637
194	1.74	107.8	190	1.021	251	57	3246
226	1.74	147.6	208	1.086	275	49	2380
286	1.76	109.0	192	1.494	253	-33	1096
314	1.83	86.3	182	1.723	241	-73	5371
233	1.83	97.2	189	1.234	249	16	268
232	1.84	56.2	161	1.437	213	-19	349
244	1.89	83.3	183	1.331	242	-2	3
189	1.91	65.2	172	1.103	227	37	1393
248	1.91	83.0	184	1.345	243	-4	20
272	1.91	85.2	185	1.466	245	-27	720
259	1.97	110.0	203	1.276	268	9	83
260	2.00	38.4	150	1.729	199	-61	3762
201	2.01	82.1	188	1.067	248	48	2288
268	2.03	140.2	221	1.214	292	24	553
			ASF[b]=	1.32		Sum=	49936
						s =	49

[a]Predicted V_{SI} calculated here using: $V_{s1} = 37.2 q_{c1N}^{0.291} I_c^{0.484}$

[b]*ASF = average (Measured V_s / Predicted V_s)*

[c]Residual Standard Deviation, *s = SQRT [(Σ column (8))/(j-2)]* where *j* = number of samples, 23

APPENDIX F

SUMMARY OF COMPILED LABORATORY SHEAR MODULUS AND MATERIAL DAMPING DATA FROM SOUTH CAROLINA AND SURROUNDING STATES

A summary of the compiled laboratory shear modulus and material damping data from South Carolina and surrounding states is presented in this appendix. Information for test samples from Charleston, South Carolina is summarized in Table F.1. Information for test samples from the Savannah River Site, South Carolina is summarized in Table F.2. Information for test samples from the Richard B. Russell Dam, South Carolina is summarized in Table F.3. Information for test samples from North Carolina is summarized in Table F.4. Finally, information for test samples from Opelika, Alabama is summarized in Table F.5.

Table F.1- Dynamic laboratory test samples from Charleston, South Carolina.

Sample Index	Location / (Lat., Long.)	Boring No.	Depth (m)	USCS Soil Type	*PI* (%)	*FC* (%)	Tested By[*]	Dynamic Test Type[#]	Geology
C-1	Daniel Island (32.833,-79.927)	C-79	10	Sand with Silt	2	8	UTA	RC/TS	Holocene age soil
C-2	Daniel Island (32.833,-79.927)	C-79	11	Fat Clay	79	93	UTA	RC/TS	Holocene age soil
C-3	Daniel Island (32.833,-79.927)	C-79	20	Sandy Silt	132	68	UTA	RC/TS	Wando Formation/ Top of the Cooper Group
C-4	Mark Clark Exp. (32.739,-80.007)	B-15	31	Clay	47	92	Fugro	RC	Cooper Group
C-5	Mark Clark Exp. (32.777,-80.035)	B-35	15	Organic Silt	59	78	Fugro	RC	Cooper Group
C-6	Mark Clark Exp. (32.780,-80.034)	B-36	9	Clayey Sand	2	38	Fugro	RC	Wando Formation/ Top of the Cooper Group

[*]UTA = University of Texas at Austin; Fugro = Fugro-McClelland (Southwest), Inc.
[#]RC = Resonant Column; TS = Torsional Shear.

Table F.2- Dynamic laboratory test samples from Savannah River Site, South Carolina.

Sample Index	Location	Boring No.	Depth (m)	USCS Soil Type	*PI* (%)	*FC* (%)	Tested By*	Dynamic Test Type#	Geology
S-1	Savannah River Site	CFD-4a	17	SM	0	N/A	UTA	RC/TS	Dry Branch
S-2	Savannah River Site	CFD-5a	24	SC	34	N/A	UTA	RC/TS	Dry Branch
S-3	Savannah River Site	ITP-4b	17	SP-SC	8	N/A	Law	RC	Dry Branch
S-4	Savannah River Site	NPR-26x	32	SC	34	N/A	Purdue	RC	Dry Branch
S-5	Savannah River Site	RTF-80	24	SP-SM	0	N/A	Law	RC	Dry Branch
S-6	Savannah River Site	RTF-94	29	SC	19	N/A	Law	RC	Dry Branch
S-7	Savannah River Site	BGE-7c	12	SP-SC	N/A	N/A	GEI	RC	Dry Branch
S-8	Savannah River Site	BGE-10c	20	SP-SC	N/A	N/A	GEI	RC	Dry Branch
S-9	Savannah River Site	SFS-8c	26	SAND	N/A	N/A	GEI	RC	Dry Branch
S-10	Savannah River Site	BNH-29b	25	SM	N/A	N/A	GEI	RC	Dry Branch
S-11	Savannah River Site	LRA-F5	25	SP	N/A	N/A	GEI	RC	Dry Branch
S-12	Savannah River Site	CFD-7a	31	SM	0	N/A	UTA	RC/TS	Santee
S-13	Savannah River Site	ITP-15c	44	SP-SC	72	N/A	Law	RC	Santee
S-14	Savannah River Site	ITP-24b	60	SM	0	N/A	Law	RC	Santee
S-15	Savannah River Site	NPR-B6a	66	SM	0	N/A	Purdue	RC	Santee
S-16	Savannah River Site	NPR-B6b	71	SM	0	N/A	Purdue	RC	Santee
S-17	Savannah River Site	NPR-8a	54	SM	0	N/A	Purdue	RC	Santee

Table F.2- Dynamic laboratory test samples from Savannah River Site, South Carolina (Cont'd).

Sample Index	Location	Boring No.	Depth (m)	USCS Soil Type	PI (%)	FC (%)	Tested By[*]	Dynamic Test Type[#]	Geology
S-18	Savannah River Site	NPR-8b	57	SM	0	N/A	Purdue	RC	Santee
S-19	Savannah River Site	RTF-106	32	SP	0	N/A	Law	RC	Santee
S-20	Savannah River Site	RTF-155	47	SM	0	N/A	Law	RC	Santee
S-21	Savannah River Site	KRA-4d	36	SP-SC/ SP-SM	24	N/A	GEI	RC	Santee
S-22	Savannah River Site	KRA-7a	38	SW-SC	41	N/A	GEI	RC	Santee
S-23	Savannah River Site	KRA-10b	41	SC/SM	17	N/A	GEI	RC	Santee
S-24	Savannah River Site	PPD-2B	21	SP-SC	N/A	N/A	GEI	RC	Santee
S-25	Savannah River Site	PPD-4B	34	SC	N/A	N/A	GEI	RC	Santee
S-26	Savannah River Site	PPD-5B	49	SC	N/A	N/A	GEI	RC	Santee
S-27	Savannah River Site	LRA-F9	39	SC	N/A	N/A	GEI	RC	Santee
S-28	Savannah River Site	CFD-3b	13	SM	0	N/A	UTA	RC	Tobacco Road
S-29	Savannah River Site	ITP-1a	9	SC	26	N/A	Law	RC	Tobacco Road
S-30	Savannah River Site	BNH-3c	31	SC	N/A	N/A	GEI	RC	Tobacco Road
S-31	Savannah River Site	BNH-7b	12	SC	N/A	N/A	GEI	RC	Tobacco Road
S-32	Savannah River Site	BNH-17b	16	SM	N/A	N/A	GEI	RC	Tobacco Road
S-33	Savannah River Site	NPR-B5	18	SM	19	N/A	Purdue	RC	Tobacco Road
S-34	Savannah River Site	RTF-40	20	SM	17	N/A	Law	RC	Tobacco Road

Table F.2- Dynamic laboratory test samples from Savannah River Site, South Carolina (Cont'd).

Sample Index	Location	Boring No.	Depth (m)	USCS Soil Type	*PI* (%)	*FC* (%)	Tested By[*]	Dynamic Test Type[#]	Geology
S-35	Savannah River Site	RTF-53	22	SM	0	N/A	Law	RC	Tobacco Road
S-36	Savannah River Site	RTF-58	8	SAND	3	N/A	Law	RC	Tobacco Road
S-37	Savannah River Site	RTF-65	14	SAND	0	N/A	Law	RC	Tobacco Road
S-38	Savannah River Site	RTF-72	8	SC-SM	5	N/A	Law	RC	Tobacco Road
S-39	Savannah River Site	SFS-2a	11	SM-SC	N/A	N/A	GEI	RC	Tobacco Road
S-40	Savannah River Site	SFS-4a	16	SM	N/A	N/A	GEI	RC	Tobacco Road
S-41	Savannah River Site	LRA-F1	9	SC	N/A	N/A	GEI	RC	Tobacco Road
S-42	Savannah River Site	LPD-10c	11	SP-SC	N/A	N/A	GEI	RC	Tobacco Road
S-43	Savannah River Site	LPD-8c	7	SP-SC	N/A	N/A	GEI	RC	Tobacco Road
S-44[$]	Savannah River Site	CFD-12a	80	SM	0	N/A	UTA	RC/TS	Snapp
S-45[$]	Savannah River Site	CFD-13a	87	SM	0	N/A	UTA	RC/TS	Snapp
S-46	Savannah River Site	NPR-113	150	SM-SC	N/A	N/A	Purdue	RC	Snapp
S-47	Savannah River Site	NPR-73x	103	SM	0	N/A	Purdue	RC	Snapp
S-48	Savannah River Site	CFD-T1A	107	CH	27	N/A	UTA	RC/TS	Sawdust or Steel Creek
S-49	Savannah River Site	CFD-PS6A	27	CH	53	N/A	UTA	RC/TS	Dry Branch
S-51	Savannah River Site	NPR-96X	129	CL	19	N/A	Purdue	RC	Snapp
S-52	Savannah River Site	BNH-11U-C	11	CH	64	N/A	GEI	RC	Tobacco Road

117

Table F.2- Dynamic laboratory test samples from Savannah River Site, South Carolina (Cont'd).

Sample Index	Location	Boring No.	Depth (m)	USCS Soil Type	*PI* (%)	*FC* (%)	Tested By[*]	Dynamic Test Type[#]	Geology
S-53	Savannah River Site	CFD-2A	7	SC	19	N/A	UTA	RC/TS	Upland (stiff)
S-54	Savannah River Site	CFD-1A	3	SC	31	N/A	UTA	RC/TS	Upland (stiff)
S-55	Savannah River Site	LPD-2B	6	SP-SC	N/A	N/A	GEI	RC	Upland (soft)
S-56	Savannah River Site	CFD-8A	47	SP-SM	0	N/A	UTA	RC/TS	Warley Hill
S-57	Savannah River Site	NPR-52X	76	SM	0	N/A	Purdue	RC	Warley Hill
S-58[$]	Savannah River Site	CFD-PS11A	57	SP-SM	0	N/A	UTA[$]	RC/TS	Congaree
S-59[†]	Savannah River Site	CFD-T6C	262	SC	16	N/A	UTA	RC/TS	Middendorf
S-60[†]	Savannah River Site	NPR-130X	169	SM	0	N/A	Purdue	RC	Black Creek
S-61[†]	Savannah River Site	NPR-192X	247	SC-SM	6	N/A	Purdue	RC	Black Creek
S-62[†]	Savannah River Site	NPR-260X	326	SM	0	N/A	Purdue	RC	Cape Fear
S-63[†]	Savannah River Site	CFD-T4A	199	CL	14	N/A	UTA	RC/TS	Black Creek
S-64[†]	Savannah River Site	CFD-T5B	226	CL	12	N/A	UTA	RC/TS	Black Creek

[*]UTA = University of Texas at Austin; Law = Law Engineering and Environmental Services, Inc.; Purdue = Purdue University; GEI = GEI Consultants, Inc.

[#]RC = Resonant Column; TS = Torsional Shear.

[$]Sample marked as "disturbed". Still used in the analysis because their results were consistent with other data.

[†]Not used in this analysis because they don't follow the trend exhibited by the shallow data (Stokoe et al., 1995, p.34).

Table F.3- Dynamic laboratory test samples from Richard B. Russell Dam, South Carolina.

Sample Index	Location	Boring No.	Depth (m)	USCS Soil Type	*PI* (%)	*FC* (%)	Tested By[*]	Dynamic Test Type[#]	Geology
R-1	Richard B. Russell	AB-65	1	Sand	0	3	SADEN-FL	RC	Embankment Sand
R-2	Richard B. Russell	C-100	1	SP	0	4	SADEN-FL	RC	Embankment Sand
R-3	Richard B. Russell	D-110	1	SP	0	4	SADEN-FL	RC	Embankment Sand
R-4	Richard B. Russell	M3-RC-1	1	MH	24	86	SADEN-FL	RC	Embankment Impervious Soil
R-5	Richard B. Russell	C-287-B	1	CH	29	62	SADEN-FL	RC	Residual Soil
R-6	Richard B. Russell	C-295-C	4	SM	6	49	SADEN-FL	RC	Residual Soil
R-7	Richard B. Russell	C-292-B	12	weathered rock	4	58	SADEN-FL	RC	Saprolite
R-8	Richard B. Russell	C-317-B	7	weathered rock	0	N/A	SADEN-FL	RC	Saprolite

[*]SADEN-FL = U.S. Department of the Army, South Atlantic Division Laboratory (SADEN-FL).
[#]RC = Resonant Column.

Table F.4- Dynamic laboratory test samples from North Carolina.

Sample Index	Location	Boring No.	Depth (m)	USCS Soil Type	*PI* (%)	*FC* (%)	Tested By[*]	Dynamic Test Type[#]	Geology
N-1	North Carolina	IV-27E	2.1	MH	22	94	NCSU	TS	Residual Soil
N-2	North Carolina	IV-28E	2.1	MH	22	94	NCSU	TS	Residual Soil
N-3	North Carolina	IV-32G	3.7	MH	14	91	NCSU	TS	Residual Soil
N-4	North Carolina	I-3B	1.2	MH	14	90	NCSU	RC	Residual Soil
N-5	North Carolina	I-4B	1.2	MH	14	90	NCSU	RC	Residual Soil
N-6	North Carolina	I-5B	1.2	MH	14	90	NCSU	RC	Residual Soil
N-7	North Carolina	IV-26E	1.3	MH	6	84	NCSU	TS	Residual Soil
N-8	North Carolina	III-10D	1.2	MH	27	84	NCSU	TS	Residual Soil
N-9	North Carolina	IV-29E	1.5	MH	13	81	NCSU	TS	Residual Soil
N-10	North Carolina	III-9D	1.2	MH	29	77	NCSU	TS	Residual Soil
N-11	North Carolina	III-11D	1.2	MH	31	72	NCSU	TS	Residual Soil
N-12	North Carolina	III-25E	1.2	ML	5	78	NCSU	TS	Residual Soil
N-13	North Carolina	III-23E	2.1	ML	0	71	NCSU	TS	Saprolite
N-14	North Carolina	III-20E	2.5	ML	0	70	NCSU	TS	Saprolite
N-15	North Carolina	III-21E	1.8	ML	0	67	NCSU	TS	Saprolite
N-16	North Carolina	III-24E	1.5	ML	0	65	NCSU	TS	Saprolite
N-17	North Carolina	III-22E	1.5	ML	0	64	NCSU	TS	Saprolite

Table F.4- Dynamic laboratory test samples from North Carolina (Cont'd).

Sample Index	Location	Boring No.	Depth (m)	USCS Soil Type	*PI* (%)	*FC* (%)	Tested By[*]	Dynamic Test Type[#]	Geology
N-18	North Carolina	II-6C	3.1	ML	10	58	NCSU	TS	Residual Soil
N-19	North Carolina	II-7C	3.1	ML	10	58	NCSU	TS	Residual Soil
N-20	North Carolina	II-8C	3.1	ML	10	58	NCSU	TS	Residual Soil
N-21	North Carolina	III-15D	1.2	SM-ML	0	64	NCSU	TS	Saprolite
N-22	North Carolina	III-17D	1.2	SM-ML	0	64	NCSU	TS	Saprolite
N-23	North Carolina	III-16D	1.2	SM-ML	0	56	NCSU	TS	Saprolite
N-24	North Carolina	III-18E	1.5	SM-ML	0	53	NCSU	TS	Saprolite
N-25	North Carolina	III-19E	1.5	SM-ML	0	53	NCSU	TS	Saprolite
N-26	North Carolina	I-1A	1.1	SM-ML	8	48	NCSU	RC	Residual Soil
N-27	North Carolina	I-2A	1.1	SM-ML	8	48	NCSU	RC	Residual Soil
N-28	North Carolina	III-12D	1.8	SM	0	30	NCSU	TS	Saprolite
N-29	North Carolina	III-13D	1.8	SM	0	26	NCSU	TS	Saprolite
N-30	North Carolina	III-14D	2.4	SM	0	29	NCSU	TS	Saprolite
N-31	North Carolina	IV-30F	4.3	SM	0	20	NCSU	TS	Saprolite
N-32	North Carolina	IV-31F	5.0	SM	0	15	NCSU	TS	Saprolite

[*] NCSU = North Carolina State University at Raleigh.
[#] RC = Resonant Column; TS = Torsional Shear.

Table F.5- Dynamic laboratory test samples from Opelika, Alabama.

Sample Index	Location	Boring No.	Depth (m)	USCS Soil Type	PI (%)	FC (%)	Tested By[*]	Dynamic Test Type[#]	Geology
A-1	Opelika, Alabama	B9-3M-S1	3.0	ML	10	80	GT	RC	Residual Soil
A-2	Opelika, Alabama	B9-3M-S2	3.0	ML	10	80	GT	RC	Residual Soil
A-3	Opelika, Alabama	B8-4M-S1	4.0	ML	12	75	GT	RC	Residual Soil
A-4	Opelika, Alabama	B9-4M-S1	4.0	ML	12	75	GT	RC	Residual Soil
A-5	Opelika, Alabama	B8-5M-S1	5.0	SM	4	40	GT	RC	Saprolite
A-6	Opelika, Alabama	B7-5M-S1	5.0	SM	4	40	GT	RC	Saprolite
A-7	Opelika, Alabama	B7-7M-S1	7.0	SM	0	42	GT	RC	Saprolite
A-8	Opelika, Alabama	B8-7M-S1	7.0	SM	0	42	GT	RC	Saprolite
A-9	Opelika, Alabama	B8-8M-S1	8.0	ML	5	68	GT	RC	Residual Soil
A-10	Opelika, Alabama	B8-8M-S2	8.0	ML	5	68	GT	RC	Residual Soil
A-11	Opelika, Alabama	B7-9M-S1	9.0	SM	0	32	GT	RC	Saprolite
A-12	Opelika, Alabama	B7-9M-S2	9.0	SM	0	32	GT	RC	Saprolite

[*] GT = Georgia Institute of Technology.
[#] RC = Resonant Column.

PRINTING COSTS

Total Printing Costs	$649.26
Total Number of Documents	90
Cost per Unit	$7.214